EFFECTS OF CLIMATIC LOADING IN FLEXIBLE PAVEMENT SUBGRADES IN TEXAS

by

ASIF AHMED

Presented to the Faculty of the Graduate School of

The University of Texas at Arlington in Partial Fulfillment

for the Requirements

of the Degree of

DOCTOR OF PHILOSOPHY

THE UNIVERSITY OF TEXAS AT ARLINGTON

December 2017

ACKNOWLEDGEMENTS

I would like to express my sincere gratitude to my supervising professor, Dr. Sahadat Hossain, for his guidance, support, and encouragement throughout this research. He generously shared his experience and knowledge with me, and provided the motivation and “push” that I needed to complete my research and dissertation. I am grateful for the opportunity to work under him and for having the freedom to work at my own pace.

I would like to acknowledge the Texas Department of Transportation (TxDOT) for funding this project. I am thankful for the TxDOT officials, Al Amaroon and Boon Thian, for their support. I would also like to recognize Dr. Nur Yazdani, Dr. Xinbao Yu, and Dr. Chien-Pai Han for devoting their time as committee members and for their constructive comments.

A special thanks to my friends and research team for their cooperation and assistance throughout my graduate studies. Thanks to Dr. Sadik Khan, Dr. Md Zahangir Alam, and Dr. Mahsa Hedayati for their support and guidance. I am grateful to the excellent undergraduate researchers Aya Shishani, Kelli Greenwood, Carla Flores, Madeline McCollough, and Cory Rauss. I would also like to thank Jobair Bin Alam, Naima Rahman, Masrur Mahedi and Arindam Dhar for their friendship and good times. I consider myself lucky to be a part of such a lively research group.

I would like to express my sincere gratitude to my undergraduate thesis supervisor, Dr. Shamsul Hoque, for the role he played in motivating me toward the field of research. Most importantly, my deepest gratitude to my father, mother, and entire family for their endless encouragement and support. I thank almighty Allah for giving me the strength and patience to pursue a doctoral degree.

October 27, 2017

ABSTRACT

EFFECTS OF CLIMATIC LOADING IN FLEXIBLE PAVEMENT SUBGRADES IN TEXAS

Asif Ahmed, Ph.D.

The University of Texas at Arlington, 2017

Supervising Professor: MD. Sahadat Hossain

Expansive soils, which have been reported as a worldwide problem, cover 25% of the United States. Due to the swelling and shrinkage behavior induced by moisture variations, expansive soil contributes to volumetric deformation, which in turn affects the stability and performance of structures. The Texas Department of Transportation (TxDOT) allocates 25% of its budget to pavement maintenance and repairs, much of which is triggered by expansive soil. In order to decrease the burden of this expense on maintenance authorities, it is necessary to have an accurate understanding of expansive subgrade behavior. Applying this knowledge to the pavement design and construction processes can significantly increase the pavement's service life.

The specific objectives of this research were to (1) study the behavior of expansive soil with seasonal changes and climatic loading; (2) asses the real-time moisture and temperature variations in the expansive subgrade; (3) quantify the deformation pattern with time in response to environmental loading; (4) develop a real-time moisture, temperature, and deformation prediction model; (5) based on the investigation of the subgrade, provide solutions in order to combat the pavement deformation; and (6) evaluate the effectiveness of the proposed solution.

In order to accomplish the objectives, one farm-to-market road and one state highway were selected for observation of the behavior of expansive subgrades in North

Texas. Soil samples were collected and tested to determine the soil properties. Moisture, suction sensors, temperature sensors, and rain gauges were installed to record the variations of the variables over time. Moreover, geophysical testing was conducted to continually portray the subgrade over time. Deformation of the pavement was monitored through topographic surveying and a horizontal inclinometer.

Collected data was analyzed in a statistical environment to develop real-time prediction models. The first attempt produced a moisture variation model that captured variations due to seasonal effects and temporary variations due to rainfall. The outputs of this model were within 90% of the values measured on-site. The second attempt produced a temperature prediction model that was dependent on depth and the day of the year. The squared correlation coefficient between the observed and predicted soil temperature was more than 0.90. Application of the developed models could allow for a non-invasive estimation of the response of soil strength and stiffness properties due to variations in moisture and temperature. While examining the deformation data, it was found that seasonal variations only capture a portion of the deformation, whereas the amount of precipitation plays a significant role in further modifying the model. Temperature and suction were also correlated with deformation to finalize the deformation model. Application of the developed model facilitates estimation of deformation at any time of the year, in response to precipitation.

The study also attempted to focus, to a limited extent, on numerical modeling; however, the selection of unsaturated parameters was challenging. The selection of unsaturated permeability and flow parameters is usually laboratory-based, because a specific condition of the soil makes it impossible to capture them in real time in the field. This study attempted to determine the variations of unsaturated hydraulic conductivity based on rainfall response data. Rather than conducting the usual laboratory testing to

determine the unsaturated flow parameters by curve fitting, a novel approach was undertaken to determine the flow parameters from field soil water characteristic curves. Finally, field-based values were used in the PLAXIS 2D environment for transient analysis. The validity of the estimated parameters was confirmed, as FE results corresponded with direct field measurements. The study results indicated that FE modeling can provide effective information about the subgrade matric suction variations.

This research focused on finding a possible solution to the problem of pavement distress. It was found that controlling the moisture from the edge of the pavement can significantly improve the pavement performance. Consequently, a moisture barrier consisting of a geomembrane and a geocomposite (geonet sandwiched between two nonwoven geotextiles) was suggested. A combination of a 40-mil LLDPE geomembrane and an 8-oz. HDPE geocomposite was used to control the moisture from the edge of a 50 ft. section of FM 987. A control section along the same roadway was instrumented and monitored for comparison. Preliminary field monitoring results clearly indicated that the moisture barrier significantly reduced the water infiltration near the edge of the pavement. Moreover, the movement of the pavement was reduced by 80%, based upon previous recorded measurements of the control section.

TABLE OF CONTENTS

LIST OF ILLUSTRATIONS

LIST OF TABLES

CHAPTER 1

INTRODUCTION

BACKGROUND

Expansive soil is a worldwide problem (Nelson and Miller, 1992). In the United States, approximately 25% of all soils are expansive (Cerato et al. 2007). Volume changes of these soils occur due to adsorption or desorption of moisture, leading to cyclic swelling and shrinkage which affects the performance and stability of the structures constructed over it. Nelson and Miller (1992) estimated that 9 billion USD is spent on damages annually, while Jones and Jefferson (2012) calculated a total financial loss of 15 billion USD due to the presence of expansive soil. The Texas Department of Transportation (TxDOT) spends 25% of its total annual expenditures for maintenance and repair of damaged pavements (Sebesta, 2002). In North Texas, more than 50% of TxDOT's budget is allocated to repair and maintenance caused by distress from expansive soils (Lenz, 2011). Puppala et al. (2012) stated that due to severe pavement cracking, maintenance costs are sometimes higher than construction costs. As such, the effects of expansive subgrade soils should be addressed at both the design and construction stages to reduce future maintenance costs.

Differential volume changes, due to either swelling or shrinkage of expansive subgrades, cause damage to pavements (Chen, 1988). Pavements experience severe distress and an increase in roughness, with cracks in both longitudinal and transverse directions if the volume change phenomenon is not encountered in the design phase. Subgrade moisture, temperature, and suction variations depend on several factors, i.e., width of road, roadside drainage, presence of trees, presence of cracks, and water infiltration through cracks (Nelson and Miller, 1992; Chen, 1988).

Nelson and Miller (1992) categorized the causes of shrink-swell behavior of subgrades into three groups: soil characteristics, environmental factors, and the state of stress. Environmental factors include rainfall, vegetation, and drainage. Hedayati (2014) mentioned moisture content variation as the prime cause of subgrade deformation in expansive soil. Existing design methods suggest a rough estimation of moisture content, i.e., equilibrium moisture content (Zheng et al. 2013; Zapata et al. 2008). In-situ monitoring of moisture content provides a better understanding of the variations of moisture due to precipitation. Temperature, humidity, and suction also play important roles in expansive subgrade soil behavior. Hence, measurements of climatic conditions and environmental factors needed to be studied for a better understanding of expansive soil behavior. An accurate understanding of the behavior of expansive subgrade, the interaction of subgrade pavement structures, and the incorporation of the results into the design process can improve the pavement service life significantly.

Potential vertical rise (PVR), which is based on outlines provided by McDowell (1956), is the current standard method used for estimating the volume change of expansive subgrades. This empirical method provides estimations of pavement deformation by analyzing the subgrade soil's swelling capacity. The determined PVR is then compared to certain specified values, and remedial measures need to be taken if the criterion is not satisfied.

Although the method provides a fair estimation of the possible deformation, it bears some deficiencies in its principal assumptions, which yield over-conservative results. Moreover, the method is not case specific and does not address variations of factors affecting the swelling process, especially moisture. Recent researches suggest utilization of moisture-based methods, which evaluate the swelling/shrinkage deformations based on moisture variations in the subgrade soil. To increase accuracy of

the moisture-based methods, an estimation of moisture variations due to climatic effects is necessary.

Pavement distresses, in particular longitudinal cracks, form on the surface of the pavement as a result of the expansion and contraction of subgrade soil. Additionally, moisture intrusion from the edge of pavement causes longitudinal cracks near the edge of the pavement. These longitudinal cracks are known as edge drops. In addition to the distresses caused by vertical movement, areas of expansive soil near areas of soil that are not expansive will cause differential movement, resulting in worse pavement distresses. As maintenance costs are increasing every year, the Texas Department of Transportation is seeking feasible and economical methods to employ for repairing North Texas soils plagued by expansive soils. A combination of horizontal and vertical moisture barriers (geomembranes and geocomposite layers) were placed in a section of pavement in an effort to find a viable solution.

PROBLEM STATEMENT

Methods have been developed to relate volumetric deformation of high plastic subgrades with soil properties. Initially, researchers attempted to incorporate the movement of soil with basic soil properties, i.e., LL and PL (Houston, et al., 2011; Osman and Sharief, 1987). Based on research performed by McDowell (1956), TxDOT has been using the vertical rise (PVR) method to determine expansive soil movement. However, the method is reportedly conservative, and several assumptions might lead to errors (Lytton, et al., 2005). In addition to soil properties, field instrumentation has been used to capture the real variations of moisture and other properties to predict the soil deformation (Manosuthikij, 2008; Hedayati, 2014).

A recent development in this area is the suggestion to utilize numerical modeling to provide additional information on volumetric deformation. Abed (2007) used a 2D

PLAXFLOW analysis to examine the swelling and shrinkage behavior of expansive soil. Puppala et al. (2014) performed a 3D static analysis in Abaqus to study the swelling behavior. Recently, the effects of real-time rainfall on cyclic wetting and drying of expansive subgrades have been studied by Hedayati (2014). He also discussed the importance of an additional drying-wetting cycle rather than the typical annual wetting-drying cycle which is dependent on the rainfall pattern.

Quantification of pavement performance in response to environmental loading is required to mitigate the maintenance and repair cost. Then, based on the quantification result, attempts should be made to find solutions to the problem. Hence, this study collects the real-time response of a subgrade, develops a prediction model, attempts to capture the variations of material properties, and performs numerical modeling of the expansive subgrade, followed by proposing a method for reducing the distress of pavement.

Previous researchers (Jayatilaka and Lytton 1997, Henry and Barna 2002, Steinberg 1989) adopted different approaches, i.e., horizontal barriers, vertical barriers, and geocomposite capillary barrier drains (GCBD) to combat pavement cracking. However, each of the studies resulted in either high cost of materials or construction difficulties. Hence, a simple and cost effective solution, using a modified (horizontal/sloped) moisture barrier that included geomembrane and geocomposite layers, was placed in a section of pavement to check its effectiveness in improving pavement performance.

RESEARCH OBJECTIVES

The overall objective of this study was to perform a comprehensive analysis of pavement distress, including monitoring real-time variations of different parameters of expansive subgrade, and evaluate the pavement's deformation accordingly. The

research included site investigations, field instrumentation, monitoring, laboratory investigation, model development, and numerical modeling. In addition, it also looked for an effective solution for mitigating pavement distress in expansive soil. The specific objectives of the current research work were to:

1. Establish a field instrumentation program to monitor pavement performance.
2. Study the effects of rainfall on different subgrade soils, i.e., moisture, temperature, suction, and deformation of pavement.
3. Develop real-time data-based moisture model due to environmental loading.
4. Develop a model of pavement deformation based on climatic loading.
5. Estimate the moisture variation at the slope of pavement by employing the resistivity imaging (RI) technique.
6. Determine the soil parameters required for numerical modeling from field investigations.
7. Provide effective solution(s) to edge-cracking on expansive subgrades.

DISSERTATION ORGANIZATION

Chapter 1 describes the background, problem statement, and objectives of the research. It's the total dissertation "in a nutshell." Chapter 1 is followed by an extensive literature review presented in Chapter 2. The rest of the dissertation is divided into four papers. The first paper describes the real-time moisture model development. It entails the variations of moisture due to both seasonal changes and temporary increases due to rainfall. The second paper focuses on the development of a deformation model in flexible pavement. It also records the seasonal variations of moisture by means of geophysical testing. The third paper covers the in-situ findings in the numerical environment. It explains the extraction of significant parameters from field instrumentation data and usage of it in numerical modeling. The final paper describes the solution for

pavement edge cracking by adopting a modified moisture barrier. It depicts how this solution is different from previous solutions, and compares its effectiveness with them. These papers are followed by a summary and conclusions.

CHAPTER 2

LITERATURE REVIEW

EXPANSIVE SOILS

Expansive soils are well-known in the world of civil engineering. They respond to changes in moisture content with increases or decreases in soil volume. Expansive soils swell when moisture content increases and shrink when moisture content decreases. Areas with distinct wet and dry cycles can easily observe the effects of expansive soils. Such soils undergo volumetric deformation that gradually damages essential infrastructures such as foundation slabs, bridges, roadways, and residential homes. Present in both humid and arid/semi-arid environments, expansive soils cover nearly a quarter of the area of the United States. Annually, expansive soils alone incur more financial losses to US property owners than earthquakes, flood, hurricanes, and tornadoes combined (Jones and Jefferson, 2012). In a typical year, the associated financial losses can be as high as 15 billion dollars (Table 2:1). Several countries, like the USA, Israel, India, South Africa, Australia, etc., have reported infrastructure problems due to expansive soils (Manu, 2008). Their low stiffness, light loading, and extended presence over the country render pavements especially susceptible to deterioration. Continuous volumetric deformation of the problematic soils increases the pavement's roughness, resulting in reduced serviceability. Consequently, a better understanding of the causes of pavement distress and the behavior of expansive soils is necessary for acceptable pavement performance and design (Sebesta, 2002).

A definite relationship exists between expansive soils, moisture content, and pavement. Expansive soils expand when they gain moisture and shrink when they lose moisture, resulting in the soil layers above the expansive soils moving upward when they gain moisture and moving downward when they lose moisture. If the layers of expansive

soil experienced the same moisture changes, the entire structure built on it would just move up and down with changing moisture. However, the expansive soil layers may have areas of soils with different characteristics or different moisture contents. As a result, the soil layers above the expansive soils can exhibit differential movement, causing damage to buildings, highway pavements, and airport pavements resting on shallow foundations.

Table 2:1 Worldwide Damage of Expansive Soils (Adem and Vanapalli, 2013)

Region	Damage/Year	Reference
USA	$ 15 Billion	Jones and Jefferson (2012)
UK	£ 400 Million	Driscoll and Crilly (2000)
France	€ 3.3 Billion	Johnson (1973)
Saudi Arabia	$ 300 Million	Ruwaih (1987)
China	¥ 100 Million	Ng et al. (2003)
Australia	$ 150 Million	Osman et al. (2005)

Similarly, pavement distresses can appear as a result of the swelling and shrinking action of expansive soils. Longitudinal cracks form on the surface of the pavement as a result of the expansion and contraction of subgrade soil. Additionally, moisture intrusion from the edge of the pavement causes longitudinal cracks near the edge of the pavement, which are known as edge drops. In addition to the distresses caused by vertical movement, areas of expansive soil that are near areas of soil that are not expansive will cause differential movements, resulting in worse pavement distresses.

Many roads constructed in Texas are susceptible to cracking due to expansive clay subgrades. The costs to repair these pavements are sometimes higher than the construction costs. Brown (1996) found that the use of soil mechanics during the

pavement design process can reduce pavement cracking, and recommended that it be used during the design and construction phases of roads.

Swelling and shrinkage can cause damage to pavements. Changes in the moment and shear forces cause failure in the pavement. These forces are not accounted for in the design of pavements, which causes poor flexure strength in the pavement. The moisture variations in the subgrade soils cause shrinkage and swelling. Trees close to the pavement take water from the soil and cause shrinkage in the soil subgrade. Lack of adequate roadside ditches for drainage, as well as other poor drainage conditions, also cause shrinkage and swelling.

Shrinkage and swelling lead to cracking in all directions of the pavement and cause bumps in the road, making the ride uncomfortable for passengers in cars. Moisture can also get in the subsoil through the cracks and the subgrade soils, causing loss of support for the pavements. Figure 2:1 and Figure 2:2 present various types of heave that are related to distresses in pavements. Damages to pavements can be major, and the cost of maintaining and repairing them can be very high.

Figure 2:1 Heaving problems in flexible pavements (Manosuthikij, 2008)

Figure 2:2 Pavement distress due to expansive soil movement (Manosuthikij, 2008)

EFFECT OF CLIMATIC FACTORS

Climatic factors, especially moisture and temperature variations, induce substantial changes to structural characteristics of pavement system and have major impacts on their long term performance. Therefore, better understanding of these parameters would enhance pavement design efficiency significantly.

Moisture and temperature variations tend to affect properties of bound and unbound layers of the pavement system. Major sources of moisture variation are rainfall, intrusion from cracks, freeze-thaw cycles, leakage, and evapotranspiration (Hedayati, 2014). An increase in moisture content reduces the stiffness of the subgrade soils, which weakens the support for the overlaying pavement. Furthermore, variations of moisture content may cause swelling and shrinkage in high plastic subgrade soils. Surficial cracks are generated due to this behavior and impose additional maintenance expenditures on departments of transportation (Zapata and Houston, 2008).

Temperature variations influence the modulus of the subgrade soil and properties of the asphalt layer. Freeze-thaw cycles cause expansion and contraction cracks that may penetrate deep into the bounded layers. Moreover, the viscosity of the asphalt pavement is reduced at high temperatures and may cause significant deformation. This problem is of particular concern in Texas, where surface temperatures can be as high as 55ºC in summer (Hedayati, 2014).

To consider the possible effects of moisture and temperature in the design procedures, many researchers have developed a regression analysis to relate subgrade characteristics with environmental factors. Such models estimate the moisture/temperature profile beneath the pavement, in combination with translation techniques, and correlate possible variations in structural properties of subgrade soil (Hossain, 2012). For accurate analysis, the profiles should be estimated in the entire depth contributing to overall pavement performance. Nelson et al. (2001) defined this depth as the active zone, which might be as deep as 3.6 m. However, limited information is available on variations of moisture and temperature in the entire depth of active zone.

SOURCE OF WATER IN PAVEMENTS

Water can enter the pavement structure in several ways. Cedergren et al. (1973) presented a pictorial view of water intrusion in pavement, as shown in Figure 2:3. Ridgeway (1982) listed several sources of free moisture intrusion, such as cracks in pavement surface, infiltration through shoulder and side ditches, free water from pavement base, high groundwater table, etc.

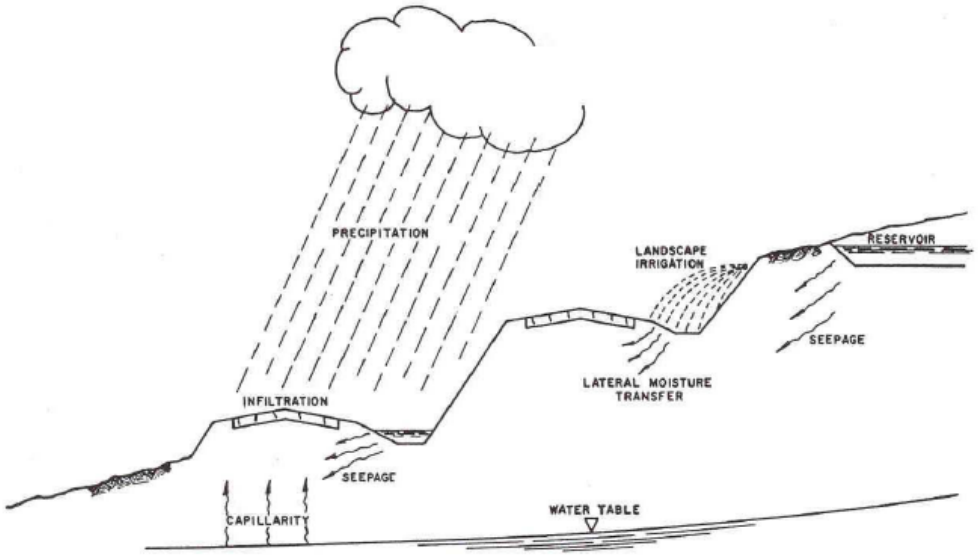

Figure 2:3 Potential sources of water in Pavement Structure (Cedergren et al. 1973)

Hedayati (2014) conducted resistivity imaging on a cross section of a farm-to-market road in Dallas, Texas. He reported moisture intrusion from the edge of the pavement, i.e., grass side slope.

PAVEMENTS AND EXPANSIVE SUBGRADES

The Texas Department of Transportation (TxDOT) spends 25% of its construction and maintenance budget on the repair of pavement distresses. Because

expansive subgrade is seldom identified as the source of pavement failure, maintenance routines typically only consist of roadway surface treatment (Figure 2:4). Consequently, surface roughness can reappear from six months to two years later. This is a common problem for 18 out of 52 TxDOT districts (Wanyan et al, 2010).

Figure 2:4 Pavement distress in Texas Highways

Farm-to-market (FM) roads are flexible pavements, with an average daily traffic (ADT) of less than 400 vehicles (AASHTO, 2004). Due to their higher flexibility and displacement tolerance, they tend to perform better than rigid pavements (Dafalla et al., 2011). However, the low structural elastic modulus of FM roads renders them more vulnerable to damages resulting from expansive subgrade. Figure 2:5 illustrates the two causes of pavement and slab distresses (Fredlund, et al., 2006).

Differential movement between the edge and center of the slabs causes pavement and slab distresses. Moisture readily infiltrates soil that is exposed outside the slab, resulting in greater moisture variations with increasing distance from the center. The slab can exhibit either a center lift (i.e., edge drop) as a long-term distortion, or an edge lift as a seasonal distortion. Edge drops happen when capillary action causes an increase in moisture in the soil beneath the slab; edge lifts occur when the perimeter soil becomes

wetter than the soil beneath the slab. The resulting differential movement causes a crack in the structure that grows with continuous loading.

Loss of support also contributes to pavement and slab distresses. Soil shrinkage can lead to separation between the slab's edge and the supporting soil. Consequently, the stress concentration in the slab increases, resulting in top-down cracking. The support index, "C," is used to define the amount of support provided by the foundation soil. A higher climate index corresponds to a more stable moisture balance.

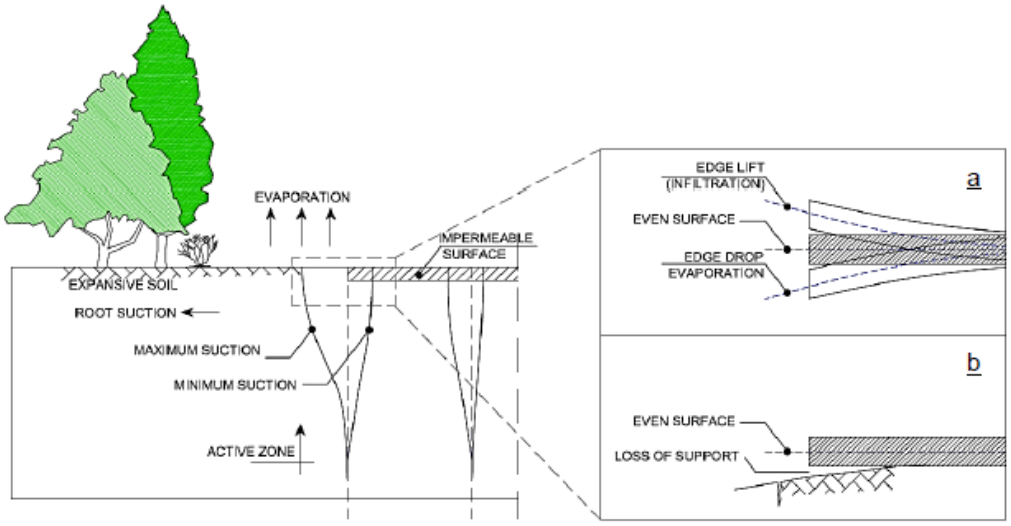

Figure 2:5 Loss of pavement support due to expansive subgrade (Hedayati, 2014)

Movement between the edge and the center of the slabs, coupled with loss of support, can lead to edge cracks/drop off, longitudinal or transverse cracking, reflection cracking, and swelling (Dessouky et al., 2012; Buhler and Cerato, 2007). The above distresses and their causes are discussed in the following sections.

Edge Drop-Offs

Excessive differential movement, absence of shoulder support, base weakening by frost action, insufficient drainage, moisture variation in soils (Hearn, et al., 2008), and

weak cohesive soils (Heath et al., 1990) contribute to longitudinal cracking 0.3 to 0.6 m from the outer edge of the pavement (Figure 2:6). Swelling-shrinkage behavior and excessive moisture variations intensify the cracks, which develop where the moisture reaches its maximum penetration under the pavement (Gupta et al. 2008).

Figure 2:6 Edge drop (Hedayati, 2014)

Longitudinal/Transverse Cracking

Longitudinal cracks are common to nearly all low-volume pavements in North Texas, and occur as a consequence of differential heaves in expansive subgrade soils (Figure 2:7). Cracking begins when the heave is at a maximum, progressing when the highly plastic subgrade dries during the dry seasons (Gupta et al., 2009; Sebesta, 2002). Longitudinal cracks begin as a single crack or multiple cracks and grow to a cracking pattern resembling an alligator over time.

Asphalt hardening and surficial thermal contraction can result in transverse cracks, which appear across the pavement centerline or in a lay-down direction (Figure 2:7). The progression of existing cracks and the development of additional cracks under traffic loading indicate a swelling subgrade.

Figure 2:7 Longitudinal and transverse cracking (Hedayati, 2014)

Reflection Cracking

Reflection cracking occurs when existing cracks in the highly plastic subgrade propagate throughout the pavement structure due to differential movement across the pavement layers (Figure 2:8). Moisture is free to move into the pavement through the cracks. Loading has been found to accelerate degradation of pavement exhibiting reflection cracking (AASHTO, 2004).

Figure 2:8 Reflection cracking (Hedayati, 2014)

Upheaving/Waves in Profile

Upheaving and waves in the profile develop from the uneven expansion of subgrade soil along the road profile (Figure 2:9). Dynamic loading on the distressed

pavement can amplify pavement distortion and increase surface roughness. Pavement roughness is a function of vertical differences between the ideal and actual surface profiles and quantifies the satisfaction of users traveling the road.

Figure 2:9 Wavy profile in pavement (Hedayati, 2014)

In the last four decades, swelling problems have attracted wide attention due their adverse effect on infrastructures. According to Dafalla et al. (2011), research on roads and pavement is still ongoing. In order to interpret the interaction between swelling and pavement performance, it is necessary to have a good understanding of the swelling mechanism. In the following sections, current procedures of measuring swell are discussed.

MEASUREMENT AND PREDICTION METHODS

For proper design and construction, clay swelling must be taken into account and predicted. In fact, many agencies require a prediction method to be employed before design and construction take place on clay soils. Three categories of prediction methods exist: Oedometer tests, empirical relations, and section-based methods (Lytton, Aubeny, and Bulut, 2005).

Oedometer Tests

The first method of prediction involves the consolidation theory. Oedometer tests employ a constant seating pressure in order to determine the maximum possible swell.

The oedometer test makes use of a consolidation machine. To perform the test, an undisturbed sample is allowed to swell to its maximum by submergence in water (ASTM, 2008). Advantages of this method include its low cost and simple instructions. However, disadvantages of this method include its sensitivity and dependence on the person who performs the test. Sample disturbances and lack of the operator's skill can cause discrepancies in the test results. To increase test accuracy, further simplifications to the method have been suggested (Fredlund et al., 2016; Rao et al., 1988). The equation associated with the consolidation test serves as a basis for the general swell prediction equation, as shown in the following equation.

$$\Delta H = Cs \frac{H}{1 + e_0} \log\left(\frac{\sigma'_f}{\sigma'_s}\right)$$

Where,

ΔH = Overall vertical movement

Cs = Swelling index

H = Depth of swelling layer

e_0 = Initial void ratio

σ'f = Final stress state

σ's = Swelling pressure

While multiple researchers have agreed upon the use of the above equation, they have interpreted the parameters associated with the equation in different ways. Notable researchers who have interpreted the parameters include Fredlund (1983), Dhowian (1990), Nelson and Miller (1992), and Nelson et al. (2006).

Empirical Relations

The second method of prediction involves empirical or semi-empirical methods. In these methods, laboratory measurements are correlated to field measurements and to

various soil properties. These soil properties include penetration test results (both standard and cone), soil water chemistry data, and mineralogy. The volume change, as a result of swelling, can be influenced by the aforementioned soil properties, environmental influences, and stress conditions. Climate, drainage, vegetation, permeability, and temperature are environmental conditions that can influence the swelling of a clay soil. In addition, the stress conditions that can influence the swelling of a clay soil include stress history, in-situ soil stress conditions, loading conditions, and the soil profile.

Current Prediction Method in Texas

For Texas roads, the Texas Department of Transportation (TxDOT) recommends testing method TX-124E, Determination of Potential Vertical Rise (PVR) to predict soil swelling. McDowell (1956) laid the foundation for this testing method, in which the potential swelling of the soil is predicted by using the soil's liquid limit, plasticity index, surcharge pressure, and initial water content. A collection of curves is produced from these parameters that enables potential swelling. Maximum (0.47*LL+2), minimum (0.2*LL+9), and initial water contents are used to determine the percentage of volumetric change of the soil. The potential vertical rise (PVR) is determined for each layer, and then the PVR for a site is determined by determining the sum of the PVRs of all layers. Recommended PVR values can be found in Table 2:2. If these recommendations cannot be met, adjustments to the subgrade are necessary (TxDOT 1999).

Table 2:2: Recommended values of PVR in different types of road (TxDOT, 1999)

Type of Highway	Maximum Allowed PVR (in)
IH/US	1
SH	1.5
FM	2

IN-SITU INSTRUMENTATION AND MONITORING

Moisture variation and infiltration, as well as temperature variation, can have crippling effects on pavement. Moisture levels affect the soil properties, which can affect the subgrade soil, which can, in turn, affect the pavement layers. Therefore, it is important to monitor the pavement to understand these behaviors and their effects. Moisture varies within the pavement layers, and the effects of moisture variation are more prevalent in the unbound subgrade layer than in the bound layers, such as the surface and base layers. Inversely, the deeper layers (subgrade) are less affected by temperature variations. On-site instrumentation and monitoring of said instrumentation is vital to observing these effects. Moisture and temperature variations combine to cause deformation, cracking, and increased roughness of the pavement (Zapata and Houston, 2008). To properly observe the effects of both moisture and temperature in the form of deformation, cracking, and increased roughness, the following instruments are typically utilized: moisture and temperature sensors, suction probes, rain gauges, surveying points, inclinometer profiling, resistivity imaging, and ground-penetrating radar. In the following subsections, specific instruments and associated literature are detailed.

SENSORS FOR IN-SITU MONITORING

Moisture Sensors

Soil moisture is affected by soil type, air temperature, pavement temperature, soil temperature, precipitation, and vegetation. Because various factors can affect moisture sensor data, the most reliable and most acceptable method for data collection of moisture variation involves the direct measurement of moisture over time (Bayomy and Salem, 2004). Time domain reflectometry (TDR), dielectric sensors, and neutron probes can all be used to collect moisture data. Proper installation of these sensors can help avoid

widespread moisture data errors. In fact, improper installation accounts for up to 45% of the errors made in moisture data measurements provided by such instrumentation.

Dielectric sensors measure soil dielectric constants, which can be related to soil moisture content. When the moisture content of the soil increases, the dielectric constant increases by a significant amount. This allows the development of a correlation between the dielectric constant and the moisture content. Through calibration equations, this correlation leads to an eventual relationship between the dielectric constant and the gravimetric water content, as shown in following equation.

$$\omega = \frac{\theta}{G_s\ (1-n)}$$

Where:

ω = Gravimetric moisture content

θ = Volumetric moisture content

Gs = Specific gravity of soil solids

n = Porosity of soil

While in-situ moisture content variation has been studied by multiple researchers, an accurate equation for predicting the variation of moisture content over time has not been developed. Researchers have observed seasonal changes in moisture content of the soil (Chen, 1988; Puppala et al., 2012; Jones and Jefferson, 2012; Wang et al., 2013; Kodikara et al., 2014). Marks and Haliburton (1969) observed that the seasonal moisture content variations were present, but all observed data hovered around particular values correlating to 1.1 to 1.3 times the plastic limit of the soil. In addition to seasonal fluctuations, temporary environmental conditions (such as precipitation events) can have significant effects on the moisture content of the soil. Accurate predictions would involve

correlating the observed moisture content data of the soil with both seasonal and temporary environmental effects.

Temperature Sensors

Temperatures within the soil, pavement, and air can affect the pavement surface. Ground temperatures in particular can be helpful in construction projects when heat losses are experienced. In addition to measuring for building heat losses, ground temperature measurements are useful in construction projects involving thermal energy storage equipment and heat pumps (Florides and Kalogirou, 2004). Where unsaturated soil is concerned, data associated with moisture evaporation, modulus of elasticity, and variation of suction can be augmented by temperature data (Nguyen et al., 2010). Instrumentation of temperature sensors is simple; temperature sensors are placed in the soil without regard to soil disturbance.

In addition, temperature variations within soil layers may be correlated with ambient temperatures. While seasonal temperature variations are typically observed throughout soil layers, the temperature variation is most evident at shallower depths.

Pavement Deformation Monitoring

Elevation measurements are compared to detect pavement deformation. Topographic surveying is used In order to measure elevation changes at the surface level. A survey of the pavement site is conducted, with data points taken along the edges and in other locations across the pavement surface. Horizontal inclinometers can be installed to determine changes in elevation in the subsurface layers. When they are installed properly and in the appropriate location, elevation changes at the base, subbase, and subgrade levels can be monitored. A horizontal inclinometer (Figure 2:10) is typically installed in a pipe that is placed in narrow trenches and can aid in observing small vertical deformations over time. Local deformations inside the pavement structure

can be determined by utilizing the horizontal inclinometer and survey data together (Machan and Bennett, 2008). The inclinometers can detect small pavement deformations earlier than they can be observed in survey data. As the inclinometer is moved through the pipe, it measures angles. Using these angles and trigonometry, the inclinometer produces a vertical profile, which can be compared with previous readings to determine elevation changes.

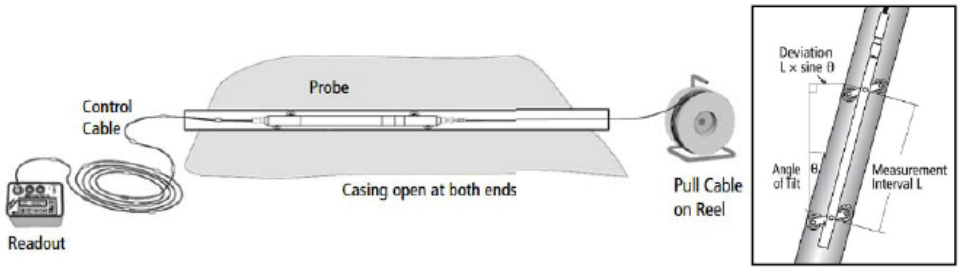

Figure 2:10 Installation of horizontal inclinometer (Hedyati, 2014)

SOIL WATER CHARACTERISTIC CURVE (SWCC)

Soil suction can be defined as the negative pore water pressure on the soil – the soil's affinity for water or the tendency of a soil to absorb water (Hardcastle, 2000). Soil suction is composed of matric and osmotic suction. Matric suction can be defined as surface tension effects or the adsorption of clay minerals. Osmotic suction is basically due to the presence of salts in the soil water.

The soil water characteristic curve (SWCC) is one of the most important parameters in unsaturated soil mechanics. It has been defined as the variation of water storage capacity with respect to suction (Fredlund et al., 1994). Once the suction is known, the water content at a point can be obtained from the SWCC. It is also called the water retention curve.

Formulation of SWCC

The Guide for Mechanistic Empirical Pavement Design provides the approach to take to determine the SWCC from basic soil properties (NCHRP, 2004). The equation used for predicting SWCC was provided by Fredlund and Xing (1994) and is shown in following equation. The basic parameters required for determining the curve are optimum moisture content (wopt), maximum dry unit weight (γmax), specific gravity of soil solids (Gs), percent finer of passing #200 sieve (P200), effective grain size corresponding to 60 percent finer (D60), and the plasticity index (PI).

$$\theta_w = C(h) \times \left[\frac{\theta_{sat}}{\left[\ln\left(e + \left(\frac{h}{a_f} \right)^{b_f} \right) \right]^{c_f}} \right]$$

Where, $C(h) = \left[1 - \frac{\ln\left(1+\frac{h}{h_r}\right)}{\ln\left(1+\frac{1.45\times10^5}{h_r}\right)} \right]$

In which,

θw = volumetric water content;

θsat = saturated water content;

af, bf, cf = parameters related to air entry value, rate of desaturation of soil and curvature of suction respectively;

θsat is determined by the following equations (NCHRP, 2004):

$$\theta_{opt} = \frac{w_{opt} \times \gamma_{d\,max}}{\gamma_{water}}$$

$$S_{opt} = \frac{\theta_{opt}}{1 - \frac{\gamma_{d\,max}}{\gamma_{water} \times G_s}}$$

$$\theta_{sat} = \frac{\theta_{opt}}{S_{opt}}$$

Correlating SWCC Fitting Parameters to Soil Properties

Zapata et al. (2000) determined the fitting parameters of Fredlund and Xing's (1994) equation by statistical analysis of well-known soil properties. The soils were divided into two categories: (i) Plasticity Index (PI>0) and (ii) PI=0. For the first group, P200 and PI were the main soil properties used for correlation. D60 was the main soil property for the second group. For the soils with PI greater than zero, the product of P200, as a decimal, was multiplied by the PI as a percentage, to form the weighted PI (wPI). This value was used as the main soil property for correlation.

For soils: PI>0:

When $(P_{200} \times PI) > 0$, Zapata et al. (2003) provided following equations for estimating the parameters used in Eqn. 1.

$$\mathrm{wPI} = \%\mathrm{Passing\ \#200} \times \mathrm{PI}$$

$$\mathrm{a} = 11 + 4(\mathrm{wPI}) + 0.00364(\mathrm{wPI})^{3.35}$$

$$\mathrm{c} = 0.5 + 0.0514(\mathrm{wPI})^{0.465}$$

$$\mathrm{b/c} = 5.0 - 2.313(\mathrm{wPI})^{0.14}$$

$$\mathrm{h_r/a} = 32.44\mathrm{e}^{0.0186(\mathrm{wPI})}$$

For soils: PI=0:

The correlations for PI=0, the parameters are as follows:

$$\mathrm{a} = 0.8627(\mathrm{D_{60}})^{-0.751}$$

$$\mathrm{b}' = 7.5$$

$$\mathrm{c} = 0.1772\mathrm{Ln}(\mathrm{D_{60}}) + 0.7734$$

$$\mathrm{h_r/a} = 1/(\mathrm{D_{60}} + 9.7\mathrm{e}^{-4})$$

A sample SWCC determined from soil properties is shown in Figure 2:11 (Zapata et al., 2000).

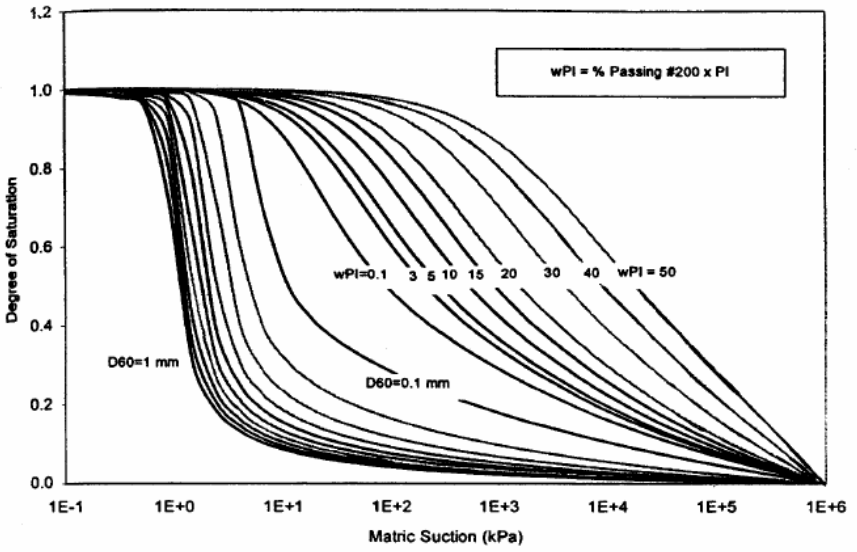

Figure 2:11 Predicted SWCC based on D60 and wPI (Zapata et al., 2000)

Determination of SWCC by WP4C Dewpoint Potentiometer

There are several methods of determining SWCC in the laboratory, including pressure plates, filter papers, and commercially available humidity cells, i.e., the WP4C Dewpoint Water Potentiometer. However, most of the methods are time consuming, expensive (Houston et al. 2006), and sensitive to test conditions and the skills of the operator (Hedayati et al., 2014). Moreover, a limited number of practicing geotechnical laboratories (about 20%) performs suction-based tests (Zapata et al., 2000). Consequently, researchers have tried different approaches to determine, estimate, or predict the SWCC. Fredlund et al. (1997) used grain-size properties, and Houston et al. (2006) used the one-point-suction-measurement technique.

In the current study, a WP4C Dewpoint Potentiameter was utilized to determine the SWCC of the soil, as it made the task less time consuming. The equipment, manufactured by Decagon Devices Inc., uses the chilled mirror hygrometer technique to measure the total suction of soil. The device is shown in Figure 2:12. The suction-

measuring range of the device is 0-300 MPa, and it has an accuracy of +/- 0.5 MPa in 0-5 MPa range and +/- 1% from the 5-300 MPa range (Decagon, Devices, 2017). It requires several 15 mL cups for testing the specimens. The cups are inserted into the drawer of the equipment chamber for measurement. The chamber is temperature controlled and can range from 15 to 40 degree Celsius.

Figure 2:12 WP4C Dewpoint Potentiameter by Decagon Devices, Inc.

The device can render the suction state of the soil in a relatively short time. In 'precious' mode, the device takes several subsequent readings until the successive readings occur within a pre-determined tolerance. It usually takes 15-20 minutes to record a value. Hence, a complete SWCC can be obtained in a timely manner. The WP4C can measure matric suction up to 450 MPa (Decagon Devices 2017). There are two modes of operation: continuous mode and fast mode. In continuous mode, the sample reading is obtained continuously, which is suitable for long-term monitoring. In the fast mode, it offers a quick measurement. The drawback of this method is that it is less accurate.

Sample preparation for this device is a bit challenging, as it is a relatively small specimen size (15 mL cup). As the device uses the chilled mirror hygrometer technique, the samples cannot be filled to the top because they would come into contact with the sensor, which would affect the reading. Hence, care should be taken prior to the insertion of the sample. The cups are shown in Figure 2:13. The specimens were prepared with de-aired/distilled water in order to minimize the effect of osmotic suction, as it measures total suction, while the objective of the test was to obtain matric suction. Approximately half of the cups were filled with the sample prior to measurement. Subsequently, the soil around the cups was carefully removed, and the cups were thoroughly cleaned prior to insertion into the device.

Figure 2:13 15 mL cups for soil sample used in WP4C (Decagon Devices)

MOISTURE VARIATION AT SLOPE BY RESISTIVITY IMAGING

Resistivity Imaging (RI) is an emerging non-destructive method for monitoring the moisture variations of the soil. The theory and background of RI are described in the subsequent sections.

Background of Resistivity Imaging

Electrical resistivity imaging (ERI) has become one of the most applied and user-friendly geophysical techniques in geomorphologic and geotechnical research. It is a

multi-electrode profiling technique that records hundreds of subsurface data points which are used to produce a multi-colored, two-dimensional cross section of the earth. In recent years, electrical resistivity surveys have progressed rapidly from the conventional sounding survey. It is a non-destructive test, and its purpose is to determine the subsurface resistivity distribution by making measurements on the ground surface and conducting geo-physical properties, i.e., structure, water content, or fluid composition (Samouelian et. al., 2005). This method is widely used in hydrogeology, environmental, and geotechnical research, as it has the potential to reveal the subsurface image (Aizebeokhali, 2010). It has been used for the investigation of morphotectonics, weathering studies, landform evolution in mountain areas, permafrost detection, and exploration of underground karst structures (Zhou et al. 2001).

Theory of ERI

ERI is an active geophysical method which measures the electric differences at specific locations while injecting a controlled electric current at other locations. The theory is in an entirely homogeneous half-space. A resistivity value can be calculated for the subsurface by knowing the current injected and measuring the resulting electric potential at specific locations. However, homogeneity within the subsurface is very rare, and the electric current, when introduced, will follow the path of least resistance. Figure 2:14 illustrates the concept of subsurface electric current flow and the influence of subsurface heterogeneities.

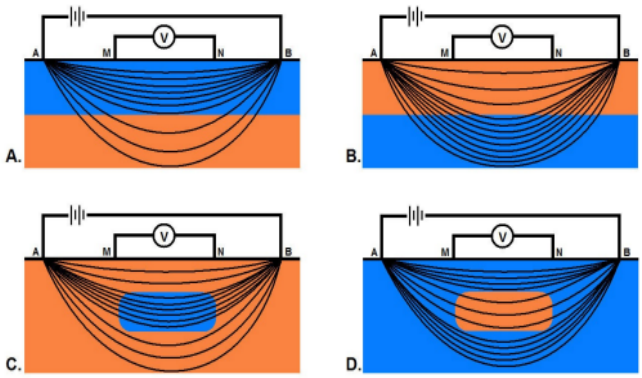

Figure 2:14 Variations in subsurface electric current density (Aizebeokhali, 2010)

For a simple soil body, the resistivity ρ (ohm_ m) is defined as

$$\rho = R\,(A/L)$$

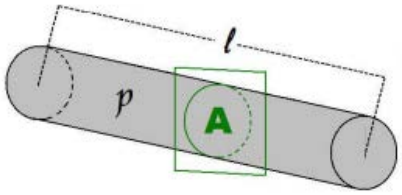

Figure 2:15 Relation between resistance and resistivity (Tabbagh et al., 2000)

Where, R is the electrical resistance, L is the length of the cylinder (m) and A is the cross section area (m2). The electrical resistance of a cylindrical body is defined by the Ohm's law

$$R = V/I$$

Where, V is the potential difference measure in Volt and I is the current in Ampere. The current density J (A/m2) is determined for all the radial directions with,

$$J = I/2\pi r2$$

Where, 2πr2 is surface of a hemispherical sphere of radius r. The distribution of current flow in a homogeneous soil is shown in the figure below.

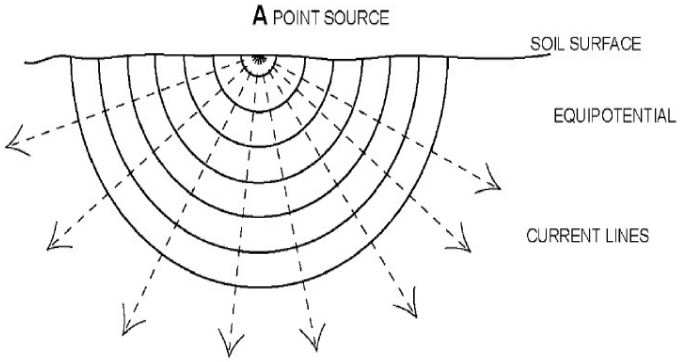

Figure 2:16 Distribution of current flow in a homogeneous soil (Samouëlian et al., 2005)

Four electrodes are required to compute the electrical resistivity. Electrodes A and B are known as current electrodes, and M and N are known as potential electrodes. The current is passed through A and B, and the potential difference is measured by M and N. Figure 2:17 shows the details;

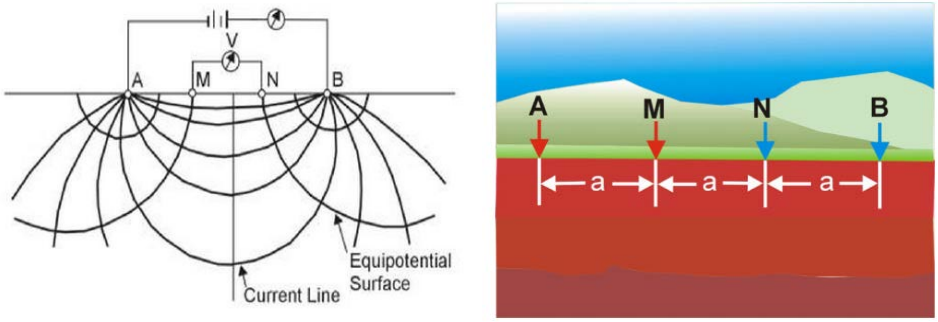

Figure 2:17 Equipotentials and current lines for a pair of current electrodes (Manzur, 2013)

Multi-Electrode System

A multi-electrode system is comprised of a large number of electrodes that are located along a line. It carries out an automatic switching of these electrodes to acquire profiling data. This technique, called resistivity imaging or electrical resistivity tomography (ERT), finds applications in the environment, groundwater, and civil engineering and archaeology fields.

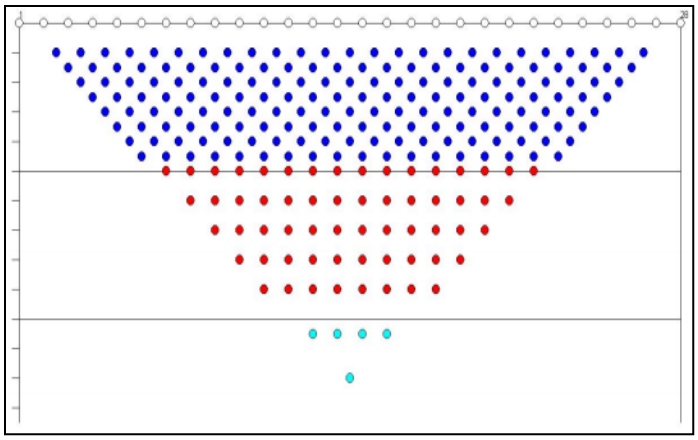

Figure 2:18 Multi-electrode system (Tabbagh et al., 2000)

Electrical Resistivity as a Function of Soil Properties

Electrical resistivity is a function of subsurface soil properties. The variables of the function are particle size distribution, mineralogy, voids, porosity, connectivity between the particles, degree of saturation, concentration of soluble minerals, temperature, etc. Typical ranges of electrical resistivity with soil properties are shown in the Figure 2:19 below.

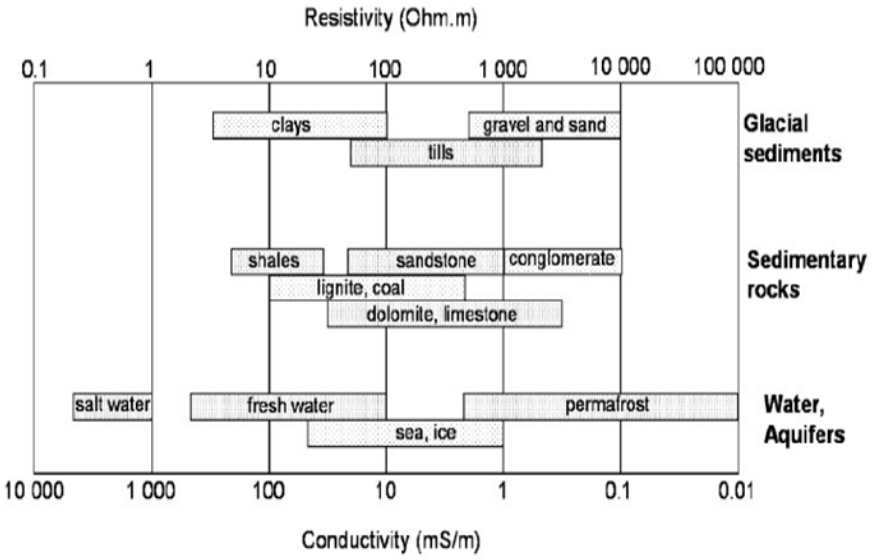

Figure 2:19 Typical range of electrical resistivity (Samouëlian et al., 2005)

PREVIOUS FIELD INSTRUMENTATION STUDIES

Baymon and Salem (2004) instrumented five sites in Ohio and monitored them for five years, from 1999-2003 (Figure 2:20). They reported monthly average moisture content with time. Seasonal variations were found in all of the sites; however, the value of the average moisture content was found to be dependent on the site soil condition. For example, the average moisture content of the Lewiston site was approximately 20% after two years of monitoring, whereas it was approximately 40% at the Pack River site. The authors plotted the average moisture over months, but there was some large time interval which might lead to not capturing the instant variation. The temperature variations reported over time were found to follow a perfect seasonal trend, which was essentially sinusoidal.

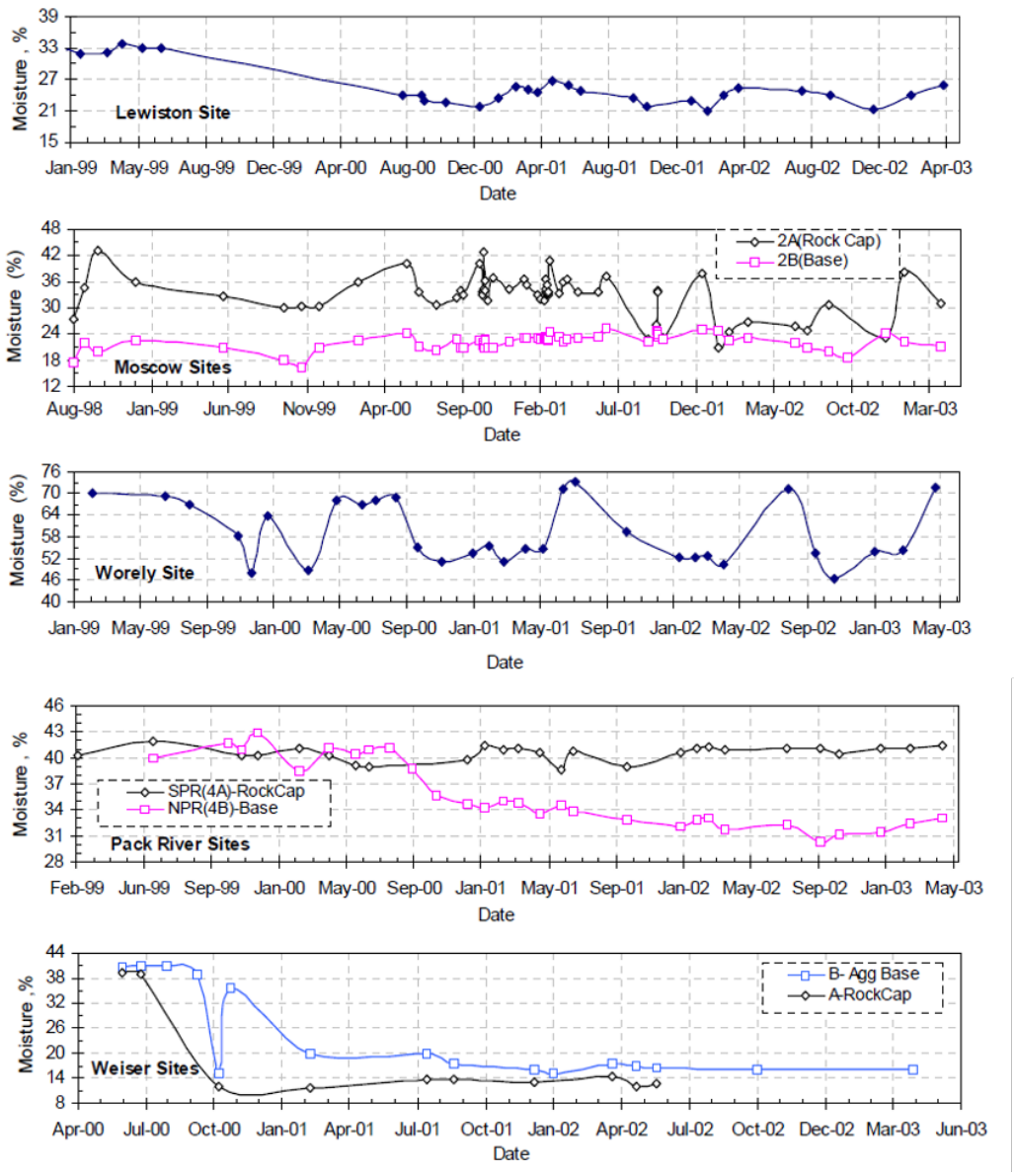

Figure 2:20 Long-term subgrade moisture content in Idaho, USA (Baymoy and Salem, 2004)

Fredlund et al. (2006) studied the effects of expansive soils on foundation slabs. They performed numerical modeling of variations of suction due to moisture flow and reported associated volumetric deformation. It was found that strengthening the slab did

not contribute to controlling the deformation of the foundation. The authors found up to 70 mm deformation at the edge of the slab. In other words, improved structural properties did not help to reduce the expansive soil problems.

Manosuthkij (2008) instrumented four sites in Texas with TDR sensors placed in the side slope of asphalt roads. He reported mean moisture content as the difference between the maximum and minimum moisture content of each month, and concluded that edge cracking might occur when the difference is greater than 20%. Edge cracking was reported after the summer (August and September), when all of the sensors indicated that the moisture variation was more than 20% (Figure 2:21). The author also reported suction values for that time period, which were found to be 1635 and 1098 kPa, respectively, and represented a dry condition, and hence the beginning of cracking at the slope. Wanyan et al. (2010) reported the moisture variation value as 15%, indicating susceptibility for edge cracking. None of the authors reported saturation values or temporary moisture increases in their studies.

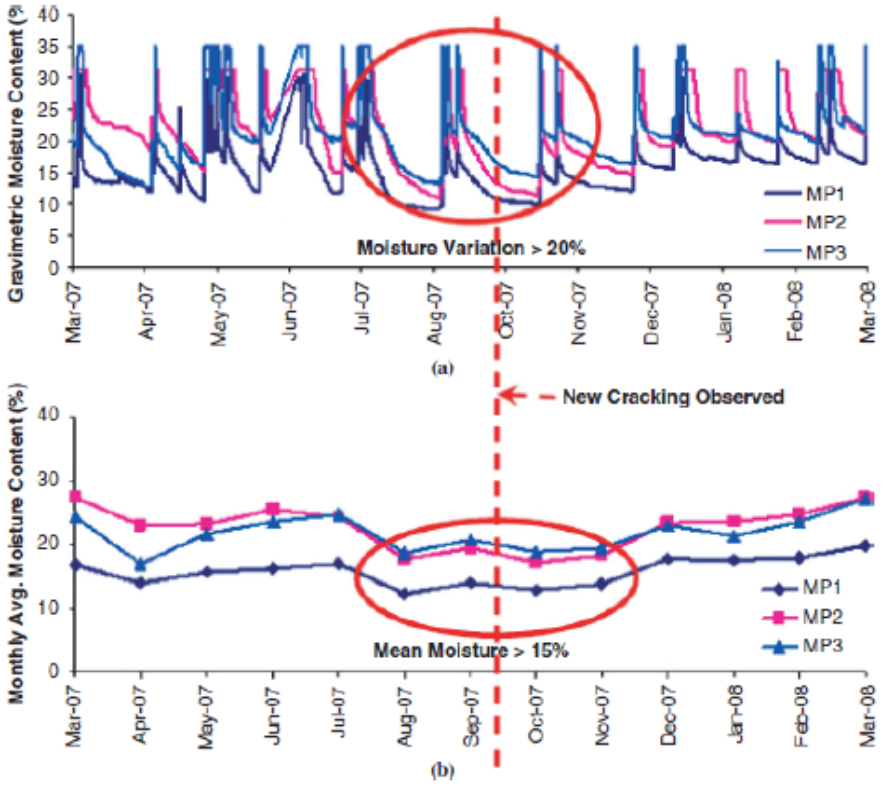

Figure 2:21 In- situ instrumentation results in Texas, USA (Manosuthikij, 2008)

A similar study was conducted in Canada by Nguyen et al. (2010) to monitor the suction variations under both driving lanes and side slopes, at different depths up to 2.2 m. The authors reported that the variation of suction in the soil is mainly a function of climatic conditions, i.e., precipitation and freezing temperatures, rather than soil properties and conditions. Strong sensitivity was recorded at shallower depths and side slopes. Suction variation was limited to 150 kPa under driving lanes, whereas variation as high as 800 kPa was found at the side slope (Figure 2:22). The authors tried to define the zone of suction variation which could cause distress to the pavement, but they did not report any surveying or similar deformation data over time for measuring the deformation.

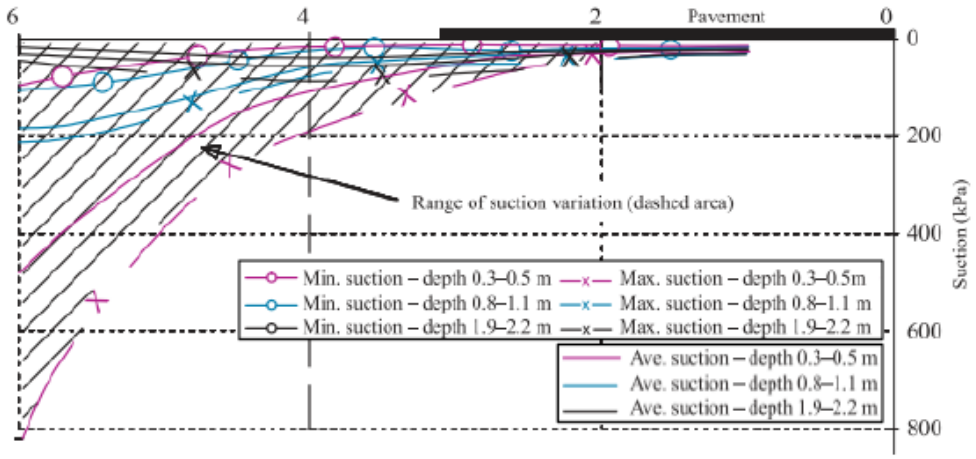

Figure 2:22 Suction variations beneath highway pavement in Canada (Nguyen et al., 2010)

In addition to the seasonal variations, temporary variations of suction due to precipitation were more pronounced in the shallower depths and side slopes (Figure 2:23). It was reported that suction is more sensitive to rainfall when the ground water table is stable and deep. Finally, it was concluded that more distress was observed at the pavement shoulder than at the pavement centerline.

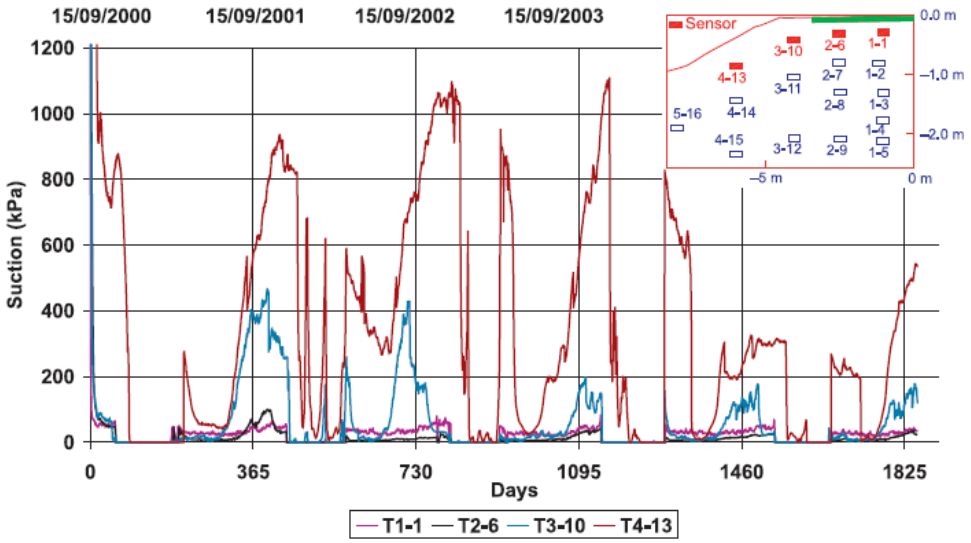

Figure 2:23 Temporary variations at side slopes and shallow depths in Canada (Nguyen et al., 2010)

Heydinger (2003) instrumented two sites in Ohio to monitor the moisture and temperature variations. Moisture data was collected 14 times a year; hence, the average variation was not the real time data with temporary variations. The author found that subgrade moisture had a seasonal pattern (Figure 2:24). However, sensors installed 2 inches from the surface showed the most variation and recorded temporary variations due to precipitation. It was concluded that developing a sinusoidal moisture variation model was independent of precipitation. The study further investigated the effect of moisture variations on changes in resilient modulus, but did not incorporate any deformation analysis.

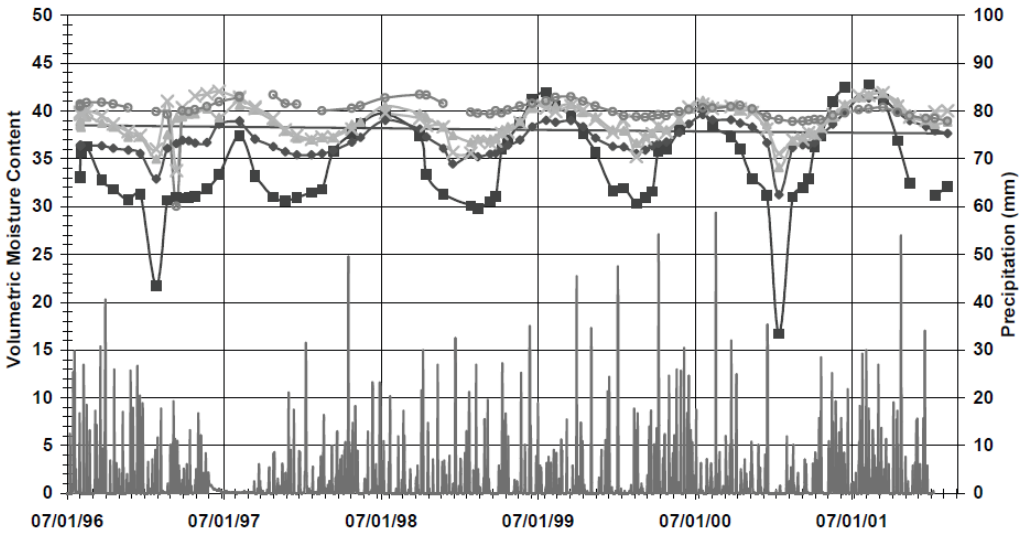

Figure 2:24 In-situ moisture measurements in Ohio, USA (Heydinger, 2003)

A study by Kodikara et al. (2014) included real time moisture variations. The authors monitored 23 sites in Melbourne, Australia for more than two years, up to a depth of 1500 mm. The study found immediate response after precipitation up to 550 mm of depth, whereas the moisture probes at deeper depths (greater than 550 mm) showed periodic variations. It was reported that moisture variations in deeper soil depend on the evaporation rate at the ground surface, meaning that there can be a lag time up to three or four months. The authors developed a real-time moisture model on the basis of 12 months' of data that defined the moisture variation as cyclic and following a first degree Fourier series trend. There was no rainfall input in the developed model. In other words, the model was developed based on the increase in moisture due to rainfall, which is applicable to a specific range of moisture values. The authors reported an increase in prediction accuracy with increasing depth; accuracy at shallower depths sometimes dropped below 60%. A sample predicted vs. measured moisture graph is presented in Figure 2:25.

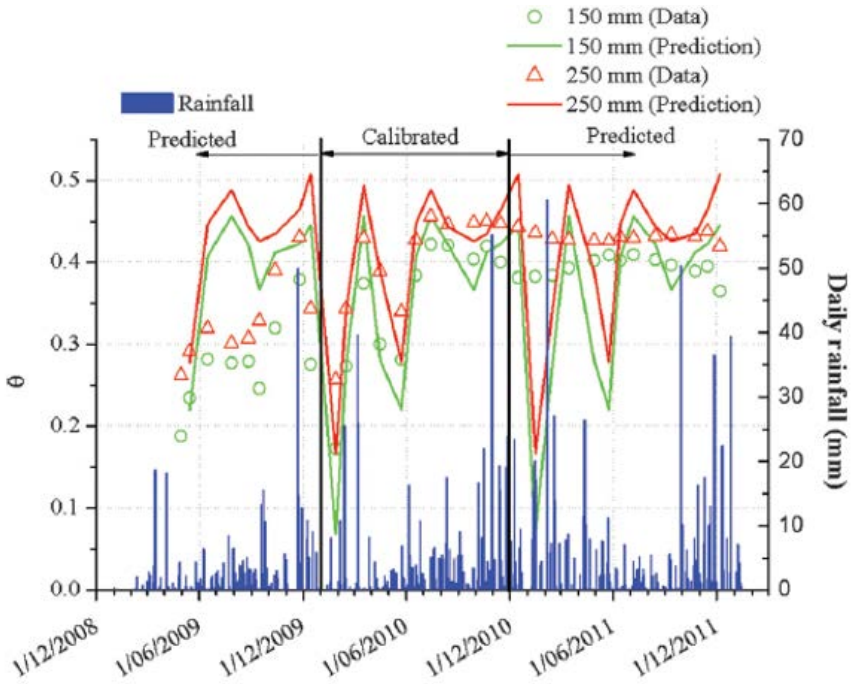

Figure 2:25 Measured vs. predicted data at different depths in Australia (Kodikara et al., 2014)

Clarke (2006) measured subgrade resistivity over a period of nine months at a site in Oklahoma, to determine the active zone, edge moisture variation distance, and long-term equilibrium moisture beneath the sites. The author also monitored the seasonal fluctuations of moisture at the edges (Figure 2:26). The study found the active zone to be 1.6 m, and most of the extreme changes at the surface diminished with depth.

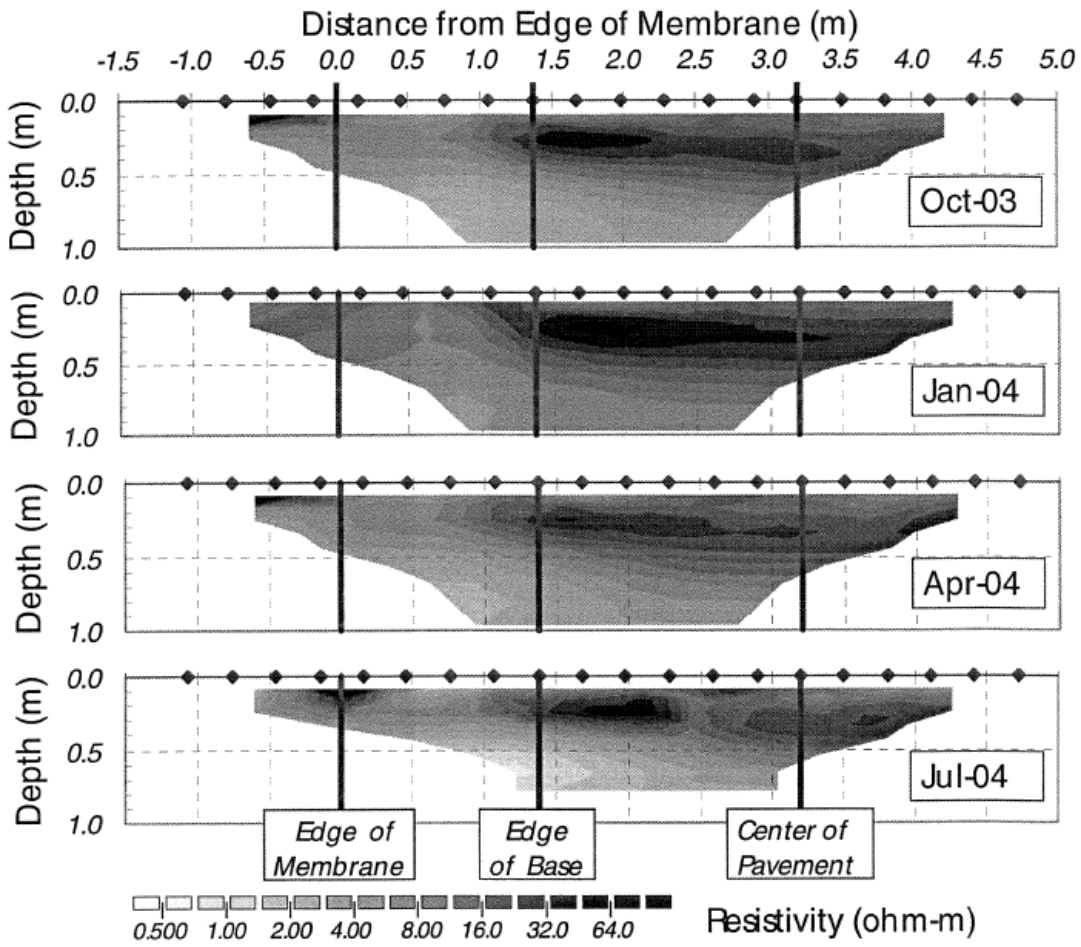

Figure 2:26 Resistivity values at 3-month intervals in pavement slope in Oklahoma, USA (Clarke, 2006)

As discussed earlier, swelling and shrinkage are the main problems associated with expansive soil. The depth to which this phenomenon occurs is referred to as active zone depth. Nelson et al. (2011) proposed a method for predicting the heave as a function of moisture infiltration. They conducted the study for residential homes, and reported that if the active zone is too large, an estimation of heave might be impractical. Talluri et al. (2011) concluded that a good match might be observed for volumetric

deformation if the active zone depth is confined to 2-3 ft. while using the suction-based methods. They also reported over-prediction of heave if the depth increases.

Rasul et al. (2015) monitored the moisture dynamics beneath a road system in Sweden, using electrical resistivity. The authors identified an obvious negative correlation between resistivity values and precipitation measurements and concluded that the road surface layers and the road shoulders exhibited high variations of resistivity. From this, the authors identified the road shoulders as important areas for moisture distribution and suggested a more frequent data acquisition schedule.

Extensive field instrumentation was carried out by Hossain (2012) at a highway slope in Dallas, Texas. The author used dielectric sensors to measure the variations of moisture and suction at different depths of a slope built on expansive clay. The variation of suction was found to be from 0 to 800 kPa during field monitoring. Moisture sensors were installed at different depths, i.e., 4 ft., 8 ft., 12 ft., and 20 ft. at crest, and at the middle of the slope. Higher variations were found up to 8 ft. of depth, very little variation was found at 12 ft., and no variation was observed at 20 ft. depth. The effects of rainfall intensity and duration were also included in the study. It was found that long-duration, low-intensity rainfall delayed the penetration of rainwater longer than high-intensity rainfall. Based on the swell test results and field monitoring for two years, the author concluded that the depth of the active zone in Texas is 3.2 m.

PAVEMENT STRESS ANALYSIS

Burmister (1943) performed the first closed-form solution for a two-layered, linearly elastic, half-space problem. The pavement stress analysis was later extended to a three-layered system. The pavement layers were considered as homogenous and linear elastic. The stress and strain obtained from the analysis were later compared against the failure criteria.

Huang (1993) later improved the assumptions of the elastic theory. The assumptions are: (i) layers are homogenous and isotropic; (ii) all layers are infinite laterally; (iii) all layers have finite thickness except for the subgrade, which is considered infinite; (iv) pavements are loaded statically; and (v) the compatibility of stress and strain is assumed to be satisfied at all layer interfaces.

Puppala et al. (2014) reported that matric suction exceeding 1500 kPa induces shrinkage cracking in the summer months. The authors only considered cracking that was caused by the shrinkage of the clay subgrade and determined the strain based on the gravimetric moisture content. Crack generation due to excessive tensile strain in the pavement was not considered. The difference in moisture content is defined as the difference between the amount of moisture after completion of the shrinkage test and the original moisture content. The authors found the following relationships:

$\epsilon_{sh, vert} = 0.23 \Delta w$

$\epsilon_{sh, vol} = 0.66 \Delta w$

where,

$\epsilon_{sh, vert}$ = vertical shrinkage strain

$\epsilon_{sh, vol}$ = volumetric shrinkage strain

Δw = variation of gravimetric moisture content

The authors also compared vertical swell strains with measured swell strains and other existing models. It was found that both the PVR and Lytton (2004) models provided predictions that lie below the field measurements.

LIMITATIONS OF PREVIOUS STUDIES

Previous studies have discussed the importance of accurately measuring volume changes caused by the expansive behavior of clay. In most of the cases, the studies were laboratory-based or with limited field instrumentation. For example, Heydinger

(2003) collected moisture data only 14 times a year, which can result in not capturing the instant variations of moisture. Replication of field behavior in the laboratory is complex; hence, a comprehensive study based on continuous field data is necessary. Real-time damage due to transient volume changes should always be addressed in pavement design. Therefore, it is essential to include climatic factors and their effect on the design process of pavement to improve the sustainability of structure.

ROAD CONDITIONS AND CLIMATIC EFFECTS

Shrinkage and heaving of soil are affected by the types of clay minerals present, state of soil compaction, environmental conditions, and site and road conditions. The variables dealing with soil are the most understood due to their ability to be tested in a laboratory environment. Environmental conditions are studied in various ways. The Thornthwaite moisture index parameter (commonly used in the United States) and equilibrium moisture index (commonly used in South America) are used to observe rainfall and evapotranspiration effects. These approaches both require other soil properties to determine suction. The suction properties are then used in the estimation of the swell properties. The current Thornthwaite index values should be reviewed and, if necessary, revised to account for global warming and other seasonal moisture variations.

Influence of Drainage Ditches on Expansive Soils

Expansive soil behavior can be influenced by drainage systems, including drainage ditches. Ponding can occur in poorly-designed ditches and raise subgrade saturation levels. The higher saturation levels can raise the swell magnitudes and can increase shrinkage movements. Therefore, pavement design should adequately consider the drainage ditches. Stallings (1999) reviewed ditches near pavements and evaluated their conditions. The impacts of moisture and matric suction changes in the subgrade soil were used to assess the drainage ditches in this research, using a similar methodology.

Influence of Trees on Expansive Soils

Vegetation interacts with the available moisture in subsoils, and volume changes and deformation result, which can influence swelling and shrinkage of soils. Soil moisture patterns are disrupted by moisture depletion through transpiration, shade levels, organic material buildup, precipitation runoff retardation, and water channel formation (Snethen, 2001). Maximum damage results from large trees in humid and arid climates (Snethen, 2001). Small trees, bushes, and grasses mostly affect moisture at shallow depths in arid and semi-arid regions. The effects of vegetation are influenced by number, size, location, and types of trees. Vegetation effects are generally unnoticeable during wet seasons, but dramatic effects can result during dry periods (Snethen, 2001).

Certain types of trees are known to dry out subgrade soil and cause cracking in pavements (Sillers et al., 2001; Jaksa et al., 2002). The potential influence of trees on pavement can be evaluated using the lateral distance from the trees and the height of plants. Current pavement design on high PI clays pulls from information related to the effect of vegetation on foundations. A safe planting distance with regard to trees was recommended by Ward (1953) in the United Kingdom. Bozozuk (1962) studied the drying settlements of elm trees. Large ground movements in the United Kingdom in the mid-1970s were linked to the drying effect of trees due to severe drought (Cameron, 2001). The widespread damage sparked many research efforts (e. g. Cutler and Richardson, 1981; Driscoll, 1983). Root system aggressiveness was studied in Australia (Baker, 1978). The depth and radius of drying was observed to depend on the species and on the drying effect of trees in open grasslands (Biddle, 1983, 2001). Tucker and Poor (1978) compared differential movements to distance and height ratios. Wesseldine (1982) researched the damaging effects of one species of tree in New Zealand, establishing a damage threshold of 0.75 D:H for single trees and 1.0 to 1.5 for groups of trees.

Climatic extremes may play a large role in causing and increasing damage to pavements and lightly-loaded structures (Snethen, 2001). The types and proximity of vegetation are particularly important to the severity of damage caused by the vegetation. The relative average rank analysis of multiple tree types reveals that poplar, elm, oak, and ash are the four most influential trees (Bryant et al., 2001). Experience and observations led to the establishment of guidelines for standard distances from trees to structures (Snethen, 2001). Soils that have liquid limits greater than 40 and plasticity indices greater than 25 may be particularly influenced by vegetation (Snethen, 2001). This research studies the influence of vegetation on soil moisture availability and matric suction.

REMEDIATION STRATEGIES FOR EXPANSIVE SOILS

Subgrade soil should be strong enough to prevent rutting and stiff enough to minimize resilient deflection. The practical load-carrying capacity of subgrade soils is difficult to evaluate due to the variety of soil types and seasonal variations. The selection of design-bearing values for clay subgrades is particularly difficult. Stabilization of foundation soils is one way to improve the bearing capacity (Raymond and Ismail, 2003).

Three methods are employed to combat the shrinking and swelling nature of subgrade soil (Rojas et al. 2006). They include replacing the expansive soil; stabilizing the soil with lime, cement, and/or fly ash; and using moisture barriers to prevent moisture content changes in the expansive soil. The first two can be lumped together as alteration of the soil, and the third is based on controlling the subgrade moisture (Jayatilaka and Lytton 1997). Replacing the subgrade soil in a pavement may not be feasible due to the volume of soil that would have to be replaced. Another method for controlling subgrade moisture involves pre-wetting the subgrade (Jayatilaka and Lytton 1997).

Puppala et al. (2011) studied the moisture content variations and soil suction associated with an expansive soil beneath pavements and estimated the surficial crack widths associated with changes in soil moisture content. They developed models that represented expansive soil shrinkage and swelling behavior in response to seasonal temperature variations, as well as moisture content changes. The authors suggested geosynthetic liners, compost-amended soil covers, and chemical treatments with additives as solutions to expansive subgrades.

Wanyan et al. (2014) presented a methodology for using the soil moisture content and soil properties to predict longitudinal pavement cracking. They concluded that the two most effective ways to improve the performance of pavement were to improve the soil's mechanical properties and reduce the soil moisture content variation. Pavement shoulders were seen as the starting point for pavement cracking, due to greater moisture variations and weaker pavement materials at this location. It was concluded that stronger pavement only delays the onset of problems related to expansive soil.

Dessouky et al. (2014) studied pavement repairs for low-volume pavements constructed over expansive soils and suggested that the problems associated with pavements constructed over soil with low-to-moderate plasticity can be solved with a combination of geogrid reinforcement and lime treatment. The study suggests a cement-treated base for areas with high-plasticity soil. They did not compare the results of this method with other possible methods.

Mahedi (2018) used cement and slab stabilization for expansive soil as a method of treatment. The author also conducted some non-destructive testing to evaluate the pavement condition due to expansive behavior of subgrade (Mahedi, Hossain, Faysal and Khan, 2017; Mahedi, Hossain, Faysal, Khan and Ahmed 2017)

Commonly-used remediation methods for expansive soils include treatment, replacement, overlaying structures, stability of moisture levels, and project relocation. The following sections describe the various remediation methods.

Admixture Stabilization

In admixture stabilization, liquids, slurries, or powders are mixed and blended with soil to improve soil strength and stiffness.

Lime

Lime stabilization is widely used to improve soil strength; improve resistance to fracture, fatigue, and permanent deformation; improve resilient properties; reduce swelling; and resist the damaging effects of moisture. Lime stabilization is most effective in moderate-to-high plastic soils (Little et al., 2000). Clays can either be modified or stabilized by lime (Little, 1999). In modification, calcium cations are exchanged, and the hydrated lime reacts with the clay mineral surface. Stabilization is characterized by a long-term pozzolanic reaction, in which calcium silicate hydrates and calcium aluminate hydrates react with aluminates and silicates from the clay mineral surface.

A lime mixture design protocol was developed by Little (1999), which included a selection of mineralogically-reactive soil or aggregate, establishment of an optimum lime content, and evaluation of resistance to moisture-induced damage through a capillary suction test. The addition of lime reduced the soil's swelling potential, liquid limit, plasticity index, and maximum dry density while increasing the optimum water content, shrinkage limit, and strength (Croft, 1967). The optimum addition of lime has been found to be 1% to 3% by weight (Bell 1996); however, lime is typically used in percentages between 2 and 8 in soil stabilization (Basma and Tuncer, 1991). Resistance to deformation and stability in pavement is dictated by the aggregate, soil, or stabilized layer shear strength (Little, 1999). Tensile strength properties can be approximated through

strength tests. The indirect tensile strength of lime-soil mixtures is approximately 0.13 times the unconfined compressive strength (Thompson, 1966). The flexural tensile strength of lime-soil mixtures is approximately 0.25 times the unconfined compressive strength (Chou, 1987).

The curing time for lime-and-lime-fly-ash-stabilized materials is much longer than that of Portland-cement-stabilized layers. The resilient properties of lime-soil mixtures are very sensitive to the level of compaction and molding moisture content. Lime stabilization may substantially increase shear and tensile strengths; however, the layer becomes more susceptible to load-induced tensile stresses. This can cause fatigue failure unless proper design steps are taken.

Cement

Cement can be used to effectively stabilize granular materials, silts, and clays; byproducts; and waste materials commonly used in pavement bases, subbases, and subgrade construction (Little, 2000). Coarse-grained soils are more effectively and economically stabilized with cement. It is difficult to mix cement with soils with a PI greater than 30. To combat this, the soil can first be treated with lime to reduce the PI and improve workability (Hicks, 2002). Cementitious links between the cement itself and the soil particles stabilize the soil (Croft, 1967). Clay soil benefits from reduced liquid limits, plasticity indices, and swelling potential, as well as increased shrinkage limits and shear strengths (Nelson and Miller, 1992). Types I/II and V cement stabilizers were studied for their effectiveness at treating sulfate-rich soils in Texas (Puppala et al., 2004). The study of these stabilizers indicated that the soil properties were significantly improved by the use of cement stabilization. A cement-stabilized and sand-based course material was studied in Georgia (Rollings et al., 1999).

Evaluation and Comparison of Stabilization Methods

The type of soil, environmental conditions, and drainage considerations influence the selection of the correct stabilizing agent (Figure 2:27). The particle size distribution and Atterberg limits are the main criteria in determining what stabilizing agent should be used with regards to soil type. Cementitious binders are preferred in wetter areas. Cohesive soils are well-suited for lime stabilization, as are silts, if pozzolan is added. The suitability of using a stabilizer for enhancing strength and reducing swell potential of expansive, sulfate-rich soils was evaluated by Puppala et al., 2003. The stabilizers in this study, in order of decreasing effectiveness, were sulfate-resistant cement, lime mixed with fibers, ground granulated blast furnace slag (GGBFS), and Class F fly ash.

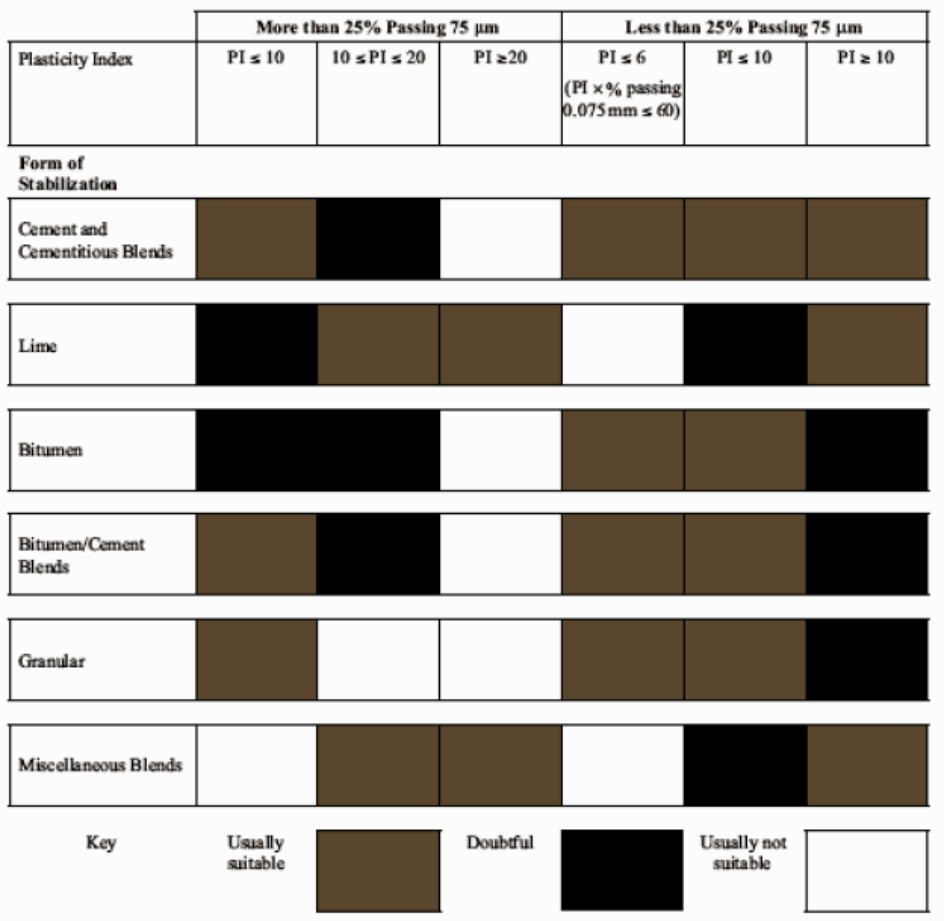

Figure 2:27 Guides to select stabilization method (Hicks, 2002)

Al-Rawas et al. (2005) studied the effects of lime, cement, and combinations of both on the swelling potentials of expansive soil. By adding a single stabilizer, the swelling potential increased and then decreased. With a combination of both, the potential decreased and then increased. All the stabilizers reduced the shrink and swell potential of the expansive soils.

Kota et al. (1996) suggested doubling the application of lime, using low calcium or non-calcium stabilizers and geotextile or geogrid reinforcement, stabilizing the top with non-sulfate fill, pretreating with barium compounds, and stabilizing asphalt with sulfate-

bearing or compact soils to lower densities and minimize the damages caused by sulfates and calcium-based stabilizers.

Moisture Control

The M-E Design Guide recommends using full-width paving to eliminate the lane/shoulder cold joint, which is a major source of water infiltration in the pavement structure of conventional and deep-strength HMA pavements. The guide also recommends inserting a granular layer between the subgrade and base course to reduce erosion, allow bottom seepage, and minimize frost susceptibility that could increase pavement roughness, providing for adequate side ditches with flow lines beneath the pavement structure; placing the edge drains under the shoulder at shallower depths; and installing drains deeper than 3 feet (1.0 meter), for groundwater problems.

Table 2:3 AASHTO definitions for pavement drainage levels (AASHTO, 2004)

Quality of Drainage	**Water Removal Within**
Excellent	2 hours
Good	1 day
Fair	1 week
Poor	1 month
Very Poor	No drainage

Huang (1993) provided the definitions corresponding to various drainage levels from pavement structures in Table 2:3. Excellent drainage removes water within two hours, and very poor drainage provides no water removal.

Moisture Barriers

Horizontal Moisture Barriers

Horizontal moisture barriers stop water from penetrating pavements. A smaller variance in moisture in the soil leads to fewer swelling and cracks in the pavement and reduces the road roughness. Browning (1999) concluded that horizontal moisture barriers do not reduce moisture variance or provide smoother pavement.

Vertical Moisture Barriers

Vertical moisture barriers have been used across the United States to control expansive subgrade soils. According to Jayatilaka et al. (1993), the sites in wet and semi-arid climates with cracked soils and shallow root zones benefit most from vertical moisture barriers.

The first vertical moisture barrier was used in San Antonio, Texas on IH-40 in 1978 (Steinberg, 1992). Vertical moisture barriers stop the lateral migration of moisture in the subgrade, which prevents swelling and shrinkage during wet and dry periods (Picornell and Lytton, 1986). They are expensive and complicated to construct. Deeper barriers (8 feet) are better than shallow barriers (6 feet) because they maintain constant moisture and reduce vertical movement, but they are more expensive (Gay and Lytton, 1998). Therefore, vertical moisture barriers are only used on major highways.

Evans and McManus (1999) found that moisture barriers in the United States were too expensive and had many disadvantages for low-volumes roads. They provide easy paths for moisture and cause deep swelling, and can also act as storage reservoirs in flat terrain with poor drainage. They developed an economical method for low-volume roads – a spray-on seal surface for a subgrade in Australia. Evans and McManus's method includes equipment to make a deep and narrow trench, install plastic sheeting, and put cementitious backfill in the trench. This new barrier costs $3.10 per lineal foot.

Figure 2:28 shows Evans and McManus's method for install plastic sheeting into the trench without damaging it.

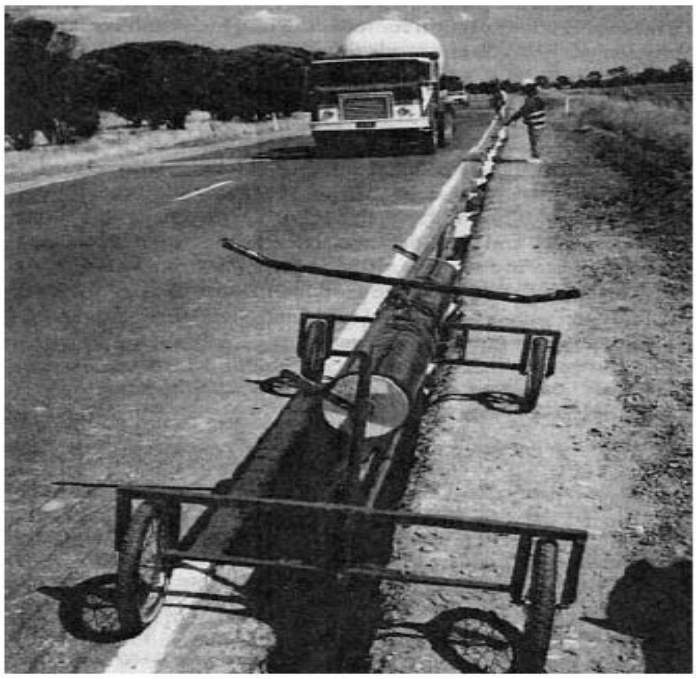

Figure 2:28 Installation of plastic sheet into the trench (Evans and McManus, 1999)

Drainage Improvement

Subsurface drainage is recommended by the M-E Design Guide to lower the ground water level, intercept the lateral flow of subsurface water beneath the pavement structure, and remove the water that infiltrates the pavement's surface. Special solutions should be considered, when possible, such as placing a permeable layer over swelling soil to keep it stable and saturated when the climate is suitable (Department of the Army, 1983).

Rollings and Christie (2002) found a lack of drainage leads to problems in collapsible and expansive subgrade soils, such as water ponding, soft spots, and the

presence of plants in the drainage ditches. They recommended lining drainage ditches with asphalt and gravel to prevent leakage and installing cross drains throughout the median so the water drains to the side of the roadway.

Geosynthetics

A layer of geosynthetic material forces the potential bearing capacity to higher shear strength surfaces and absorbs additional shear stresses. During rutting, the geosynthetic material distorts and exerts upward force, supporting load and adding carrying capacity (Hufenus et al, 2006). Geosynthetics are not used in flexible pavement design because of uncertainties and the lack of an accepted design technique.

The eight types of geosynthetics, geotextiles, geogrids, geonets, geomembranes, geosynthetic clay lines, geopipe, geofoam, and geocomposites (Koerner, 2005) are shown in Figure 2:29. Geotextiles and geogrids are the most popular. Geotextiles are made of woven, non-woven, or knitted synthetic fiber fabric. Geogrids are plastics formed into a grid-like configuration. Geofoams are lightweight foam blocks that can provide lightweight fill. Geocomposites consist of a combination of geotextiles, geogrids, and/or other geosynthetics in a factory-fabricated unit.

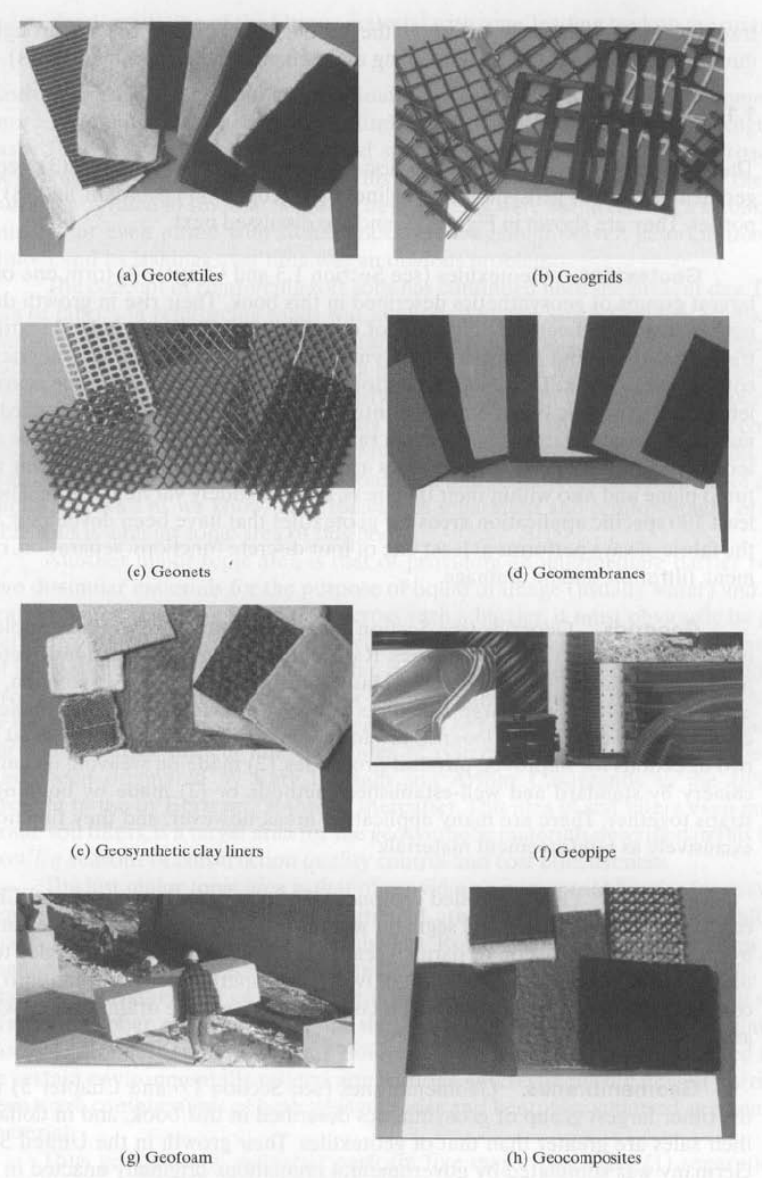

Figure 2:29 Different types of geosynthetics (Koerner, 2005)

Geogrids have higher tensile strengths than geotextiles and should be used on weak subgrades with CBR values less than three (Tutumluer et al., 2005). According to the SpectraPave2™ analysis results, the use of geogrids can effectively reduce the aggregate thickness requirements. Geogrids with higher tensile strength and high

aperture stability moduli give overall higher geosynthetic stiffness and perform better than geotextiles (Giroud and Han, 2004a, b). Geogrids were first used for the reinforcement of pavement in London, England in 1982 to control reflective cracking; they are becoming more common (Austin and Gilchrist, 1996).

Grout columns or cutoff walls and geomembranes are used as vertical moisture barriers. They are expensive, but maintain uniform moisture in the barrier. Geomembranes were tested in San Antonio, Texas and it was concluded that they have the potential to check moisture variations (Steinberg, 1992).

TxDOT studies show that fiber-rich compost can lead to less cracking in shoulders due to the fiber interlock that maintains moisture levels. It has been well established that stabilization methods such as lime, cement, and fly ash reduce heaving in expansive soils. Sulfate-resistant cement, combined lime-fiber, and GGBF treatments are being explored because of the number of soluble sulfates in the soil (Puppala et. al, 2003)

Other Remediation Methods

Deep Dynamic Compaction

Compaction should occur at higher moisture contents because it reduces the swell and swell pressure (Mowafy et al, 1985). Deep dynamic compaction maximizes the density of soil, but only temporarily, due to infiltration.

Rollins and Christie (2002) concluded that the bumps, cracks, and edge failures of pavement are caused by problems in the subgrade soil such as collapsible, expansive, and compressible soil; poorly-compacted fill; and poor drainage. Deep dynamic compaction was recommended for zones with collapsible soils since the soils extended to 20 feet below the ground surface, and it is the most economical method (approximately $1 to $1.20 square foot of surface area).

A combination of methods was recommended for expansive soils. First, a 3-ft. excavation of the expansive material and recompaction with the same soil treated with 5% lime was recommended, to reduce the plasticity of the clay (from PI of 70 in untreated to 17 in treated soils) and increase the CBR (from about 5 in untreated to 50 in treated soils). Second, it was recommended that a continuous rubber asphalt layer, covered with a six-inch layer of soil, be installed under the drainage ditches on either side of the interstate, to prevent infiltration into the subgrade. Finally, they recommended placing the base courses above the liner and using an asphalt-wearing surface to minimize the potential for cracking.

Undercut and Backfill

The Highway Subgrade Stability Manual from the Illinois DOT suggests undercutting and backfilling for soft subgrades. The method either covers the subgrade with a thick layer of granular material, or removes a portion of the subgrade and replaces it with the granular material. It is simple, inexpensive, and can be used on a large scale (Thompson, 1982). Ahlvin (1962) used Equation 8 to find the required depth of granular material:

$$t = F\left[P\left(\frac{1}{8.1CBR} - \frac{1}{p\pi}\right)\right]^{1/2}$$

Where

t = Thickness of material layer required in inches

P = Single or equivalent single wheel load in pounds

CBR = CBR of underlying subgrade soil

P = Tire contact pressure, psi

F = 0.23logC + 0.15

C = Number of load repetitions

Decreasing Clay Content

Mowafy et al. (1985) concluded that decreasing the clay content can reduce the swelling potential. They contended that there is a “critical” clay content, where the amount of swell is zero, and that below that value, the soil will shrink and above the value, it will swell. To achieve “critical” clay content, clay soils can be mixed with coarse fractions of granular materials in the field.

Waterbound Macadam Base

Waterbound macadem is a single-sized coarse aggregate that was widely used in South Africa in the 40s and 50s. It was placed and then compacted on a subbase and filled with fines, and then further compacted and slushed (Horak, 1983). The roads with waterbound macadem have withstood heavy traffic, provided drainage, and have high shear force resistance due to granular interlock (Horack and Triebel, 1986). For it to be successful, the granular layer must be thick enough and the backfill material must be able to limit rutting (Thompson, 1982).

USE OF GEOSYNTHEICS BY TXDOT AND RECENT STUDY IN USA

Moisture barriers are used to prevent moisture from intruding into subgrade soils. Some moisture barriers are made of geosynthetics, which are primarily used in pavements for separation, reinforcement, and drainage (Barksdale et al. 1989).

The Texas State Department of Highways and Public Transportation placed a horizontal geomembrane in one test location and vertical geomembranes in eleven test locations (Steinberg 1989). The vertical geomembranes were deep vertical moisture barriers. The twelve sites were continuously monitored. The results of the study suggest that deep vertical moisture barriers can help pavement serviceability and may be cost-effective. Lower maintenance costs were associated with the test sections. However, pavement cracking in the outer lanes and reduced serviceability over time were both

observed. The study concluded that the deep vertical fabric moisture barrier effectively countered the effect of expansive soil on the pavement. However, they are not widely used because of their cost and difficult construction. A typical cross section of a pavement using a vertical moisture barrier is shown in Figure 2:30.

The first vertical moisture barrier was used on Highway Loop 410 in 1979, and the second one was used on Highway 37 the next year (Steinberg 1981). These sites experienced less roughness over time compared to the sections without a vertical moisture barrier (Steinberg, 1985).

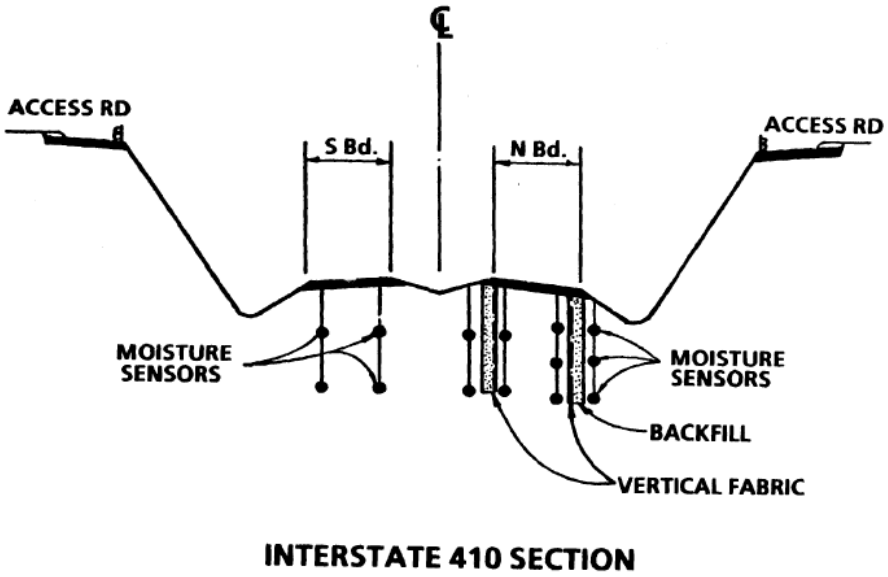

Figure 2:30 Interstate 410 Section with vertical moisture barrier (Steinberg, 1989)

After these sites showed improvement, many other pavements had vertical moisture barriers installed, as reported by Steinberg (1980; 1985; 1989; 1992). Again, the construction difficulties came into the picture, and edge cracks reappeared within years. Such a crack is shown in Figure 2:31. As the installation was deeper (at least 2.4m in

most of the cases), the backfilling of the trench was a crucial criteria. If the backfilling was not done in a proper manner, it acted as a passage for moisture intrusion.

Figure 2:31 Crack at pavement edge after installing vertical barrier (Steinberg, 1989)

Picomell et al. (1984) studied the effectiveness of the moisture barrier on Highway 37. The moisture was evaluated on the inside of the barrier; the roughness of the pavement was also measured. The moisture in the soil was found to remain constant with the installation of the moisture barrier. Bump height and serviceability were also evaluated in the different sections. It was concluded that the moisture barriers controlled the roughness of the pavement.

Gay (1994) studied the development of roughness on pavements and found the moisture barriers to be effective in reducing it. Jayatilaka et al. (1993) found that moisture barriers were only effective when medium-cracked soils were present in the subgrade. They also found that even if these medium-cracked soils were present, in semi-arid and extremely dry conditions, the moisture barriers were ineffective.

Most of the moisture barriers in Texas are installed to a depth of 2.4 meters. Picomell et al. (1987) developed a procedure to find the appropriate depth for moisture barriers, based on the climate and characteristics of the subsoil. Two assumptions were made for this procedure. If the soil is very desiccated, the barrier will prevent water from reaching the shrinkage crack fabric. If the soil is very wet, the barrier will prevent excessive drying of the soil under the edges of the pavement.

The worst condition considered for the design of a pavement is the worst drought possible for a site. This can be found with meteorological data and by using a return period equal to the design life of a pavement. Rainfall runs off to the ground that is between the shoulder and the drainage ditch, because pavements are impermeable, and can infiltrate the subsoil. A rainfall multiplying factor (RMF) that varies from 1 to 5, based on the width of the pavement and the soil profile adjacent to the edge of the pavement, can be used to compute the amount of excess rainfall. The finite element method was used to model the moisture flow and analyze the nonlinear elastic deformation of the soil.

This procedure determines the depth of the moisture barrier, using edge distortion and maximum crack depth criterion. Using the edge crack criterion, the barrier depth is determined as the smallest depth that maintains an angular distortion of 1/360 or less at the edge of the pavement. Using the maximum crack criterion, the depth of the barrier is determined as the largest depth of the crack expected with the hydraulic regime imposed on the pavement or the existing crack depth. Picornell suggests that the edge distortion criterion be used if the initial conditions are at equilibrium condition or wetter, and the crack depth criterion be used if the conditions are less than equilibrium. Picornell and Lytton (1987) suggested that the barrier should go to the depth of the roots to stop longitudinal cracks, and 25 percent deeper to stop the development of roughness.

Abd Rahim and Picornell (1989) developed a computer program to predict the behavior of different barrier types. They considered the subsoil as being divided into different-sized parallelepipeds, with moisture movement only through the cracks between the soil blocks. The program performs a water balance for the soils on the side of and underneath the pavement. Trial runs of the program showed that the moisture barrier can cause faster swelling of the soils under the pavement if the pavement has cracks that allow infiltration into the soil. The program requires information about the size of the soil blocks to form the shrinkage crack fabric, and this data is not readily available in literature for typical subsoil conditions in Texas.

Chen and Bulut (2015) studied the effect of moisture intrusion into the subgrade soil through the unprotected outside area of a pavement with vertical moisture barriers. Cracks began in the outside area and moved toward the pavement. In addition, this study found that cracks in the outside area led to reduced benefit from the vertical moisture barriers; they were found to be effective only to a certain degree. At some point, the depth of the outside cracks may completely counteract the effect of the vertical moisture barrier; therefore, it was suggested that a horizontal moisture barrier should be used. The whole study was conducted in a numerical environment, using Abaqus.

Vertical moisture barriers were employed by the Texas Department of Transportation, beginning in the mid-1990s, when expansive clays required repeated maintenance work (Jayatilaka and Lytton 1997). Vertical moisture barriers were able to reduce the development of pavement roughness, with deeper barriers being more effective, but the construction costs were high, and difficulties were experienced. Jayatilaka and Lytton's study established that maximum vertical movement due to expansive soils occurs at the edges of pavement.

Al-Qadi et al. (2004) studied the effectiveness of a geomembrane as a moisture barrier underneath the Virginia Smart Road. Ground-penetrating radar (GPR) and time-domain reflectometry were utilized. Two (2) mm thick low modulus polyvinyl chloride (PVC) was sandwiched between a nonwoven polyester geotextile to work as a moisture barrier. The typical cross section is shown in Figure 2:32.

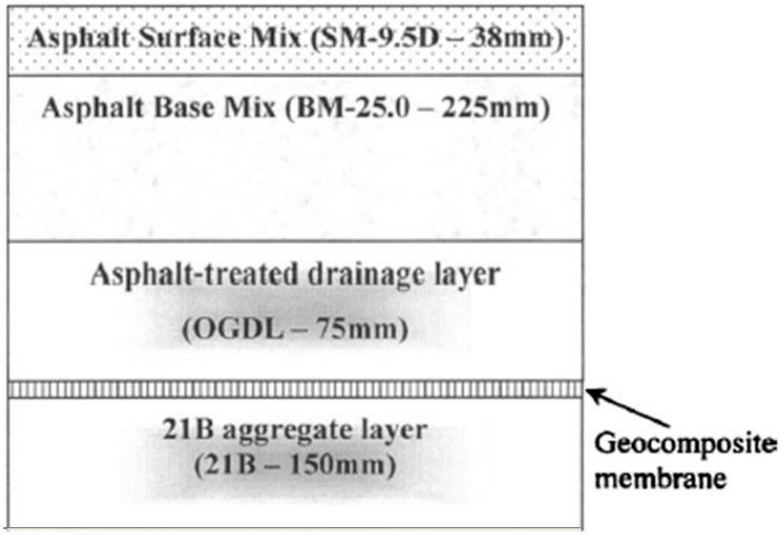

Figure 2:32 Typical cross section for moisture barrier (Qadi et al., 2004)

The authors concluded that the barrier effectively reduced the amount of water that was able to reach the subgrade soil. A 30% reduction in moisture accumulation was reported in the soil a few days after rainfall. Precipitation was shown to have little effect on the layers of soil underneath the moisture barrier, as depicted in Figure 2:33. The barrier was installed during the construction phase of the road.

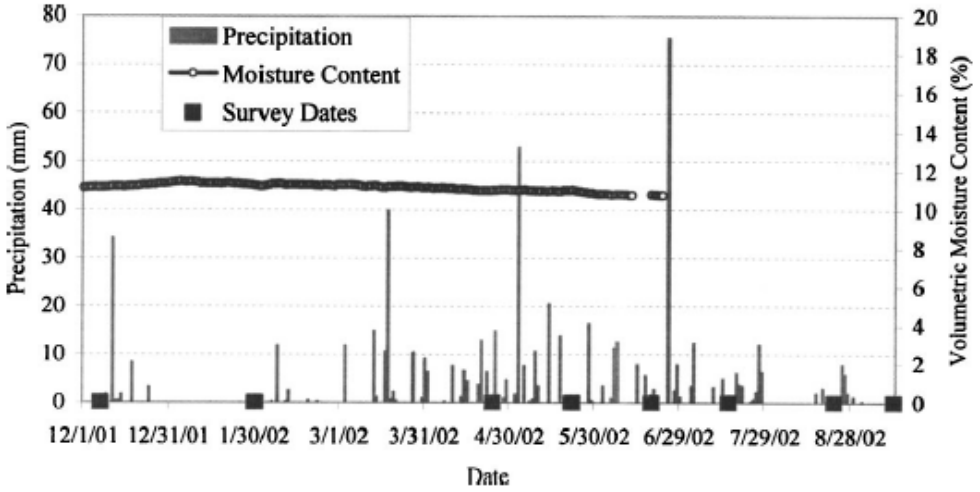

Figure 2:33 Base-layer moisture content measured by TDR under moisture barrier (Qadi et al, 2004)

Henry and Barna (2002) studied the application of a geocomposite capillary barrier drain (GCBD) installed beneath the base and subgrade of a pavement structure. The authors concluded that the GCBD was able to protect the subgrade from moisture. The study used expensive materials, but suggested the use of less expensive materials for further investigation.

Christopher et al. (2000) tested the potential use of horizontal moisture barriers to control the drainage in different types of pavements in Maine (Figure 2:34). The authors used a special geocomposite, comprised of geotextiles and geonets, and installed them during the road's construction phase. It was reportedly successful in draining water and preventing it from entering the subgrade; however, the system required a separate drainage collection system with perforated pipes, which increased the complexity of the construction.

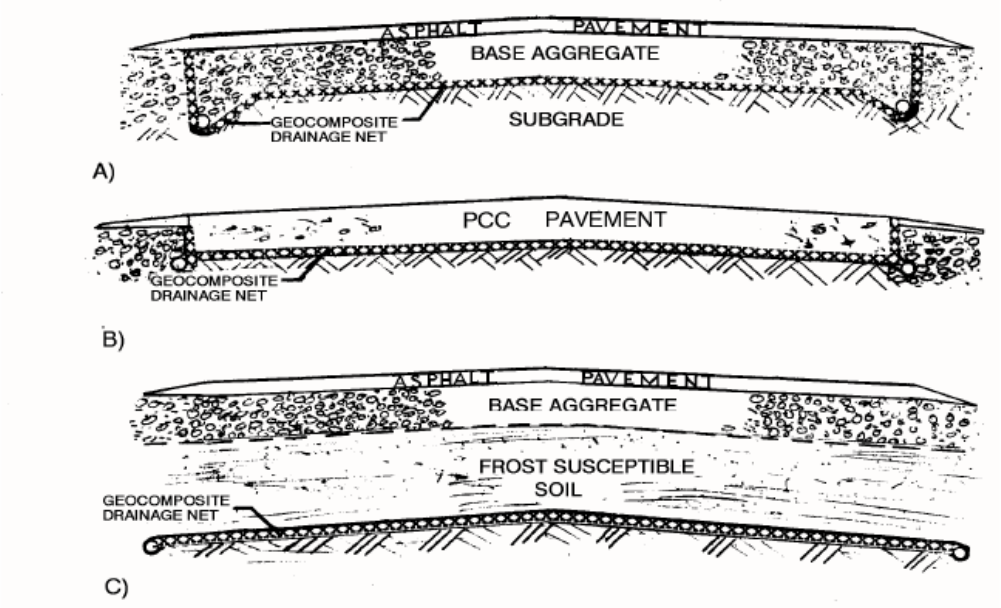

Figure 2:34 Potential use of horizontal geocomposite drainage layers (Christopher et al. 2000)

CHAPTER 3

REAL-TIME MOISTURE AND TEMPERATURE MODELING IN EXPANSIVE SUBGRADES IN TEXAS

Ahmed, A.[1], Hossain, M.S.[2]

[1]Graduate Research Assistant, Department of Civil Engineering, The University of Texas at Arlington, 416 Yates Street, NH 119, TX 76019; Email: asif.ahmed0@mavs.uta.edu

[2]Professor, Department of Civil Engineering, The University of Texas at Arlington, 416 Yates Street, NH 404, TX 76019; Email: hossain@uta.edu

(Part of this paper has been submitted to 97th Annual Meeting of Transportation Research Board, Submission ID: 18-04285)

ABSTRACT

Moisture and temperature variations significantly influence the strength and stiffness of expansive subgrade soils, shortening the service lives of pavements built on such soils and increasing the associated maintenance costs. Accurate measurements of soil moisture and temperature can be obtained through soil sampling and testing; however, this process can be extensive and costly. Thus, developing models that can accurately predict the moisture variations and temperature profile in an expansive subgrade becomes of great interest. The objective of the current study is to develop moisture and temperature models, using real-time field monitoring data from two hot mix asphalt roads in North Texas. Collected data was analyzed in a statistical environment to solve two first degree Fourier series. Based on the collected data, the first solution produced a moisture variation model that captured both variations due to seasonal effects and temporary variations due to rainfall. The outputs of this model were within 90% of the values measured on-site. The second solution produced a temperature prediction model that was dependent on depth and the day of the year. The squared correlation coefficient

between the observed and predicted soil temperature was more than 0.90. Application of the developed models could allow for a non-invasive estimation of the response of soil strength and stiffness properties due to variations in moisture and temperature.

INTRODUCTION

Expansive soil is a worldwide problem and accounts for approximately 25% of the soil in the United States alone (Nelson and Miller 1992, Buhler and Cerato 2007). Volume changes of these soils occur due to adsorption or desorption of moisture, leading to cyclic swelling and shrinkage. On average, expansive soils incur more financial losses to the nation's infrastructure than earthquakes, floods, hurricanes, and tornadoes combined (Puppala et al. 2011). Nelson and Miller (1992) estimated that 9 billion USD of damages are directly related to expansive soil problems annually, while Jones and Jefferson (2012) calculated a total financial loss of 15 billion USD. Statewide, the Texas Department of Transportation (TxDOT) spends 25% of its annual expense budget on maintenance and repair of damaged pavements (Sebesta, 2002). Addressing the effects of expansive subgrade soils in both design and construction stages could reduce future maintenance costs and extend the service lives of pavement systems.

The strength and performance of a pavement built on an expansive subgrade are most influenced by temperature and moisture (Lytton, 1988). Hedayati (2014) reported moisture content variation as the prime cause of subgrade deformation in expansive soil, which typically induces pavement cracking. Fluctuations in moisture content are influenced by the pavement subgrade compaction site, environmental site conditions, location of roadside trees, and the presence of nearby drainage ditches (Puppala, 2011). Moisture variation causes significant changes in the shear strength, resilient modulus, and permeability of subgrade soil (Fredlund et al., 2012, Khoury, et al., 2012). It also affects the hydraulic conductivity, shear strength, chemical diffusivity, specific heat, and

thermal conductivity of a soil (Lu, 2015). The success or failure of a pavement system is dependent on the support provided by subgrade layers. An increase in moisture content has been shown to decrease the resilient modulus, which quantifies the support that the subgrade can offer (Mehrota, 2013).

Researchers have developed different subgrade moisture prediction models over the years. They ranged from simple to complex in nature, i.e., single input of soil property to statistical and numerical modeling. For example, Swanberg et al. (1946) estimated moisture variation from only plastic limit value. To categorize subgrade and climatic conditions, some studies (Russam 1965, Thornthwaite 1948) subdivided geographic areas into regions with a specific index, referred to as Thorntwaite's Moisture Index (TMI). With the advancement of technology, researchers have incorporated complex mathematical relationships between soil properties and environmental conditions to predict moisture variations. Currently, the Mechanistic-Empirical Pavement Design Guide (MEPDG) recommends using the enhanced integrated climatic model (EICM) to predict moisture changes (Zapata and Houston, 2008).

Other moisture variation estimation methods include soil sampling at regular time intervals (Zhang and Briaud, 2010), assuming seasonal variations or constant equilibrium moisture content several years after construction (Zapata and Houston, 2008). Hall et al. (1999) estimated upper and lower equilibrium moisture content of specific sites rather than predicting the real-time variations. Recent research has incorporated numerical modeling. For example, Abed (2007) used 2D PLAXFLOW analysis to examine the swelling and shrinkage behavior of expansive soil due to moisture variation. Puppala et al. (2014) performed 3D static analysis in Abaqus to study the swelling behavior.

Irrespective of developed methods from soil properties or computational techniques, neither can accommodate the temporary moisture variations due to rainfall.

Various field studies have reported that, following rainfall, the increase in moisture content can be up to 20% in amplitude from the baseline moisture content (Nguyen et al., 2010, Hedayati et al., 2014, Hossain et al., 2016). Hedayati (2015) reported that this additional increase in moisture can severely deteriorate the pavement structure, a matter which is overlooked in the current models. Therefore, to reflect the real-time scenario, it is necessary to develop a moisture prediction model that incorporates both seasonal and temporary variations.

Temperature variations also play an important role in the behavior of expansive subgrade soils. For instance, temperature gradients in the subgrade can result in moisture flow (Vaswani 1975). Additionally, some soils have displayed changes in maximum compacted density, optimum moisture content, shear strength, liquid and plastic limits, and hydraulic conductivity as a result of a change in temperature (Winterkorn et al. 1972, Romero et al. 2001). Since experimental results have asserted that increasing temperatures weaken clay (Kuntiwattanakul 1995), it can be concluded that temperature has an effect on the performance of clayey soil. In the case of low-volume roads, the asphaltic layer, whose stiffness decreases with increasing temperature, serves more as a surface seal than as the main load-carrying component. Therefore, the behavior of the subgrade layer in response to variations in temperature is of great interest (Lytton 1988).

Apart from moisture and temperature, a variety of factors can influence the shrink-swell behavior of expansive subgrades, including the plasticity and suction of the soil, surrounding vegetation, and the presence of nearby drainage ditches (Puppala et al. 2011). Among such influences, the moisture variations and temperature profile of the soil are typically the determining factors for the performance of a pavement system built on an expansive subgrade. While moisture content can accurately be measured, soil

sampling and the consequent required testing can be a lengthy, destructive, and expensive process (Kodikara et al. 2014). The lack of site-specific temperature data poses another problem when considering the effects of temperature on the behavior of soil (Lei et al. 2011). The objective of the current study is to develop moisture and temperature models, using real-time field monitoring data from two hot mix asphalt roads in North Texas. The sites were instrumented with Time Domain Reflectometry (TDR) sensors to record the hourly moisture and temperature variations. After monitoring for two years, collected data was analyzed in a statistical environment to develop temperature and moisture prediction models, incorporating both seasonal and sudden increases due to climatic factors. In addition, the predicted models were compared against the measured values at the current study sites. Finally, the developed model was checked against a previous study to verify its accuracy.

METHODOLOGY

Site Selection

A study was performed to determine the causes of roadway cracking and provide possible remedial measures. Two sites were selected, based on the recommendations of the Texas Department of Transportation (TxDOT) engineers. The first site, 1.80 miles of of frontage road, is located at the intersection of FM 2757 and I20, on a two-lane, rural, hot mix asphalt pavement in Kaufman County, Texas. The second site is located on State Highway 342 in Red Oak, Ellis county, Texas.

Several structural distresses were observed on the roadway during the initial field investigations. The site had experienced continuous edge and surficial cracks, as well as bumps, punch-outs, and surface unevenness. Edge cracks of up to 3 inches width and several feet long were observed. In some cases, the depth of crack was more than 1 foot,

which resulted in complete separation of the edge from the pavement structure, as shown in Figure 3:1.

Figure 3:1 Distress condition in pavements

Site Description

The test site in Kaufman County was located on a farm-to-market road identified as FM 2757 in Forney, Texas. The low-volume road consisted of two lanes, each measuring 11 ft. wide, with no shoulder. The side slopes on both sides were covered with grass and dense trees. Small bodies of water were present to both the east and the west of the road. Movement of moisture from the bodies of water could contribute to moisture content variations in the soil underneath the pavement. Edge cracks of 3 inches in thickness penetrated 12 inches, and other surficial pavement distresses indicated the presence of expansive subgrade soil and intrusion of rainwater.

The SH 342 test site was situated in Lancaster, Texas, on the border of Dallas County and Ellis County. Each of the two lanes were 11 ft. wide, and an 11 ft. shoulder was present on each side of the road. The pavement was fairly level with the ground and was flanked by grass and dense trees on both sides. To the west, a rail line ran parallel to the roadway. Further northeast, the road overpassed Bear Creek, while a residential

area was located a short distance to the southeast. Edge drop, up to several inches in depth, was observed in the pavement shoulder. No bodies of water were observed nearby.

Instrumentation Plan

Both sites were instrumented with 5TM soil temperature/moisture sensors, a 100ECRN high-resolution tipping bucket rain gauge, and 85 mm horizontal inclinometer casings to monitor moisture/temperature variations, rainfall recordings, and vertical deformation. Field instrumentation allowed for continuous monitoring of moisture content, temperature, rainfall, and vertical deformation. Data loggers were programed to take hourly readings of moisture content, temperature, and rainfall data. Furthermore, the pavement site was visited on a monthly basis to obtain inclinometer readings. Sensor locations are illustrated in Figure 3:2, and Table 3:1 describes the notation of sensors for both FM 2757 and SH 342. For example, K 1/2 corresponds to the Kaufman (FM 2757) site. The sensor is located in borehole-1, and sensor number 2 is in that borehole. Referring to the table, the sensor is located at a depth of 8 ft. Figure 3:3 depicts some photos of field installation.

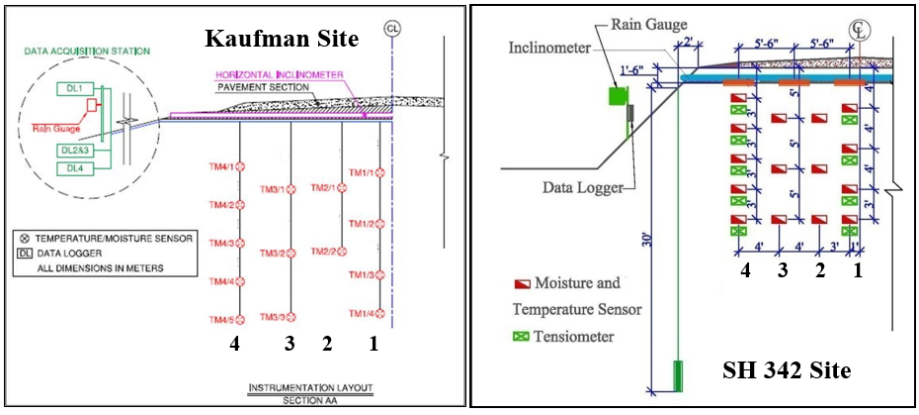

Figure 3:2 Instrumentation at two field sites

Figure 3:3 Instrumentation at SH 342

During installation, soil samples were collected from several boreholes for determining the basic soil properties. Atterberg limits, grain size distribution, specific gravity, and unit weight tests were conducted to aid in understanding the soil behavior.

Table 3:1 Sensor Notations for Both Sites

Tag for Kaufman Site	Tag for SH 342 Site	Borehole	Sensor No.	Depth (ft)
K 1/1	S 1/1	1	1	4
K 1/2	S 1/2	1	2	8
K 1/3	S 1/3	1	3	12
K 1/4	S 1/4	1	4	15
K 2/1	S 2/1	2	1	5
K 2/2	S 2/2	2	2	10
K 3/1	S 3/1	2	1	5
K 3/2	S 3/2	3	2	10
K 3/3	S 3/3	3	3	15
K 4/1	S 4/1	4	1	3
K 4/2	S 4/2	4	2	6
K 4/3	S 4/3	4	3	9
K 4/4	S 4/4	4	4	12
K 4/5	S 4/5	4	5	15
In addition, there is a sensor at SH 342 at BH-2 at 15 ft. depth designated as S 2/3; Number 3 sensor at Borehole 2 at 15 ft. depth				

Soil Properties

According to particle size distribution, samples from both sites were composed of more than 85% clay, indicating the presence of very fine subgrade soil. The liquid limit of the samples varied between 50% and 64%, and the plasticity ranged between 28% and 42%. The soil was classified as high plastic clay (CH) according to the Unified Soil Classification System (USCS) and based on sieve analysis and Atterberg limits results. The specific gravity ranged between 2.68 and 2.72, with an average of 2.70. Optimum moisture content was determined to be 22%, and dry density at the optimum moisture content was found to be 18.9 kN/m^3.

MOISTURE VARIATIONS IN SUBGRADE

Since expansive clay renders pavement susceptible to edge cracking due to moisture variations (Lytton 1988), moisture sensors were installed in four boreholes, at both sites, to investigate the effect of moisture variations on expansive subgrades. Only results from the edge borehole of the Kaufman County site and the center borehole of the SH 342 site are presented below, as the data mirrors what was recorded by the remaining sensors.

Figure 3:4a represents data collected from April 2012 to December 2014 at the Kaufman site. Sensors K 4/1 and K 4/2, at respective depths of 3 ft. and 6 ft., exhibited both seasonal effects and temporary saturation due to rainfall. Wetter seasons yielded a rise in the moisture variation curve, which then dipped during drier periods. Additionally, rainfall events registered instantaneous spikes in moisture content, ranging from 1% to 8% in amplitude. The peaks suggested that the soil became temporarily saturated before returning to equilibrium. At greater depths, moisture content remained stable. K 4/4 and K 4/5, located at 12 ft. and 15 ft. depth, maintained respective moisture contents of 16% and 20%.

Data collected at SH 342 from March 2014 to June 2015 produced the curve shown in Figure 3:4b. All sensors maintained stable moisture contents that responded only to individual rainfall events. Unlike the case in Kaufman County, there were no characteristic rises or falls indicating a seasonal effect on moisture variation. Previous studies confirmed that soil properties determined whether or not a seasonal effect on moisture variation existed at a given location (Heydinger 2003, Manosuthikij 2008). Furthermore, the shoulder at SH 342 might have delayed the movement of moisture, eliminating the seasonal contribution. Nevertheless, SH 342 only experienced temporary variations due to rainfall. S 1/1, S 1/2, and S 1/3 (located at respective depths of 4 ft., 8 ft., and 12 ft.) yielded average moisture contents of 12%, 6%, and 16%, respectively. Moisture contents rose to 14% at 8 ft. and 8% in amplitude at 12 ft. due to temporary saturation induced by continuous rainfall. At 15 ft., S 1/4 registered no appreciable changes in moisture content and remained just below 20%.

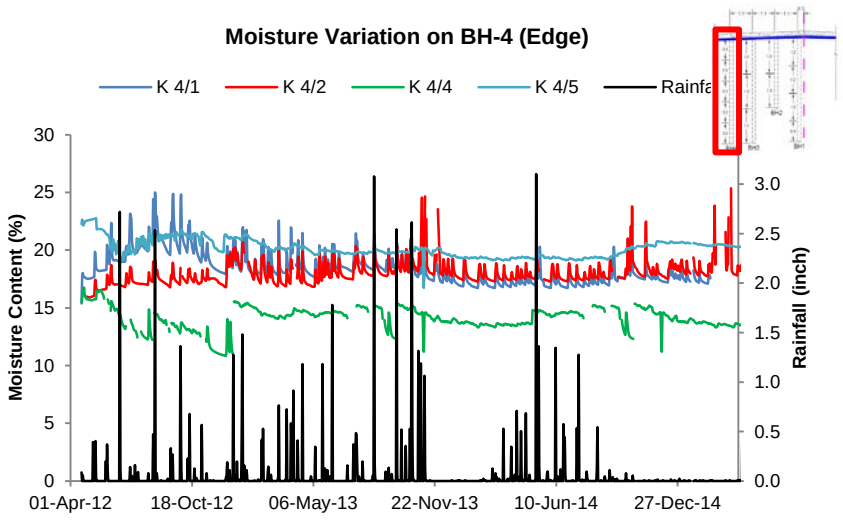

(a)

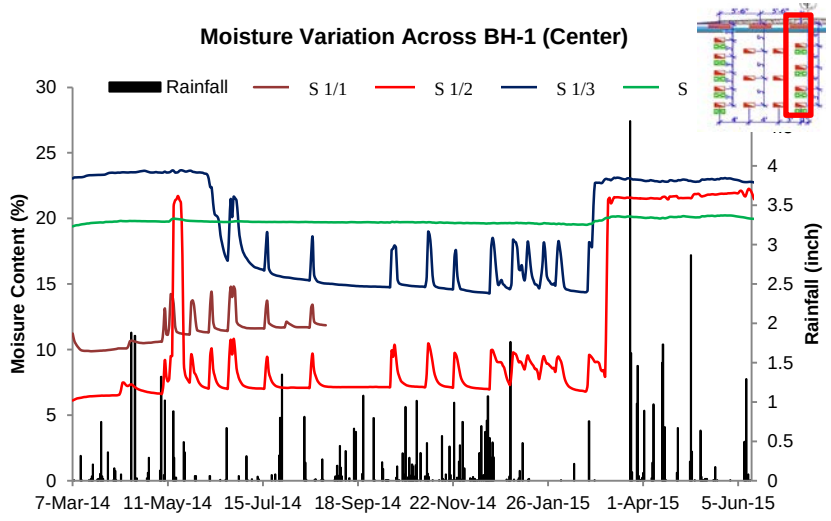

(b)

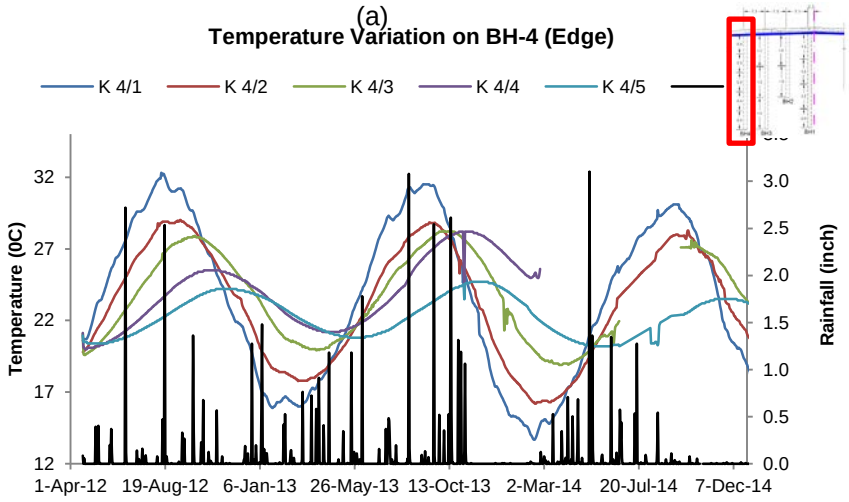

(c)

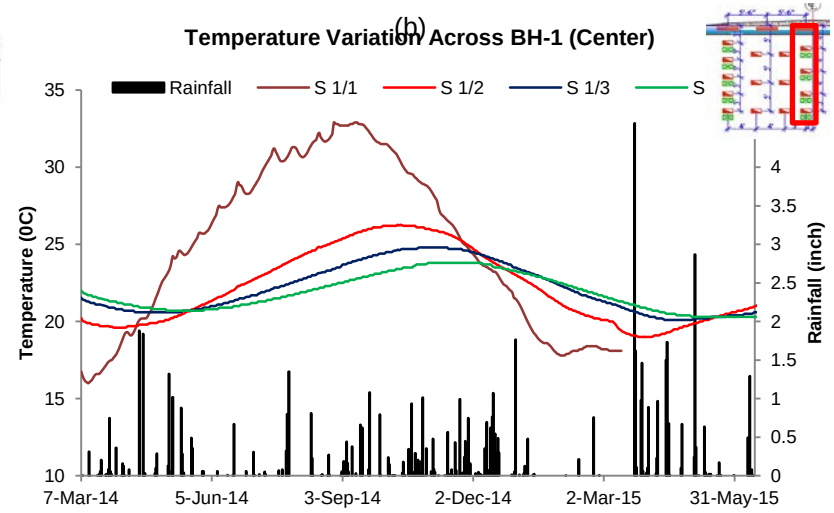

(d)

Figure 3:4 Moisture Variation at (a) Kaufman (b) SH 342; Temperature Variation at (c) Kaufman (d) SH 342

THEORY OF MOISTURE MODELING

Annual variation of subgrade moisture can be described by the following one-dimensional nonlinear diffusion function (Kodikara et al. 2014, Hedayati et al. 2015):

$$\frac{\partial \theta}{\partial t} = \frac{\partial}{\partial z}(D(\theta)\frac{\partial \theta}{\partial z}$$

where, θ = volumetric moisture content at any time t at depth z

$D(\theta)$ = Soil Moisture Diffusivity

Assuming a constant D, the previous equation can be solved as a first-degree Fourier series:

$$\theta(z,t) = \theta_0 + \theta_a \sin(\omega t - \frac{z}{d} + C_0)$$

where, $\theta(z,t)$ = volumetric moisture content at depth z at time t

θ_0 = Average moisture content over time at depth z

θ_a = Domain of moisture variation

ω = angular frequency (equal to 2π/365)

z = damping depth

C_0 = phase correction factor

The first term of the solution captures the yearly average moisture content at any depth, while the second term accounts for the seasonal variation of moisture. However, temporary variation due to rainfall must also be addressed to capture the entire moisture variation in subgrade soil (Hedayati et al. 2015). Previous studies (Heydinger 2003, Manosuthikij 2008) showed that soil and site conditions affect the seasonal and temporary variation of subgrade moisture. Some soil (low plasticity clay in Ohio) experiences a sinusoidal seasonal variation (Heydinger 2003), while other soils (expansive subgrade on high plasticity clay in Texas) tend to maintain an equilibrium

moisture content, irrespective of season (Hossain et al. 2016). Therefore, soil characteristics and specific site conditions are the most important elements in determining the moisture variation. Hence, both the seasonal and temporary variations of moisture content at subgrade were statistically analyzed and incorporated in the presented model.

MOISTURE DATA ANALYSIS

The moisture prediction model was developed using data from sensors with the most interpretable readings over the course of two consecutive years (i.e., K 1/2, K 4/2). Four sets of data were used for model development, while one sensor was randomly chosen from both the Kaufman (K 3/2) and SH 342 sites (S 1/3) for model validation.

Seasonal Trend Analysis

As discussed earlier, moisture sensors at the Kaufman County site exhibited a seasonal variation, while sensors at SH 342 maintained an equilibrium moisture content that displayed instantaneous responses to rainfall. In order to determine the seasonal trend, moisture peaks due to rainfall were removed from the Kaufman site. The seasonal output is shown in Figure 3.5. After a number of trials, the seasonal trend was found to follow the first degree Fourier series. The variables were found by solving the following equation (Sastry, 2012):

$$f(t) = a_0 + \sum_{n=1}^{\infty} \left(a_n \cos\frac{2n\pi x}{T} + b_n \sin\frac{2n\pi x}{T} \right)$$

The result of the series followed the form:

$$f(x) = a_0 + a_1 * \cos(x * w) + b_1 * \sin(x * w)$$

where, a_0 is the average value of the dataset, a_1 and b_1 are real numbers independent of the variable x, which accounts for the amplitude of the dataset, and w is the frequency

(day-1). As one year of data was used to develop the model, and seasonal trends follow annual variations, the frequency was set equal to 2π/365 (0.0.172 day-1).

Variations of the values of a_0, a_1, b_1, and w are shown in Figure 3.5. The moisture content of the sensors remained at approximately 16-17%, which can be attributed to the soil's field capacity (18). Modeling the seasonal variation was simplified by incorporating average values of the different parameters comprising the Fourier series. For example, values of a_0 were found to be 18.85, 17.64, 16.22, and 16.42 in the four graphs in Figure 3:5. The average of these four values, 17.2825, was selected for the seasonal variation model. Values for a_1, b_1 and ω were similarly obtained by calculating the average. The completed model followed the form:

$$Seasonal\ M.C. = 17.2825 - 0.46828 * \cos(x * 0.01864) + 0.5417 * \sin(x * 0.01864)$$

Since the sensor began recording data in April 2012, the first day of April was set as day one (i.e., x =1). It followed that March 31 was set as x = 365.

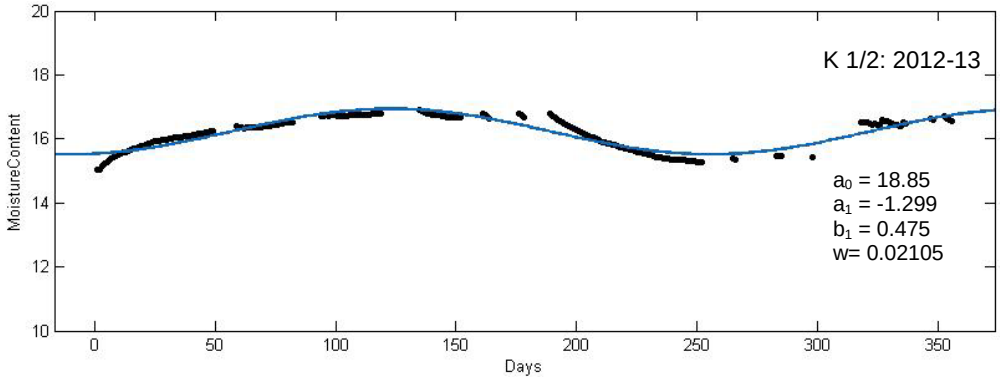

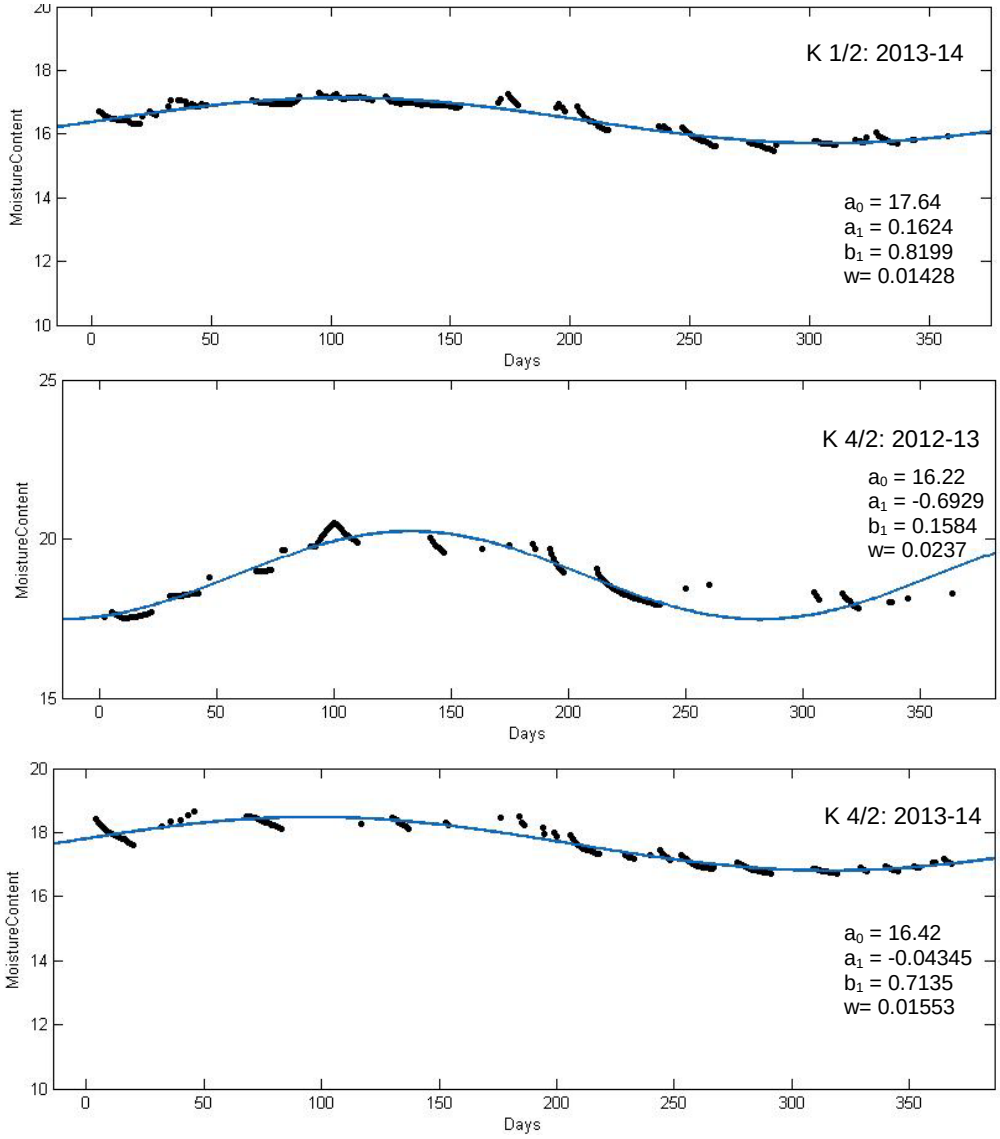

Figure 3:5 Seasonal trend of moisture variation

Moisture Fluctuation Due To Rainfall

Peaks in the moisture data (Figure 3:4a, b) depicted temporary rises caused by precipitation. The increase of moisture content was analyzed separately to determine the relationship between the rainfall and the increase in moisture content. Peaks were separated if the change in moisture content displayed a percent difference of 1% or more from the previously recorded rainfall event. A preliminary inspection of the plot showed

that, in spite of an increasing magnitude in precipitation, the resulting moisture content of the soil typically only rose up to a specific value, corresponding to the saturation point of the soil (Ahmed, Hossain, Khan and Shishani 2017). At this point, all of the medium's voids were filled with water. However, the current status of moisture content in the soil is the most determining factor for the increase of moisture the soil can experience. Thus, the more reliable plot was obtained by including only those points that exhibited an increase in moisture content due to rainfall from the equilibrium moisture content. The linear plot was concluded to best describe the trend of moisture increase due to rainfall shown in Figure 3:6. Similar results were reported by previous researchers (Hedayati 2014, Xu et al. 2012). Parameters (i.e., slope and intersection) of the four plots of Figure 3.6 were averaged to find the increase in moisture content due to rainfall. Average values used in the final moisture model were 1.39 for intersection and 2.2085 for slope.

FINAL MOISTURE MODEL

Based on the overall analysis (i.e., seasonal trend and temporary increase due to rainfall), moisture content at different depths could be explained as:

$$M.C. = [Seasonal\ Variation] + \{Variation\ due\ to\ rainfall\}$$

$$= a_0 + a_1 * \cos(x * w) + b_1 * \sin(x * w) + f(rainfall)$$

$$= [17.2825 - 0.46828 * \cos(x * 0.01864) + 0.5417 * \sin(x * 0.01864)]$$

$$+ \{(1.39 + 2.2085 * Rainfall)\}$$

where, x = days (April 01 as day 1), and rainfall is in units of inches.

The average moisture content was generally observed to remain at the soil's field capacity of 17.5% (Hedayati et al. 2015). Monitoring of moisture variation of plastic clay in Delaware County, Ohio for five years (1996-2001) exhibited an average moisture content of around 15-17% (Heydinger 2003). Similar field monitoring conducted in high plastic clay in Houston and Fort Worth, Texas for two years (2007-08) showed an average

moisture content between 15-18% (Manosuthikij 2008). Therefore, the applicability of the model is limited to specific soil conditions.

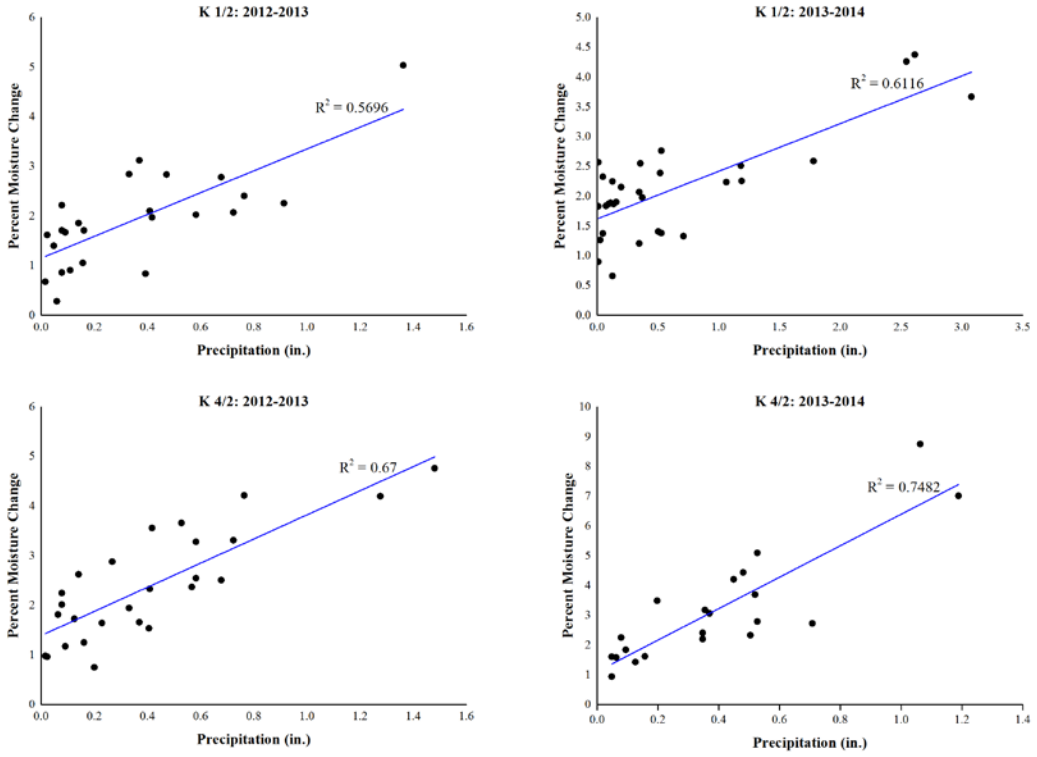

Figure 3:6 Relationship between increase in moisture content and precipitation

VALIDATION OF THE DEVELOPED MOISTURE MODEL

Sensor K 3/2 was randomly selected and tested for a period of six months (from April 2013 to October 2013) to determine the accuracy of the developed model. A sensor from the SH 342 site (S 1/3) was also selected for model validation.

Figure 3:7a illustrates that the developed model captured both the seasonal variations and temporary variations due to rainfall. A comparison of the predicted and measured values in Figure 3:8a showed that more than 90% of the data fell in the 90% confidence bands. Because seasonal variation was not observed at the SH 342 site, the

first term of the model was excluded for validation. Hence, only the increase in moisture due to rainfall was compared against the actual increase in moisture content. A comparison of the modeled and actual increases in moisture content after randomly selected rainfall events are presented in Figure 3:7b. The model's results were compared with results obtained from previous studies (Figure 3:8b), after converting gravimetric values to volumetric moisture contents (Kodikara et al. 2014). Figure 3:8b depicts the significantly improved model prediction when including the temporary variation.

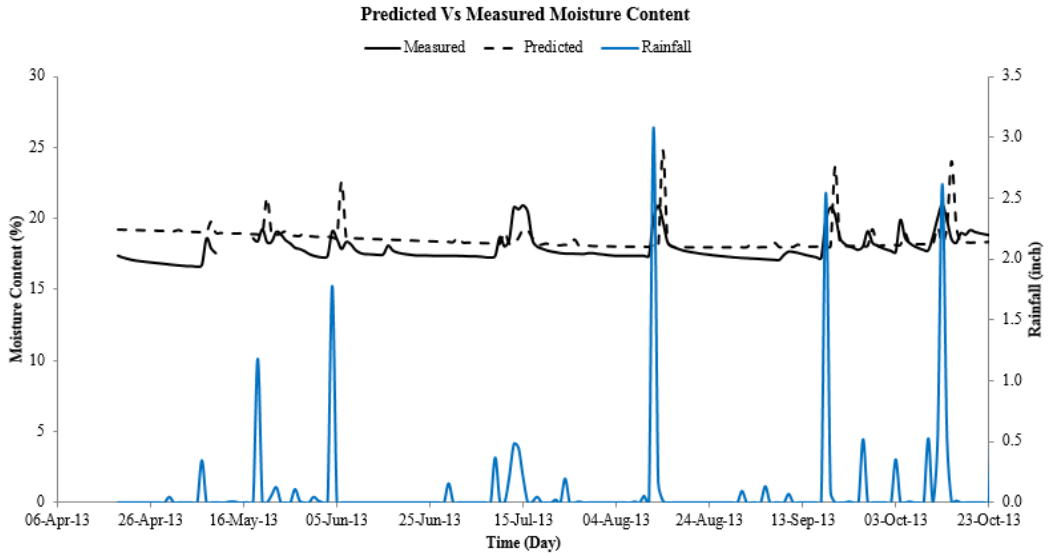

(a)

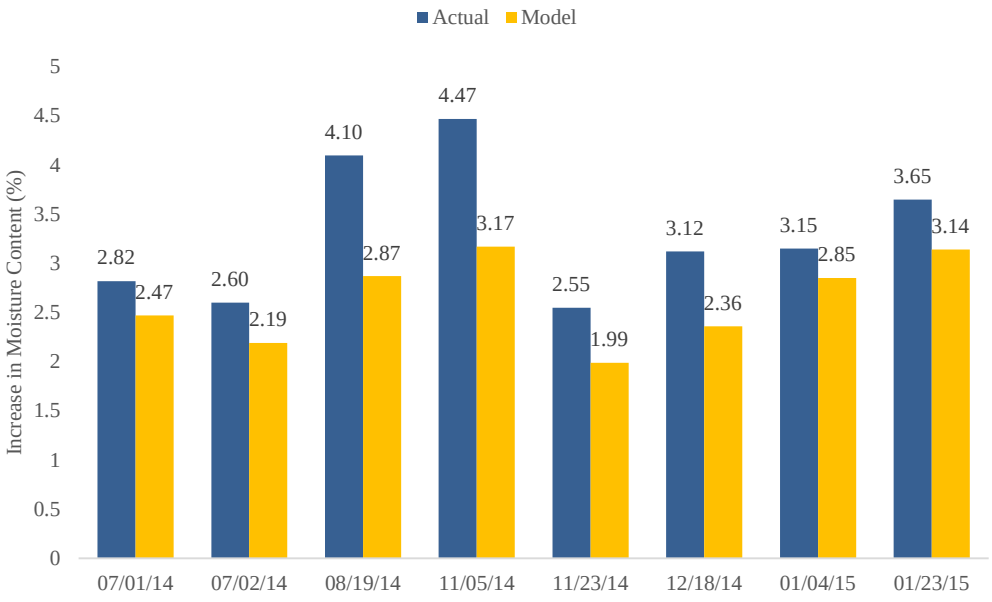

(b)

Figure 3:7 (a) Validation of moisture model at Kaufman Site and (b) SH 342 site

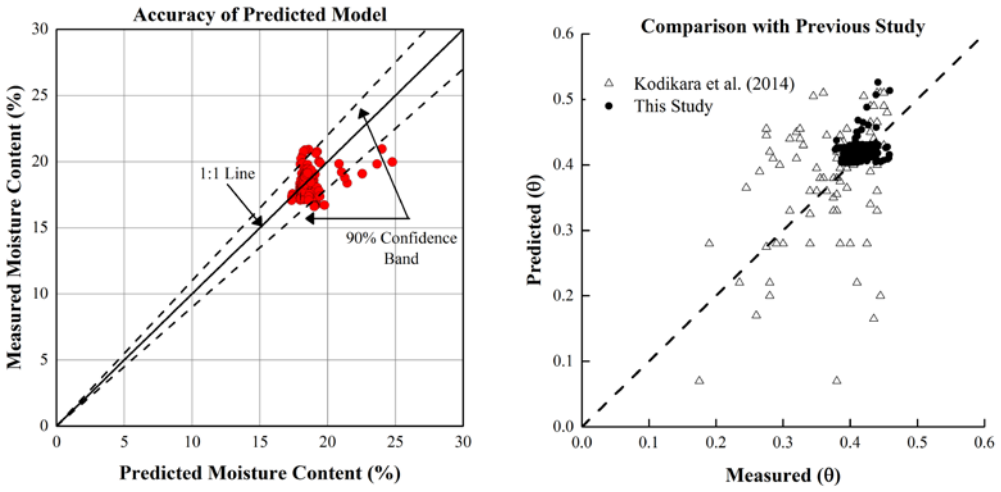

(a) (b)

Figure 3:8 (a) Accuracy of the predicted model (b) Comparison with previous study

LIMITATIONS OF THE MODEL AND FURTHER DEVELOPMENT

The developed model captures the effect of a temporary rise of moisture content due to rainfall, but the study was based on the assumption of a homogeneous soil layer. Evaporation was also neglected during the model development. To further increase the acceptance of the model, it was compared with some sensor results installed in a grassy side slope, as shown in Figure 3:10 (a). The rationale of selecting the grassy side was that it included the effect of evaporation; the sensor installed beneath the pavement did not. It was observed that the sensors exhibited seasonal and temporary variations. The sensors installed beneath the pavement also displayed seasonal and temporary variations, but the average moisture content data was different. Hence, the first term of the developed moisture model was replaced by the average moisture content of the selected sensor, and rest of it remained the same. Consequently, the modified moisture model looked as follows:

$$MC = [X - 0.46828 * \cos(x * 0.01864) + 0.5417 * \sin(x * 0.01864)] + \{(1.39 + 2.2085 * Rainfall)\}$$

Where, X = average moisture content of the location. In conclusion, to use the developed moisture model, the average moisture content of the selected site must be measured manually.

The modified moisture model was tested against the sensors installed in the grassy side slope, and Figure 3:9 depicts the measured and modeled moisture content. It can be observed that the model can record the change in moisture due to rainfall with the least error. The measured and modeled data were further plotted against a 45 degree line (Figure 3:10 b). As can be seen, most of the data is clustered around the 45 degree line. Hypothesis testing was conducted to verify the modified model.

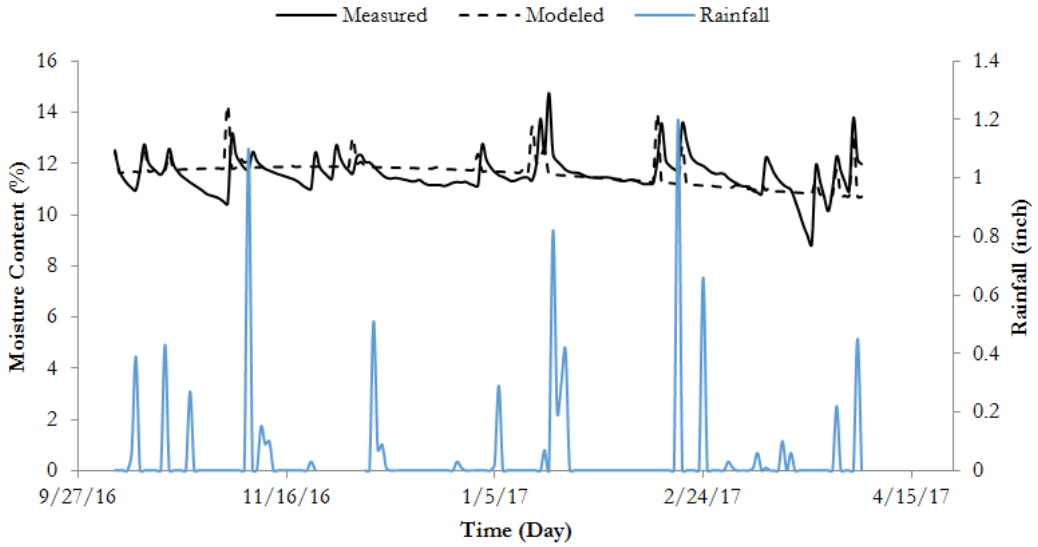

Figure 3:9 Comparison of modeled and measured moisture content in grassy side slope

An independent two-sample t-test with unequal variance was performed to determine whether there were significant differences between the actual and predicted moisture increase values. The rationale behind independent test was the non-dependency of the two set values. The mean of the predicted values of the t-test was compared against the mean of observed values. The risk level was set as 0.1, meaning that the test was conducted at 90% confidence level. The two-tailed test directed the significance level to 0.05 from 0.1. The basic hypothesis of the two-sample t-test can be described as follows:

$H_0: m_1 - m_2 = 0$

$H_a: m_1 - m_2 \neq 0$

where,

$m_1 =$ mean of the actual moisture

$m_2 =$ mean of the predicted moisture

Table 3.2: Summary of two-tailed t -test

	Mean	Std. Dev.	SE Mean	t- value	P- value
Actual	11.559	0.7	0.052	1.22	0.223
Predicted	11.639	0.523	0.039		

The test summary is provided in Table 4:2. The t-value found from the analysis was lower than that of the critical value of the two-tailed t-test. The p-value was higher than the significance level (α/2). Based on the analysis, it was concluded that the null hypothesis could not be rejected, indicating there was no significant difference between the actual and predicted values of the means. Thus, the developed prediction model was justified.

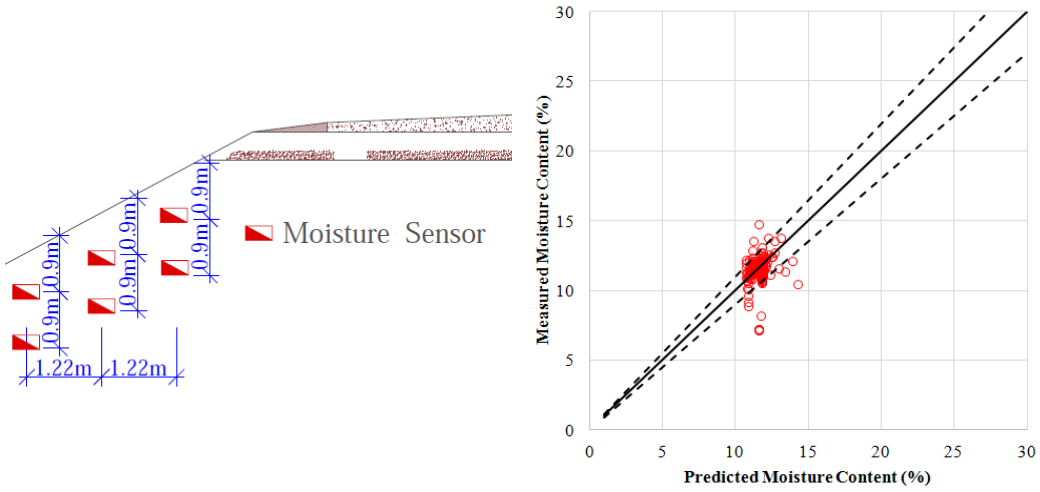

(a) (b)

Figure 3:10 (a) Location of sensors in grassy side slope (b) Predicted vs measured moisture content in grassy side slope.

TEMPERATURE VARIATIONS IN SUBGRADES

Temperature data collected from 2012 to 2014 produced the results shown in Figure 3:4c and Figure 3:4d. Sensor K 1/2 (located at 8 ft. depth at the edge borehole) recorded a maximum temperature of 31˚C in late September and a minimum of 18˚C in March (Figure 3:4c). Sensor K 1/3 (at 12 ft. depth) showed maximum/minimum temperatures of 27˚C/21.5˚C in October/March. Sensor K 1/4 (at 15 ft. depth) exhibited maximum/minimum temperatures of 24.4˚C/22.2˚C in late November/May. The domain of temperature change was found to decrease with depth. Sensor K 1/2 observed a temperature difference of 13˚C, while K 1/3 and K 1/4 showed respective differences of 5.5˚C and 2.2˚C. Conversely, time lag increased with depth. Sensors located at 8 ft. depth peaked in September, while sensors at 15 ft. depth peaked after three months, in November.

Similar temperature variations were observed in the center borehole at the SH 342 site from April 2014 to June 2015 (Figure 3:4d). S 1/1 (at 4 ft. depth) failed after peaking in August 2014 at 32.2˚C. S 1/2 (at 8 ft. depth) had maximum/minimum temperatures of 26.6˚C/18.3˚C, with a peak in October and a low at the end of March. Maximum/minimum temperatures of S 1/3 were 24˚C/20.5˚C in November/May, whereas S 1/4 showed 23.8˚C/20.5˚C in December/May. Similar temperature variations were observed for the remainder of the sensors at both sites.

Sensors at 3 ft. depth varied by 13˚C between summer and winter; at 15 ft. depth, the temperature differed only by 2.2˚C. Thus, the domain of soil temperature variation with depth decreased by 0.9˚C/ft.

BACKGROUND OF TEMPERATURE MODEL DEVELOPMENT

Soil temperature experiences daily, seasonal, and yearly changes and is influenced by time of day, cloudiness, weather patterns, precipitation, drought, and depth. With numerous factors governing soil temperature, the need arises for a widely-accepted, simple, and accurate soil temperature prediction model (Lei et al. 2011).

The thermal regime of soil can be modeled by assuming that temperature oscillates in a sinusoidal pattern around an average value (Hillel 1982). Van Wijk and Vries utilized periodic functions of weather patterns and climate to model soil temperature (Van Wijk 1963). The authors established a sinusoidal temperature variation model for homogeneous soils, similar to the models developed recently by researchers (Hedayati 2014 and Lei et al. 2011).

TEMPERATURE DATA ANALYSIS

The temperature prediction model was developed by selecting four sensors with interpretable readings from 2014 (i.e., K 1/1, K 1/2, K 1/3, and K 1/4). Temperatures at different depths of subgrades depend on the air temperature in the environment and the thermal properties of the soil. Regardless of depth, the temperature variation curves followed a similar sinusoidal pattern. However, a time lag was observed by examining the peaks of the individual curves (Figure 3:11a). Increasing depths yielded a greater time lag than the variations in air temperature. Additionally, atmospheric conditions exhibited differences of 22˚C between the maximum and minimum temperatures (15˚C and 2.2˚C at 4 ft. and 15 ft. depth, respectively). The decreasing domain of temperature variations resulted in progressively flatter curves with increasing depth. However, after approximately 126 days of monitoring (beginning January 1, 2014), the soil temperature at depths of 4 ft., 8 ft., 12 ft., and 15 ft. all reached approximately 22˚C. Because a time lag was only prominent during peaks and the temperature decrease rate was inconsistent

throughout the year, subgrade soil temperatures could not be predicted using air temperature, lag time, or decrease rate. Therefore, another approach was taken by plotting the ratio of soil temperatures at each depth to air temperature. The resulting curves, shown in Figure 3:11b, produced trends that followed a first degree Fourier series when analyzed in a statistical environment. These ratios were used in the development of a model that could predict soil temperature, given air temperature and depth. For example, if $Ratio\ (z) = \frac{T(z)}{Air\ Temp.}$ is the ratio of soil temperature at depth *z* to air temperature of that particular day, the temperature at depth *z* could be predicted from air temperature, provided that the ratio is known.

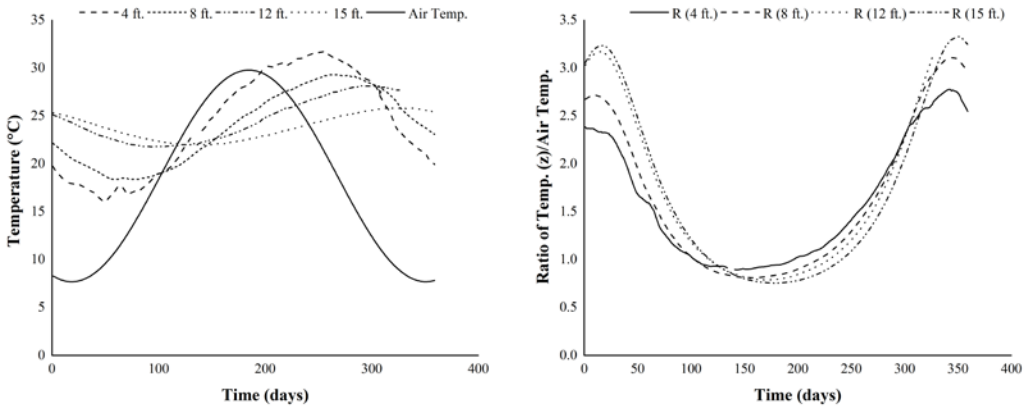

(a) (b)

Figure 3:11 (a) Temperature at different depths with air temperature (b) Ratio of temperature at depth (z) to air temperature

MODEL DEVELOPMENT

As discussed earlier, the ratio parameters followed a sinusoidal variation. The trend could best be described by an equation similar to that used when determining the seasonal pattern of moisture variation. Parameters a_0, a_1, b_1 and ω were derived using statistical software. Values of a_1, b_1 and ω decreased with depth, while a_0 increased up

to 12 ft. depth (Figure 3:12a, Figure 3:12b). Temperature variation was minimal at 15 ft. depth (less than 2.5˚C), and no moisture variation was found at that depth (Figure 3.4a, 3.4b). Hence, to obtain the parameter values, only depths up to 12 ft. were considered. Although several equations were considered to fit the parameter values (e.g., linear, exponential, power, different order polynomial, etc.), the second degree polynomial best fit the data. Ultimately, the ratio predicting equation at any depth, *z,* became:

$$Ratio\ (z) = a_0 + a_1 * \cos(x * w) + b_1 * \sin(x * w)$$

$$= (0.0751z^2 - 0.7488z + 3.747) + (-0.0669z^2 + 0.7605z - 1.4634) * \cos(x * w)$$

$$+ (-0.0572z^2 + 0.4885z - 2.06) * \sin(x * w)$$

where, the frequency ω took the form: ($-0.00005z^2 + 0.00009z + 0.0133$), and x = days (with January 01 as day 1).

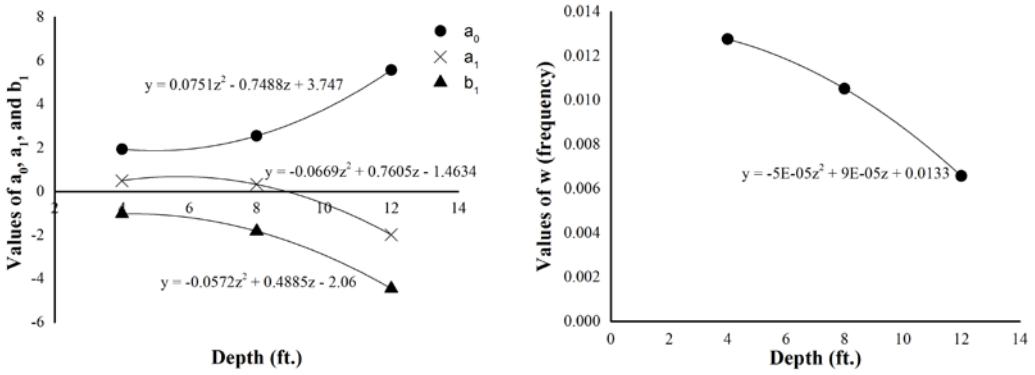

(a) **(b)**

Figure 3:12 Fitting trend of (a) a_0, a_1 and b_1 (b) ω (frequency)

VALIDATING THE MODEL

After developing the temperature prediction equation, sensor S 1/1 from SH 342 (from borehole 1 at 4 ft. depth) was randomly chosen to validate the model. As shown in Figure 3:4c and Figure 3:4d, maximum variation was observed at 4 ft. depth. Hence, only comparisons of the temperature ratio and values at 4 ft. are presented (Figure 3:13).

Similar results were observed for the remaining depths. The R^2 value was 0.91 for the measured and modeled temperature values and 0.98 for the temperature ratio. A recent temperature prediction model for a subgrade in North Carolina found that the squared correlation coefficients (R^2) between the observed and predicted soil temperatures at three locations exceeded 0.9 (Lei et al. 2015). The results agreed with a previously developed temperature model in a similar expansive subgrade (Hedayati 2014).

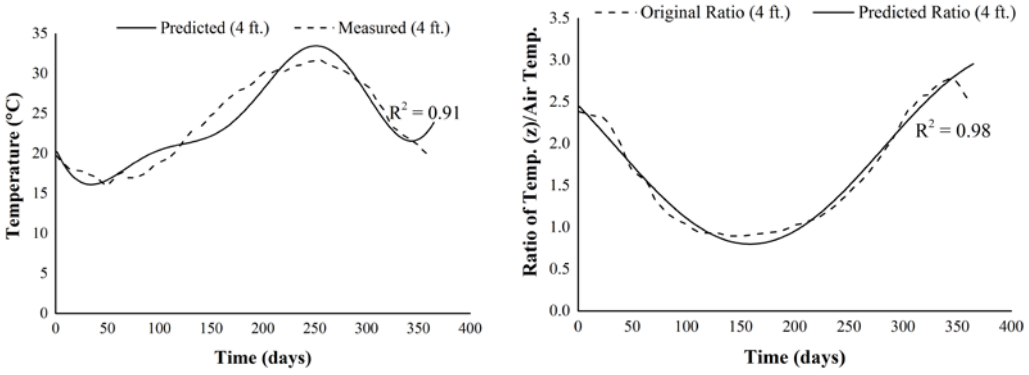

(a) (b)

Figure 3:13 Comparison of measured and predicted values (a) Temperature at 4 ft. depth (b) Temperature ratio at 4 ft. depth

CONCLUSIONS

Results obtained from two instrumented pavement sites were used to develop real-time moisture and temperature models. Moisture data showed that equilibrium moisture content varied from 6% to 20% at different depths of subgrade. Temporary increases due to rainfall ranged between 1% and 14% in amplitude. Because seasonal variations of moisture were observed at the Kaufman site, a real-time moisture model was developed that accounted for both seasonal and temporary increases. Validation of

the model indicated that the outputs of the model were within 90% of the in-situ measured values.

The presented temperature prediction model can predict the subgrade temperature at any given depth from air temperature. As the lag time and temperature decrease rates throughout the year were found to be inconsistent and non-uniform, by plotting ratios of soil temperatures at various depths to air temperatures, the ratio model yielded the subgrade temperature, given the air temperature of a particular day. The R^2 value between the observed and predicted soil temperature was 0.91.

Although the developed moisture model method incorporates seasonal effects and temporary saturation in the moisture variation, it was studied in a homogenous, single-layer subgrade and specific type of soil, i.e., high plastic clay. Moisture variations in different types of soils with heterogonous stratigraphy are considered outside the scope of the current case study, limiting the applicability of the model. In developing the temperature prediction model, soil heat parameters (such as heat absorption capacity, thermal inertia, etc.) were neglected. Moreover, the loading condition at the subgrade was assumed to be similar throughout the year. It is strongly recommended that the developed models be further modified through additional analyses of different types of soil and various geometric configurations of roads.

CHAPTER 4

DEFORMATION MODELING IN EXPANSIVE SUBGRADES IN TEXAS

Ahmed, A.[1], Hossain, M.S.[2]

[1]Graduate Research Assistant, Department of Civil Engineering, The University of Texas at Arlington, 416 Yates Street, NH 119, TX 76019; Email: asif.ahmed0@mavs.uta.edu

[2]Professor, Department of Civil Engineering, The University of Texas at Arlington, 416 Yates Street, NH 404, TX 76019; Email: hossain@uta.edu

(Resistivity Imaging Section of this paper has been published in Proceedings of GeoMEast 2017. Part of Deformation Modeling has been submitted in Journal of Materials in Civil Engineering; Submission ID: S-17-00881)

ABSTRACT

Volumetric changes due to the swelling and shrinkage behavior of the expansive subgrade pose a significant threat to pavements. Repeated wetting-drying cycles over the year create significant stress in the pavement layers, which ultimately leads to pavement cracking. The objective of the study is to develop a pavement deformation model for expansive subgrades. Moisture sensors, temperature sensors, and rain gauges were installed to record the variations of the variables over time in one farm-to-market road and a state highway. Geophysical testing in the form of Electrical Resistivity Imaging (ERI) was conducted to attain a continuous portrayal of the subgrade over time. Deformation of the pavement was monitored through topographic surveying and horizontal inclinometers. Based on the collected data, the state highway experienced up to 38 mm of movement; the farm-to-market road experienced up to 80 mm of movement. Collected data was analyzed in a statistical environment, and it was found that seasonal variations only capture a portion of the deformation, whereas the amount of precipitation amount plays a significant role in further modifying the model. Temperature and resistivity

values were also correlated with deformation to finalize the model. Application of the developed model could allow for an estimation of deformation at any time of the year, in response to precipitation.

INTRODUCTION

Pavements in expansive soil are quite common in several parts of the world (Djellali et al. 2011). Even when the pavement layers are correctly designed, an expansive subgrade can distort all of the predictions and assumptions associated with it. Repair of damages resulting from expansive soil range from 9 billion USD to 15 billion USD annually, of which more than half can be attributed to highways and streets (Steinberg 1989; Nelson and Miller 1992; Jones and Jefferson 2012). Puppala et al. (2012) reported that the cost of repair and maintenance of severely distorted pavement sometimes surpasses the cost of construction. Therefore, it is important to understand the behavior of the expansive subgrades ahead of construction in order to decrease future maintenance costs.

Expansive soil is common throughout United States, and it extends across Texas also, North Texas in particular. Sebesta (2002) reported that 25% of the Texas Department of Transportation's (TxDOT) annual expenditures are for the repair and maintenance of the problems associated with expansive soil. In most of the cases, expansive soil is unsaturated and clayey in nature (Djellali et al. 2011). Among the three types of clay minerals, i.e., kaolinite, illite, and montmorillonite, the latter one attracts more water, as it has a significantly high surface area and is characterized as high plastic clay (Das, 2013). Due to the affinity of a high volume of water, it swells when it absorbs water and shrinks when water is dissipated (Khan et al. 2017). Chabrillat et al. (2002) reported a significant amount of montmorillonite in the mid-zone of the USA. A study by Punthutaecha et al. (2006) and Puppala et al. (2013) indicated the presence of this

clayey mineral in the Dallas-Fort Worth (DFW) area, where the absorbance of water leads to volume expansion in the wet season, while the opposite occurs in the dry season (Khan et al. 2017).

Due to the volume change phenomenon, larger stresses occur in the form of cracking, heaving, and settlement of the pavement (Djellali et al. 2012). Sebesta (2002) reported longitudinal cracking, roughness, and fatigue cracking due to volume expansion and contraction. Longitudinal cracking in the pavement shoulder has been reported as the most prevalent pavement distress that is due to expansive subgrades (Sebesta 2002). The cracking phenomenon occurs because of moisture changes in the underlying subgrade and edge-moisture intrusion (Hedayati 2014, Ahmed et al. 2017). Because the moisture change is uniform, the structure only moves up and down. However, different amounts of moisture change in different soil layers, leading to differential movements and resulting in structural damage taking place in buildings, highway pavements, and airport pavements.

This paper investigates the deformation behavior of two different roads built on expansive subgrades in North Texas. Two sites were selected to accomplish the objectives: one on a farm-to-market road (FM 2757) and one on a state highway (SH 342). Moisture sensors were installed at different depths to record the moisture changes, and geophysical testing, in the form of electrical resistivity imaging (ERI), was conducted to monitor the seasonal moisture changes. Deformation behavior was recorded through topographic surveys and horizontal inclinometers. The objective of this research is to develop a pavement deformation model, based on the behavior of an expansive subgrade due to seasonal and temporary responses. It describes the monitoring results of two different roadways and the different parameters associated with deformation, and

after analyzing the parameters in a statistical environment, results in the development of a model.

METHODOLOGY

Deformation Monitoring

The timeline profile of the pavement surface and deformation was monitored through monthly topographic surveys and horizontal inclinometers. In accordance with Hedayati's findings (2014), the survey recorded the overall deformation of the pavement, and the inclinometer detected the local deformation, such as crack initiation and movement of shoulder.

Horizontal inclinometers were used to obtain the high resolution profile of settlement or heave. They can be applied to tanks, embankments, pavements, dams, and landfills. Their advantages include full-settlement/movement profile, precise measurements, and low maintenance (Slope Indicator, 2017).

A horizontal Digitilt inclinometer, manufactured by Slope Indicator, was used to record the local defection of the pavement. It consisted of a casing, horizontal probe, pull cable, and readout unit. The 85-mm inclinometer casing was installed in a horizontal trench with one set of grooves aligned in a vertical direction. There are two sensors in the inclinometer which are 600 mm apart, and the tilting angle of the device from a horizontal line was measured by the sensors. A change in inclination indicated movement. Profile accuracy remained within +/- 0.01%, using the sinus law of the measured angle. A survey was conducted at regular intervals to obtain the inclination measurements. The first survey established the initial profile, while subsequent surveys were compared with the initial one to monitor whether movement had occurred.

Moisture Monitoring

Climatic loading, i.e., precipitation, snowfall, etc., are the prime reasons for subgrade moisture changes that are directly related to volume changes (deformation). Snowfall is not a common phenomenon in Texas; hence, precipitation is the main cause of moisture content changes in the subgrades. Engineers have long agreed that environmental loading adversely affects pavement performance, however; quantitative effects are limited (Bae et al. 2007). In order to understand the effects of moisture in pavement distress, it is necessary to understand how the moisture changes over time in a subgrade. In the expansive soil in the selected study area, swelling and shrinkage of the soil are greatly affected by moisture changes, and dielectric moisture sensors were used to measure the moisture content in the subgrade of the pavement. Chapter 3 hosts the details of instrumentation of the sensors and the justification for selecting the sensors over other moisture-monitoring methods described elsewhere.

While moisture sensors returned distinct moisture content recordings, further information regarding moisture variation was desired. Geophysical testing allows for a continuous picture of the moisture variations beneath the pavement, and was performed in the form of resistivity imaging. Since sensors were not installed beneath the grassy slope adjacent to the pavement, geophysical testing also allowed for determination of the moisture variation beneath the slope, beside the pavement (Ahmed et al. 2017).

ERI measures the electric potential differences at specific locations after injecting a controlled electric current at other locations. By controlling the current injected in an entirely homogeneous half-space, a resistivity value can be calculated for the subsurface by measuring the resulting electric potential difference. However, homogeneity within the subsurface rarely exists. Additionally, electric currents will follow the path of least resistance (Ahmed et al. 2017).

Instrumentation required for RI included a super-sting R8/IP resistivity meter manufactured by Advanced Geosciences Institute (AGI) and a switch box with a 12-volt battery. RI testing was conducted with 28 electrodes placed at 0.9 m (3 ft.) intervals, resulting in a test line of 24.7 m (81 ft.). Better resolution in the horizontal and vertical directions was obtained by employing a dipole-dipole array (Manzur et al., 2016). The schematic of the layout of testing and site photos are presented in Figure 6. The collected data was analyzed in the Earth Imager 2D software (AGI, 2004), which uses a forward modeling technique to calculate apparent resistivity values from the field data. The software uses the non-linear least-squares optimization technique to yield the final output as a 2D resistivity image of the subsurface (Ahmed et al. 2017).

MOISTURE VARIATION IN PAVEMENT

As moisture has been reported as the main variable of volumetric changes in expansive subgrades, it is important to observe the variation of the subgrade moisture with time. The following section describes the moisture variations in the center and edge boreholes at the FM 2757 and SH 342 sites.

Center Borehole of FM 2757

The variations of the maximum moisture content in the boreholes observed during the monitoring cycles are presented in Figure 4:1a. During the first phase of monitoring, sensors installed at 6 ft. regularly returned the highest readings. The lowest readings were retrieved from a depth of 15 ft. These trends were common to the curves obtained during the remaining two monitoring cycles. From April to August 2013, when the total rainfall was as high as 100 mm, a slight increase was observed in all of the maximum moisture variation curves. A decrease in rainfall yielded a decrease in the maximum moisture curves. Similar values of average moisture content, trends of

maximum moisture variation curves, and responses to rainfall were displayed during the monitoring period.

Edge Borehole of SH 342

Three sensors were installed in the edge borehole of the pavement, at varying depths from 4 ft. to 15 ft. The monthly variation in average moisture content was plotted alongside monthly totals of rainfall in inches. The resulting plot is presented in Figure 4:1b. The sensor located deepest in the subgrade maintained an average moisture content of approximately 21% throughout the monitoring cycle. Full saturation of the soil prevented appreciable moisture variation. Despite a maximum increase of 85 mm in total precipitation from March to June 2014, moisture sensors installed at both 4 ft. and 8 ft. registered a decline in moisture content. The deeper sensor experienced a more gradual decrease, while the sensor closest to the ground surface responded with a 5% drop in magnitude just from March to April. Readings from the two sensors began to coincide in August 2014, when both sensors returned values of 11%. Moisture content went up to 18% and 15% respectively for 4 ft. and 8 ft. depths, due to an increase in rainfall from March to May, 2015. Both sensors registered a drop and returned to the previous 11% moisture after continuous rainfall ceased in summer 2015. A rise was again recorded following rainfall in March, 2016.

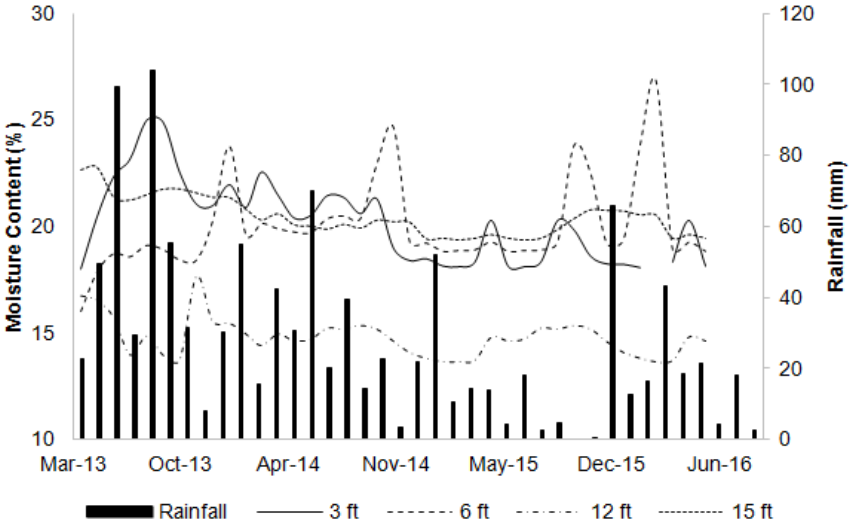

(a)

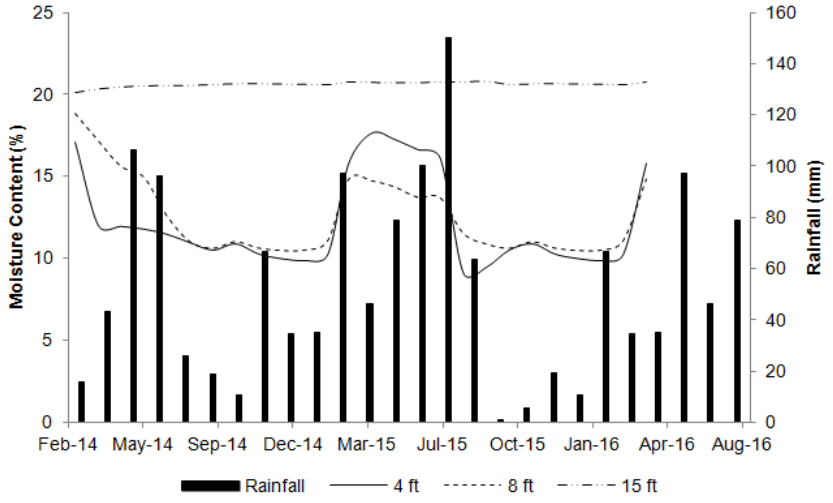

(b)

Figure 4:1 Average moisture variation in (a) FM 2757 and (b) SH 342 site

MOISTURE VARIATION IN SUBGRADE BY RESISTIVITY

The plot shown in Figure 4:3 depicts the resistivity variations across depths. Resistivity values ranged between 7 to 13 ohm-m between the months of November and

April, translating to high readings of moisture content. Thus, the period was identified as the wet season. In contrast, the period between May and October returned resistivity values as high as 23 ohm-m, corresponding to the dry season. Data obtained from geophysical testing revealed a seasonal trend in moisture content variation that was not captured by moisture sensors installed in the pavement. Given the relationship between resistivity and moisture content, a seasonal effect on resistivity suggested that a seasonal effect on moisture content variation also existed. Below a depth of 3 m (10 ft.), there were no significant fluctuations in resistivity (Figure 4:4). This corroborated the findings obtained from other studies conducted in the same area, which identified 3-3.66 m (10 - 12 ft.) as the depth of the active zone (Hossain et al. 2016). It is expected that volumetric deformation will occur beyond the active zone in response to the resistivity variations – hence, moisture change.

Figure 4:2 Resistivity setup at slope of SH 342

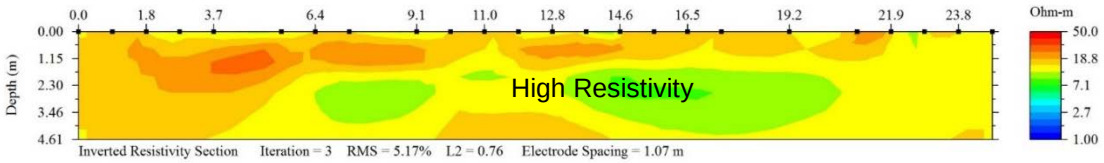

(a)

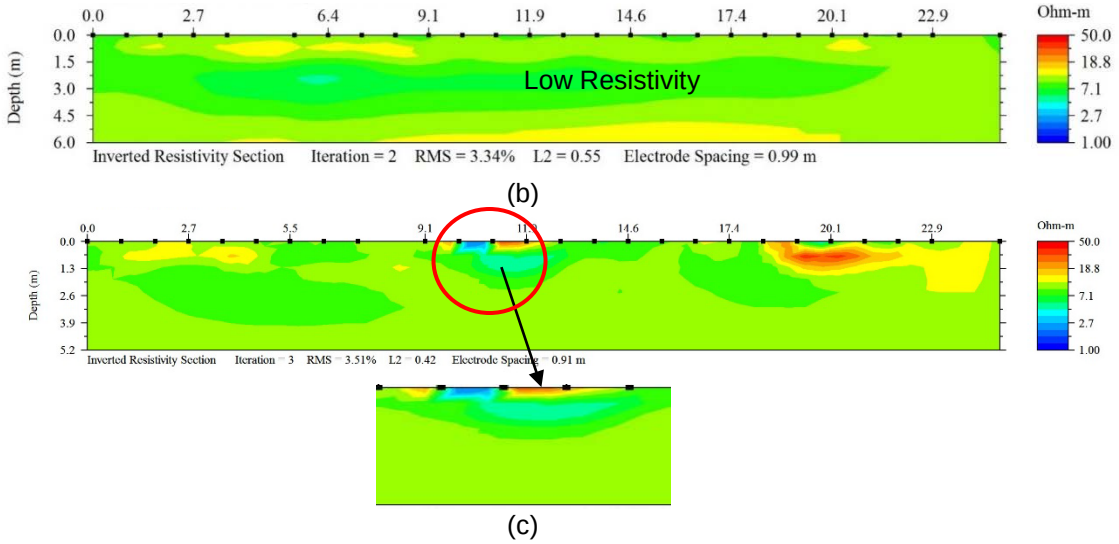

Figure 4:3 Resistivity variation in (a) dry period, (b) wet period, and (c) moisture intrusion through edge after rainfall

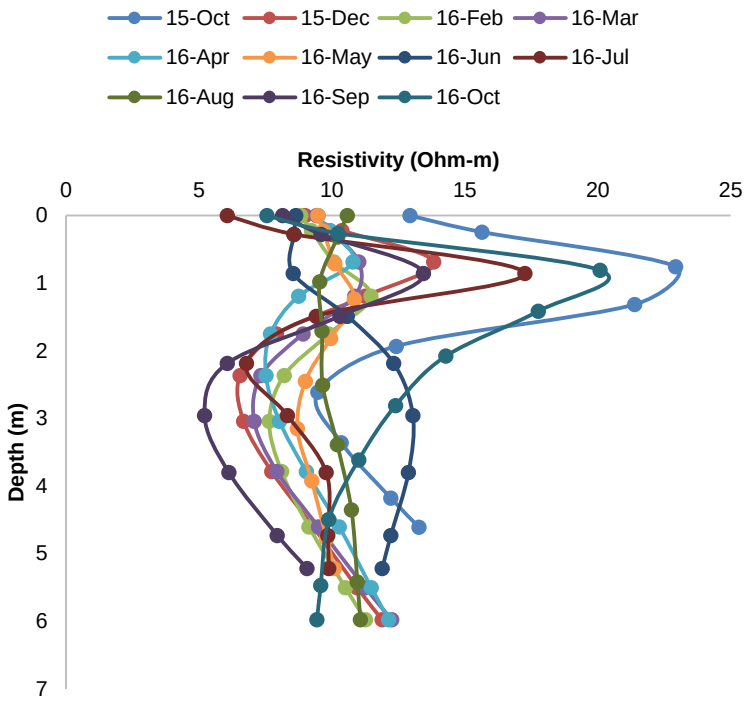

Figure 4:4 Resistivity variation across depth

A contour plot of the pavement section was drawn to gain a better understanding of moisture intrusion from edge of the pavement (Figure 4:5). No visual change of moisture can be observed in an average moisture plot, because the peak values are suppressed when it is average. While plotting the maximum moisture contour for the same pavement section, it was evident from the blue zone (Figure 4:6) that moisture was infiltrating from the edge of the pavement and was causing significant drop at the edge. So, the most critical time for pavement deformation is during the summer, a few days after rainfall, when there is opportunity for the rain to infiltrate the pavement through shrinkage cracks.

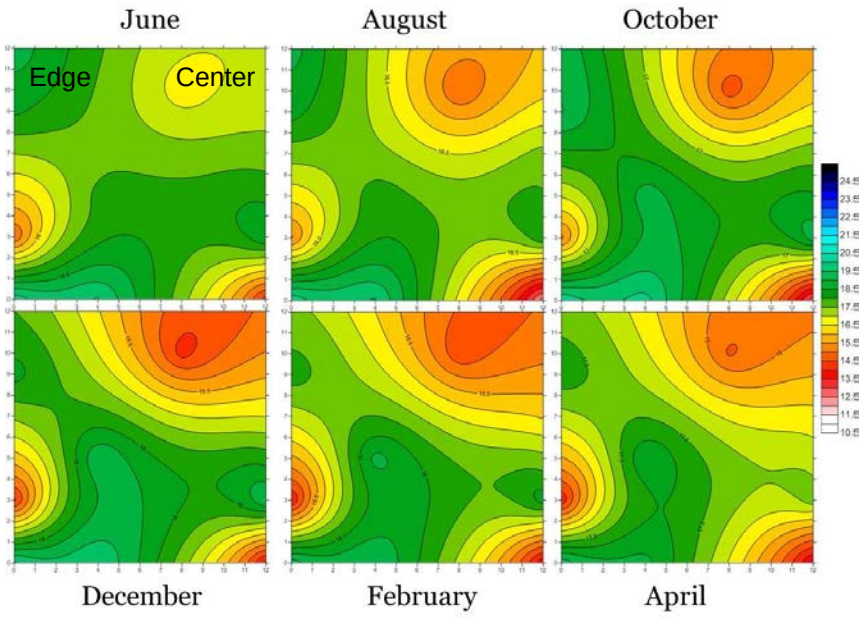

Figure 4:5 Bi-monthly average moisture content contour in pavement section

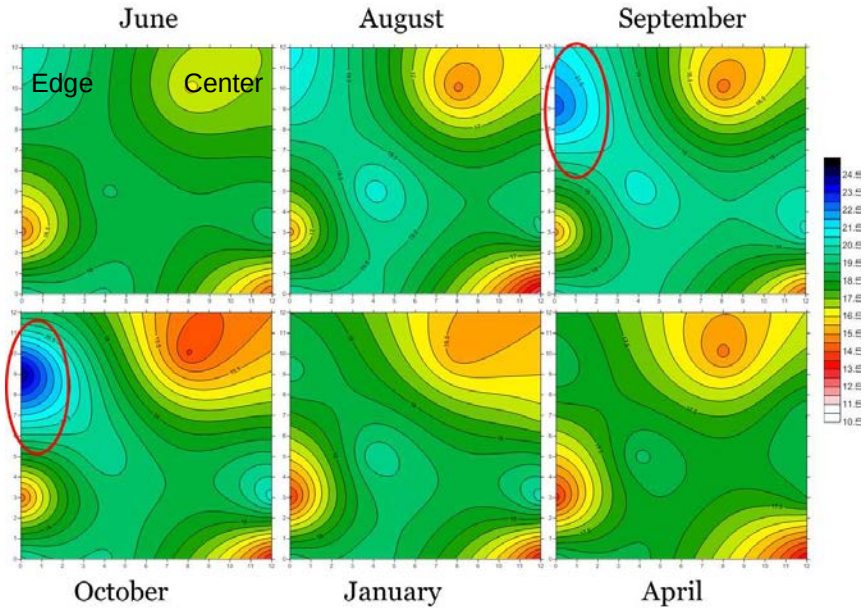

Figure 4:6 Bi-monthly maximum moisture content contour in pavement section

In addition to the seasonal and temporary variations due to rainfall, Manosuthikij (2008) reported that roadside trees also affect moisture variations of a subgrade. Hence, an observation-based inspection was carried out to determine whether trees at the study sites contributed to shrinkage cracking. The results are presented from only one site (SH 342), as it mirrors the observation from the FM 2757 site.

INFLUENCE OF TREES

Ward (1953) recommended safe planting of trees by highways and other structures in order to avoid the damage induced by shrinkage crack. The author believed that the presence of trees could utilize the subgrade moisture leading to moisture depletion in subgrades and causing shrinkage-induced cracks. Ward's research developed a "proximity rule" of D:H, where H represents the height of the tree and D represents the distance from the edge of the structure to the edge of the tree. He concluded that when the ratio is close to one, the structure could experience a shrinkage-

induced problem. Cameron (2001) described a considerable shrinkage settlement during a severe drought in UK in the mid-70's, due to the drying effect of trees.

Comparing the greenery at the SH 342 site in the summer and winter seasons (before and after the trees lost their leaves, respectively) revealed the quantity of water trees can extrat from soil at the location (Figure 4:7). Roots of roadside trees can frequently extend beneath the pavement slab in their search for water. Such phenomenon is observed in Figure 4:8**,** where a decrease in the maximum moisture content was recorded in two boreholes.

(a) (b)

Figure 4:7 Comparison of trees at SH 342 in (a) summer and (b) winter

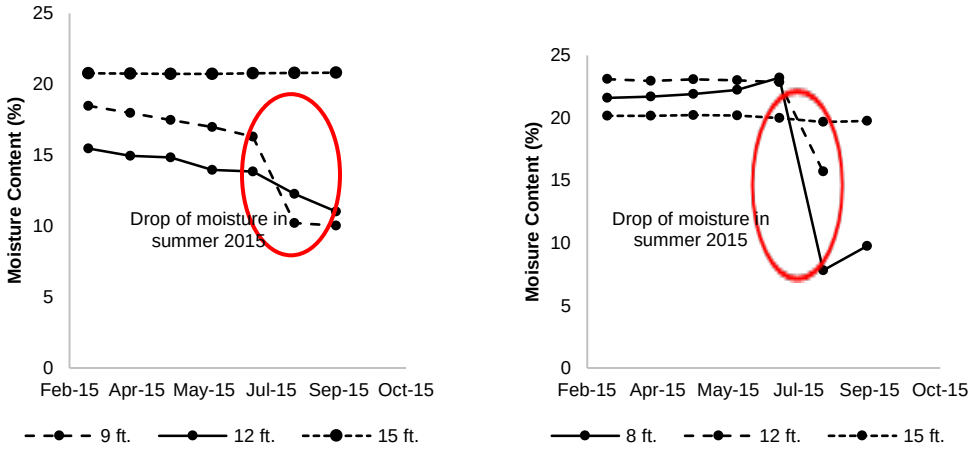

Figure 4:8 Drop of moisture content after summer

The height of the trees at the SH 342 site was estimated to average about 34 ft., and they were approximately 31 ft. from the pavement cracks, resulting in a *D/H* ratio of 0.91. In this case, the *D/H* ratio was close to the problematic level of 1.0, suggesting that the sites were likely to experience moisture depletion caused by root uptake of the large trees nearby. Desiccation of the expansive subgrade was expected to occur in the summertime, when the grasses and trees absorbed moisture from the subsoil. The resistivity at SH 342 was observed to increase from May to July 2016, indicating a decrease in moisture content (Figure 4:3 and Figure 4:4). A similar trend could have been predicted during the same time period one year earlier. Indeed, moisture sensors at the site registered a significant drop in moisture content in the summer of 2015 (Figure 4:8). Subsequent rainfalls then infiltrated the cracks, causing movement in the subgrade that ultimately produced the observed longitudinal crack in the shoulder. The study was restricted to observation, as no quantification was possible during the model development. Hence, the deformation modeling excluded the effect of trees,

After the moisture variation at the subgrade was well established through field instrumentation and geophysical testing, deformation behavior of the test site was studied, as described in the following section.

DEFORMATION BEHAVIOR OF THE TEST SITES

Deformation in Kaufman County

The profile of the pavement surface and its deformation was monitored using a horizontal inclinometer and monthly surveys. The coordinates of the first survey were set as the zero reference (May, 2012), and elevations of the points in each survey were determined by subtracting the recorded elevations from the initial reading. FM 2757 experienced distress in the summers of 2012 and 2013. The pavement maintained a constant slope in all of the readings, while severe local deformations were observed along the edge of the pavement. The most visible deformation was recorded on a survey performed on September 22, 2013, where the pavement edge had a drop of approximately 2 inches. The pavement experienced an edge drop, followed by a huge crack during this period. A similar drop was observed the following summer, in September 2014, and the pavement experienced another edge crack in October, 2015. The longitudinal cracks are shown in Figure 4:9 in successive summer periods. The crack was as deep as 7 inches (Figure 4:9 c).

(a) (b)

(c)

Figure 4:9 Crack after (a) summer 2014, (b) summer 2015; (c) 7-inch crack

Deformation in SH 342

Figure 4:10 shows the movement of the pavement obtained from the inclinometer results (2014-16). As can be seen, the pavement moved up and down due to swell and shrinkage behavior of the expansive subgrade. The inclinometer profile showed that the swelling and shrinking of the expansive subgrade caused up to 38 mm (1.5 in.) of vertical

movement across the pavement. No significant edge drop was observed at this site due to the support of the shoulder, which hindered the formation of edge cracks and subsequent deformation of the pavement. The amplitude of the pavement swelling and shrinkage was 2 inches, and it followed the same seasonal trend as was observed in Kaufman County. After the summer, it tended to shrink as a result of low moisture and swell in the wet period.

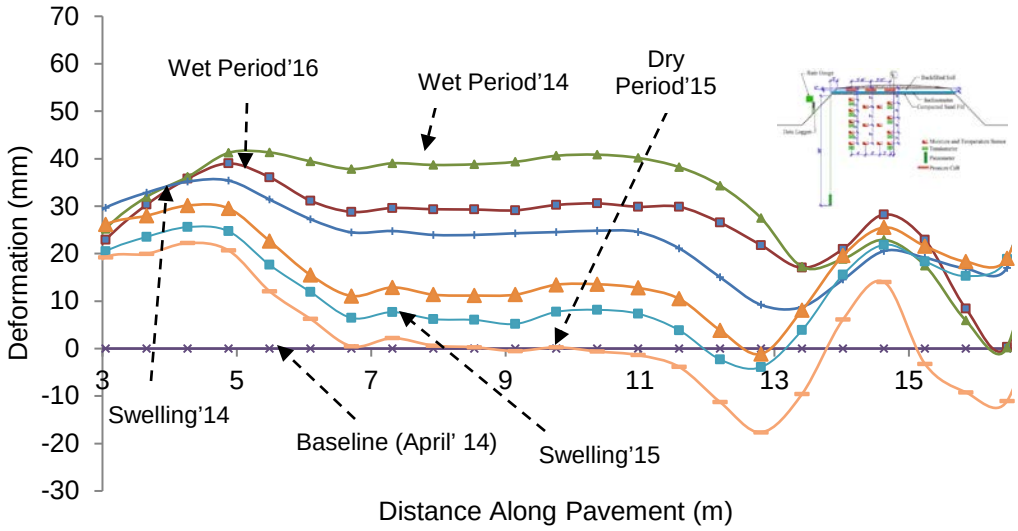

Figure 4:10 Variation of deformation in central section of SH 342

Deformation with Rainfall in Both Sites

The pavement elevations of the center point and cracked edge of the Kaufman County site are shown in Figure 4:11. The typical pattern of shrinkage and swelling was observed during the monitoring period (2014-16). After extensive rainfall events from March to May, 2015, the subgrade experienced swelling up to 60 mm. After July and August 2015, when there was hardly any rainfall, it dropped a similar amount. Previous studies (Hedayati 2014 and Puppala et al., 2012) discussed the seasonal effect on the deformation of pavement, which is also dependent on seasonal variations and precipitation.

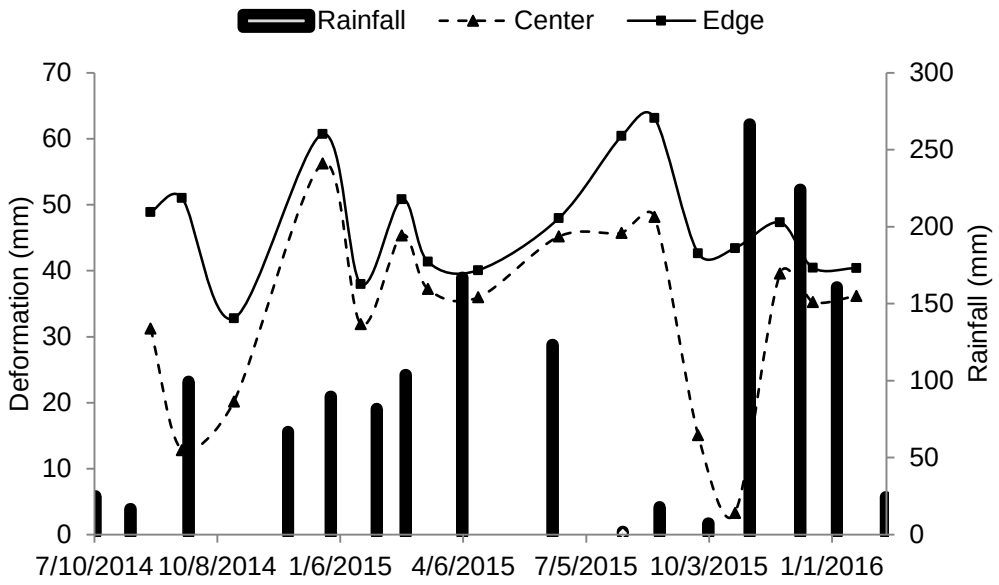

Figure 4:11 Deformation variation of edge and center with rainfall events at FM 2757 site

The movement of two points, the left edge and center of the site located at SH 342, is presented in Figure 4:12 . As can be seen, the variation of elevation corresponded with rainfall events. The deformation of two points usually follows a trend similar to that of rainfall. Hence, swelling and shrinkage behavior is observed in deformation. For instance, after a cumulative rainfall of 114.3 mm from March to May 2014, the subgrade experienced 38.1 mm of swelling, and it dropped by almost an inch after the summer of the same year. It again experienced swelling in January 2015, in response to a precipitation event of almost 50 mm, and experienced another drop after October 2015 when the amount of rainfall dropped by a considerable amount.

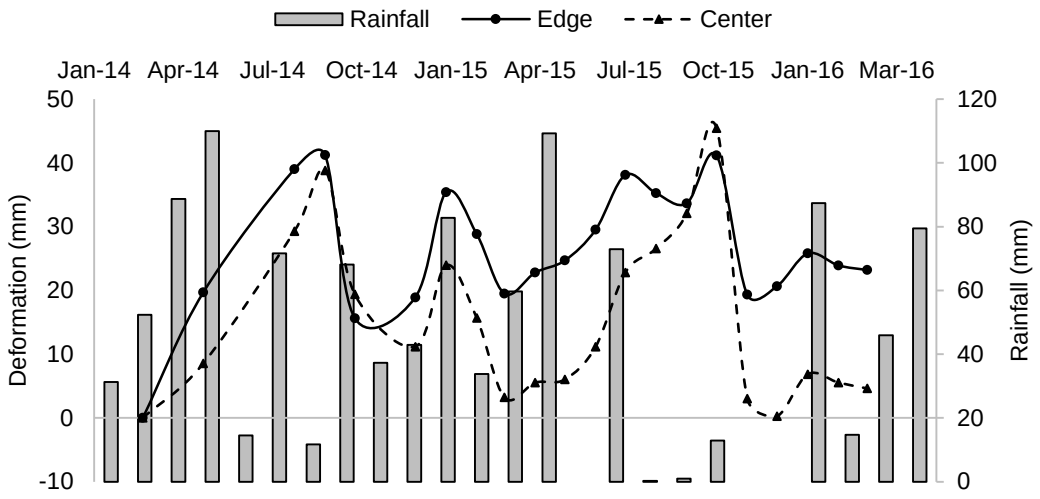

Figure 4:12 Deformation variation of edge and center with rainfall events in SH 342

Hedayati (2014) stated that moisture balance is the prime criteria for the cycle of upward and downward movements. An increased number of cycles accelerates the deterioration of pavement. Cracking is a vulnerable state for pavement deterioration, and cracking potential can be predicted by observing these movements and then be incorporated in the design process.

The difference of elevation between the left edge and the centerline of pavement was plotted against time with rainfall (Figure 4:13). Monitoring results of 2014-15 are only presented for cracking potential. The highest drop occurred in August 2014 and September 2015, resulting in an edge drop. Another huge drop was observed after September 2015. The amount of rainfall was very low during these two extreme drops of 12.5 mm. Hence, it can be concluded that the amount of rainfall has a significant impact on the potential for cracking. Based on the observation of two pavements, it can be stated that pavement is most likely to crack in August and September. Wagner (2003) reported that the months of August to October were the most vulnerable for cracks opening in Central Europe.

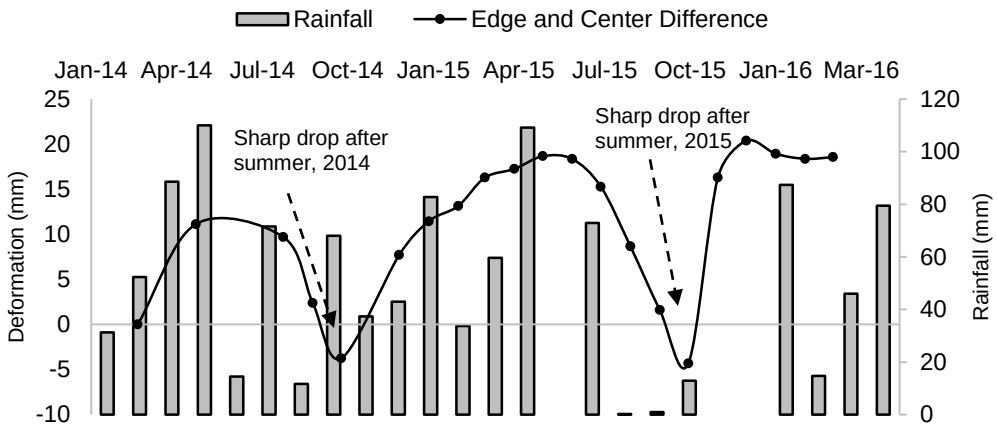

Figure 4:13 Edge drop in consecutive summers at SH 342 site

After observing the deformation patterns of the test sites, attempts were made to develop a deformation prediction model, based on the collected data.

MODEL DEVELOPMENT

Luo and Prozzi (2010) reported that longitudinal cracking near the edge of the pavement or on its shoulder, which generates when shrinkage cracks initiate in the subgrade, is one of the most prevalent pavement distresses. Therefore, the movement of the edge was considered in the model development, although the whole pavement experiences the movement. In addition, the pavement edge is the first location of crack propagation, which justifies the consideration of the edge for model development. The authors analyzed the edge pavement deformation in a numerical environment (ABAQUS). Bae et al. (2008) predicted pavement profiles, considering different parameters, i.e., pavement thickness, soil gradation, heave rate, pavement age, etc. However, the authors did not consider rainfall as a predictor variable. While conditions at both sites were considered for deformation modeling, only the deformation data from SH 342 was utilized for model development and validation.

An attempt was made to develop a pavement deformation model, considering the effects of rainfall, moisture, temperature, season of the year, and suction. According to Kutner et al. (2005), predictor variables should not be correlated with themselves while developing a model. Therefore, moisture and rainfall could not be considered as predictor variables, as moisture change is primarily governed by precipitation events. Since a rainfall event is the major source of moisture change, precipitation was considered as a predictor variable for developing the model.

Temperature was checked for the month associated with the deformation to verify its suitability as a predictor variable. Both Pearson and Spearmen correlation coefficients were checked with the pairs of the data. Figure 4:14 shows the scattered plot among the variables. The Pearson correlation yielded a value of 0.438, while Spearmen yielded a value of 0.42. The p-value was noted as 0.047, which is less than 0.1 considering a 10 percent confidence level, confirming the rejection of a null hypothesis that no significant relationship exists between the variables. For example, Figure 4:14 shows that five different temperature values were recorded for 20 mm deformation.

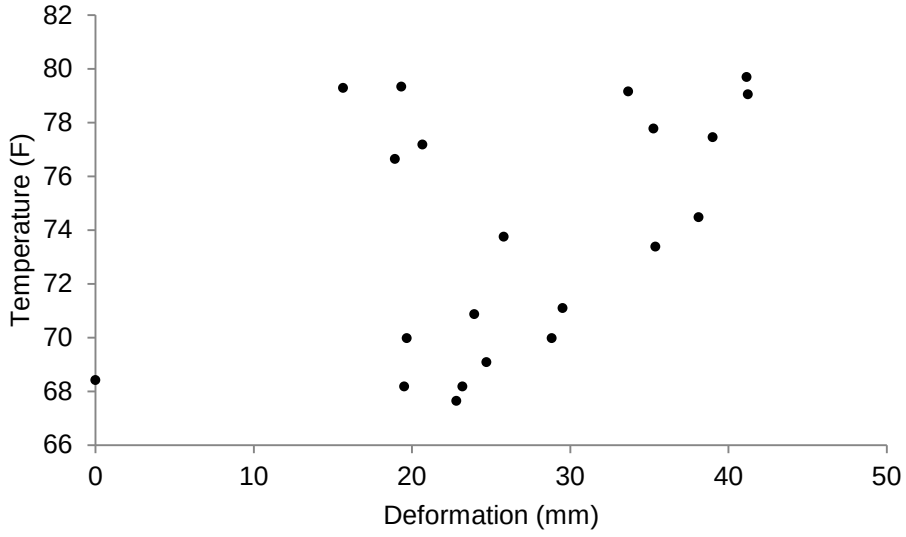

Figure 4:14 Temperature and deformation plot

The reliability and longevity of suction sensors have always been debated, but the suction values were tried against the deformation values to determine whether any significant correlation exists between them. Most of the water potential sensors use the thermal conductivity principle to measure the suction of soil (Manosuthiki, 2008). This technique measures the potential energy of water in equilibrium with water in soil (Decagon Devise, 2017). A thermal conductivity sensor consists of a porous ceramic block, including a heater. The thermal conductivity of the block varies with the water content, which is in turn connected to the matric suction applied to the block by surrounding soil (Frenlund and Rahardjo, 1993). As the two materials are in equilibrium, measuring the suction of the material provides the suction of the surrounding soil. Manu (2008) used the Fredlund Thermal Conductivity (FTC) sensor to monitor the suction beneath a pavement slope; however, he reported a high failure rate in the field and the fragility of the ceramic used in the sensor (Manosuthiki, 2008). Decagon Devices manufactures water potential sensors using the same principle, but instead of measuring the thermal conductivity, they use the dielectric permittivity of solid matrix-porous ceramic discs. The dielectric permittivity of air, solid ceramic, and water are 1, 5, and 80, respectively. Hence, the amount of water present in the pore spaces of ceramic discs directs the dielectric permittivity value of the ceramic disc. In addition, ceramic used in MPS-1 has a wide range of pore distribution. As such, a considerable range of water content can be covered by measuring the dielectric permittivity (Decagon Devices, 2017). However, the sensor has some limiting values, below which it cannot record the suction (10 kPa), thus limiting its ability to capture the real-time suction scenario at field condition. Kodikara et al. (2014) discussed two basic approaches to determine the stress and deformations of structures built on expansive soil. However, Fityus (1999) and Gould et

al. (2011) reported long-term suction monitoring as difficult and not reliable. Hence, a ground movement prediction method based on moisture content was reported by Fityus (1999) and Kodikara (2011). Puppala et al. (2011) reported ten months of field-suction monitoring data, from March 2007 to June 2008, while other values were reported as “not available” due to a malfunctioning of the sensor. Considering all of the above mentioned reasons, suction values were not considered during the model development.

The remaining parameter is the time (day) of the year. Previous researchers have reported that seasonal variations are a main cause of volumetric change (Hossain et al., 2016; and Ahmed et al. 2017). The previous section describing the seasonal variation with resistivity also confirms that the effect of season (time) of the year affects deformation. Consequently, the first step was to quantify the pavement deformation based on the recorded data.

As the edge is most vulnerable to moisture intrusion, only edge deformation values were considered and were plotted against the time period, 2014-2016 (Figure 4:15a). The overall trend followed a seasonal pattern, in addition to local rainfall in response to precipitation. After several trials, the seasonal trend was found to follow the first degree Fourier series. The variables were found by solving the following equation (Sastry, 2012):

$$f(t) = a_0 + \sum_{n=1}^{\infty} \left(a_n \cos\frac{2n\pi x}{T} + b_n \sin\frac{2n\pi x}{T} \right)$$

The result of the series followed the form:

$$f(x) = a_0 + a_1 * \cos(x * w) + b_1 * \sin(x * w)$$

where, a_0 is the average value of the dataset, a_1 and b_1 are real numbers independent of the variable x, which accounts for the amplitude of the dataset, and w is the frequency

(day-[1]). Several parameters were entered, which led to the seasonal deformation model as:

$$D = 33.56 - 7.751 * \cos(x * 0.01854) - 10.4 * \sin(x * 0.01854)$$

It must be noted that the values of the 2014-15 period were used to develop the model. To verify the developed model, edge deformation during 2015-2016 was plotted against the predicted deformation (Figure 4:15b). The excessive movement, especially the drop after the summer period, could not be captured from the seasonal variation model, but the usual seasonal change was perfectly embedded in the prediction model. Hence, it is important to include the temporary moisture variation to obtain better serviceability of the roadway. Deviation of the predicted value from the field data indicates the necessity of including the effect of rainfall in the model.

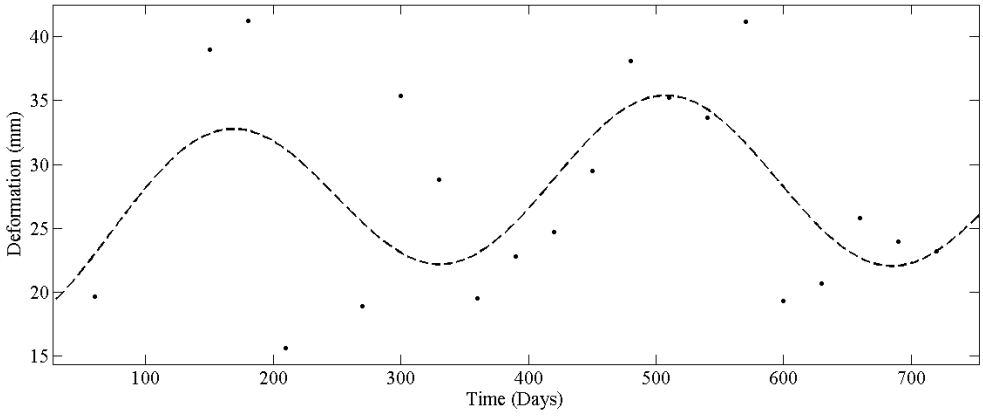

(a)

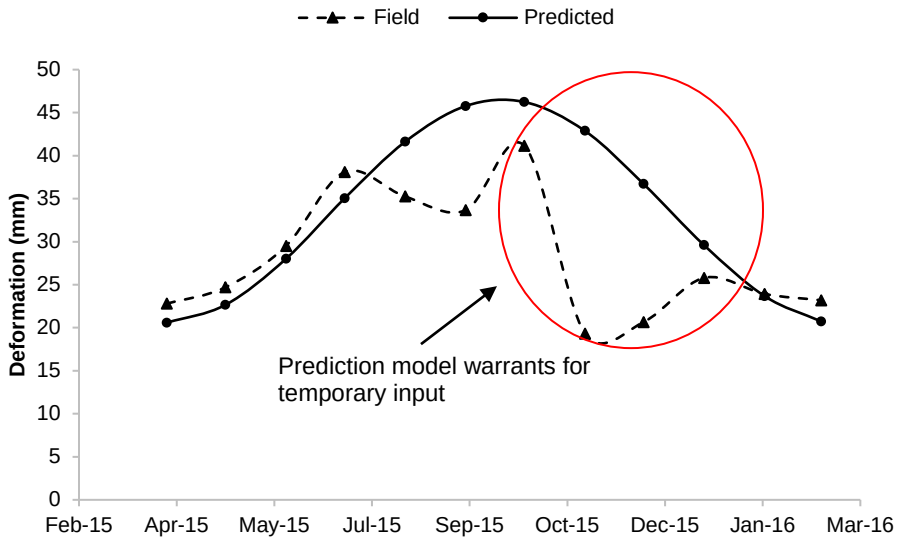

(b)

Figure 4:15 (a) Variation of the edge deformation of 2014-16 period (b) Predicted and field deformation of 2015-16 period

MODIFICATION OF THE MODEL

As seen in the prediction model, a factor is required to add the effect of rainfall events. In order to determine the effect of rainfall on the deformation values, 2014-16 edge deformation values were used to develop the model, while 2016-17 values were used to validate the model. The dataset for 2014-16 is presented in Table 4:1. The new dataset slightly modified the previous deformation model, including the seasonal effect. The frequency of value (*w)* changed to 0.01858, while the average ($a_{0)}$ of the dataset became 30.56. Hence the new deformation model took on the following form:

$$D = 30.56 - 7.751 * \cos(x * 0.01858) - 10.4 * \sin(x * 0.01858)$$

Table 4:1 Dataset for Model Development

	Day	Rain	Deform
Mar-14	0	1.23	0
May-14	60	3.49	0.7746
Aug-14	150	2.82	1.5354
Sep-14	180	0.46	1.623
Oct-14	210	2.68	0.6156
Dec-14	270	1.69	0.7446
Jan-15	300	3.26	1.3932
Feb-15	330	1.33	1.1352
Mar-15	360	2.35	0.768
Apr-15	390	4.3	0.8976
May-15	420	9.44	0.9726
Jun-15	450	2.87	1.1622
Jul-15	480	0.01	1.5
Aug-15	510	0.04	1.3878
Sep-15	540	0.51	1.3254
Oct-15	570	9.29	1.62
Nov-15	600	6.84	0.7608
Dec-15	630	3.44	0.8136
Jan-16	660	0.58	1.0158
Feb-16	690	1.81	0.942
Mar-16	720	3.13	0.9132

To check the initial prediction model, edge deformation values of the 2016-17 period were plotted against the model's (Figure 4:16). As can be noticed, the difference between the prediction and field values existed for some months. The difference of these two values was considered to have a relationship with the rainfall events. Hence, the difference of the actual and predicted values were entered on the y-axis, and rainfall was entered on the x- axis for determination of the rainfall factor.

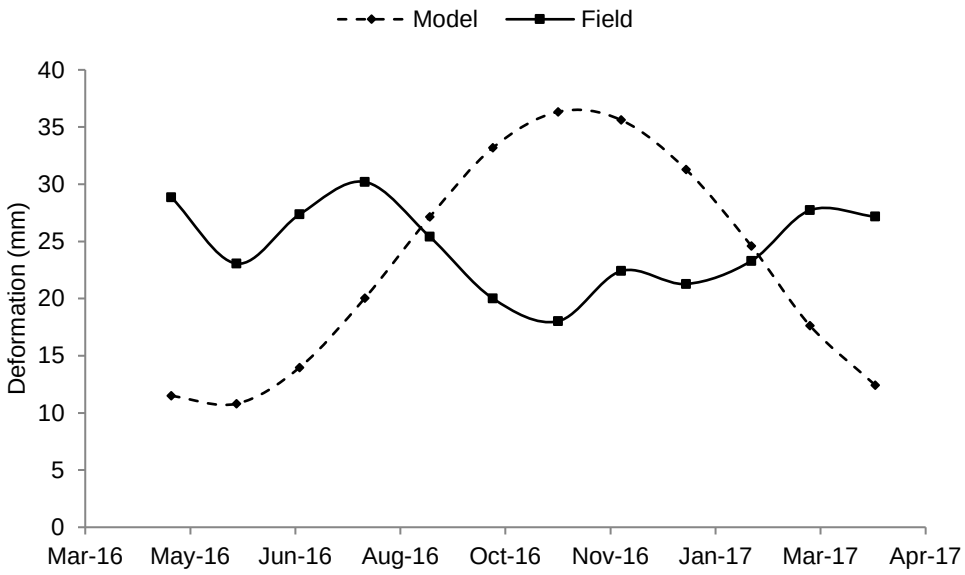

Figure 4:16 Comparison of model and field results with seasonal effects

In the preliminary stage, initial understanding was obtained through scatter plot. Beginning with the linear relationship, exponential, power, quadratic, etc. trends were tried unsuccessfully to determine the correct factor. Hence, values were considered for transformation on both the x and y axes, with log function considered for the initial transformation. A limited linear trend was found for the data. In order to increase the accuracy, a logarithm of the squared value of the difference and squared rainfall data were plotted in the y and x axes, respectively. As shown in Figure 4:17, two different linear trends were observed: first, when it corresponded with deformation factor more than 1, and the other when it was less than 1. The coefficient of determination (R^2) for both of the equations was over 0.85. The linear equations are as follows:

y (deformation factor) = 0.3169 x (rainfall factor) + 1.4849

y (deformation factor) = 0.7464 x (rainfall factor) - 2.221

where, y = squared value of log of difference between the actual and predicted value

and x = squared value of logarithm of rainfall.

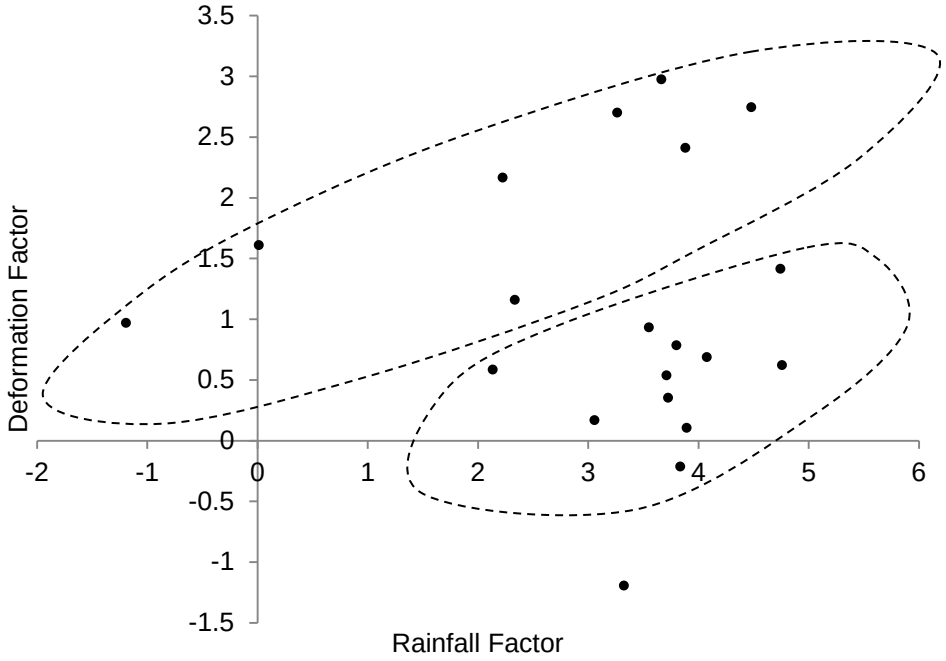

Figure 4:17 Rainfall factor for model modification

For example, in June 2016, the predicted and actual values were reported as 10.8038 and 23.058 mm, respectively. To find the deformation factor, the squared logarithm value rainfall value of the corresponding month (66.8 mm) was entered as ‘x’ in the first equation, as the difference factor was more than one. It yielded the ‘y’ value as 2.64, leading to a difference of the deformation of 19.92 mm. After adding this factor with 10.80 mm, the final predicted deformation became 30.72 mm, which was a difference of almost 7 mm from the actual one. Similar attempts were undertaken for rest of the months. The final deformation model values were plotted against the actual ones (Figure 4:18).

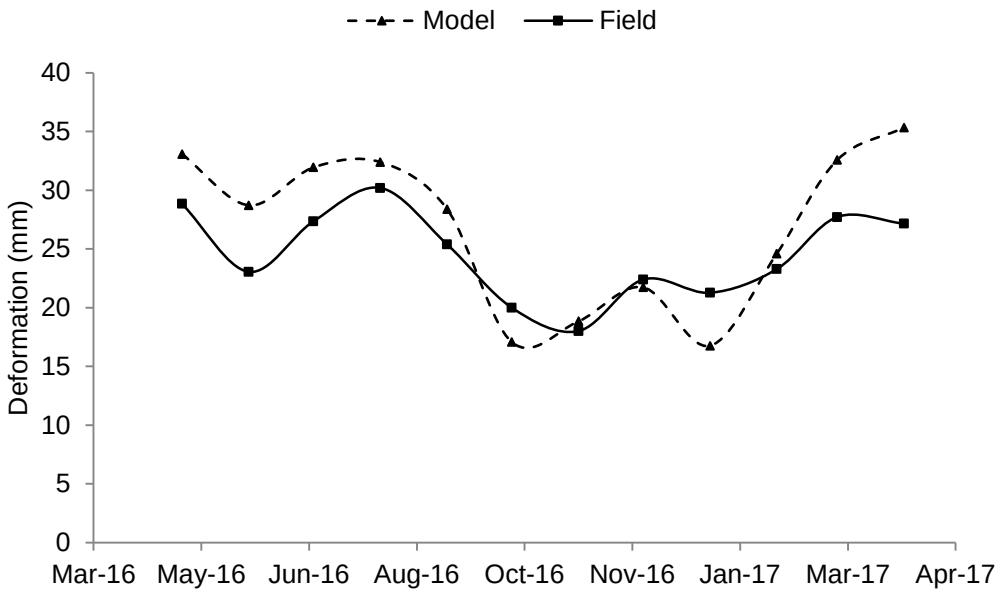

Figure 4:18 Comparison of model and field results on modified model

Based on the visual observation, it can be concluded that the improved model can capture the effect of rainfall. In order to further strengthen the findings, statistical analysis was performed.

Hypothesis testing was conducted to check whether there was a significant difference between the actual and predicted values. An independent two-sample t-test was performed to compare the mean values. The confidence level was assumed to be 90%. The basic hypothesis of the two-sample t-test can be described as follows:

$H_0: m_1 - m_2 = 0$

$H_a: m_1 - m_2 \neq 0$

where,

$m_1 =$ mean of the actual deformation

$m_2 =$ mean of the predicted deformation

Table 4:2 Summary of two-tailed t -test

	Mean	Std. Dev.	SE Mean	t- value	P- value
Actual	24.56	3.79	1.1	-1.0	0.332
Predicted	26.79	6.73	1.9		

From the test summary, it can be observed that the p- value was higher than the confidence level. In addition, the t-value was found lower than the critical value of the two-tailed test. Based on the test values, it can be concluded that the null hypothesis cannot be rejected, meaning that there is no significant difference of means between the actual and predicted values. Thus, the developed model can capture the rainfall effect at an acceptable level.

LIMITATIONS OF THE MODEL

The model was developed considering the homogenous soil layer, but not considering evaporation. The average deformation value was obtained from the field data of a specific site. Hence, it was required to perform a shrinkage-swelling test to learn the approximate average value (X) of deformation of a site other than the one tested. The first term of the developed deformation model, therefore, can be replaced by a deformation value obtained from a shrinkage-swelling test. The modified model looks as follows:

$$D = \mathrm{X} - 7.751 * \cos(x * 0.01858) - 10.4 * \sin(x * 0.01858) + \ Rainfall\ Factor$$

It is suggested that the incorporation of heterogeneous stratigraphy and the effect of evaporation would strengthen the model and requires further evaluation.

CONCLUSIONS

The study discusses the development of longitudinal cracks in flexible pavements built on expansive subgrades in North Texas. The role of moisture in the development of

cracks, intrusion of moisture from the edge, and the repetitive development of cracks every summer is also stated. Finally, it focuses on the statistical analysis of the associated parameters related to deformation. Temperature, suction, seasonal effects, rainfall, and other parameters were statistically and theoretically analyzed, and seasonal effects and rainfall distribution were determined as the dominant predictors for the deformation model. As the largest tensile stresses develop close to the shoulder, cracks initiate at the edge, for which edge deformation was considered for the model. Finally, predicted and actual edge deformation values were tested in a statistical environment, and the model was found to be in good agreement with the field values.

CHAPTER 5

NUMERCIAL MODELING OF EXPANSIVE SUBGRADES USING FIELD INSTRUMENTATION VALUES

Ahmed, A.[1], Hossain, M.S.[2]

[1]Graduate Research Assistant, Department of Civil Engineering, The University of Texas at Arlington, 416 Yates Street, NH 119, TX 76019; Email: asif.ahmed0@mavs.uta.edu

[2]Professor, Department of Civil Engineering, The University of Texas at Arlington, 416 Yates Street, NH 404, TX 76019; Email: hossain@uta.edu

(Shortened Version of this paper has been submitted to 97th Annual Meeting of Transportation Research Board, Submission ID: 18-04297

FEM Part of this paper has been accepted for 2nd Pan American Unsaturated Soil Mechanics Conference, Paper ID : 485507)

ABSTRACT

Moisture flow through unsaturated soils causes numerous geotechnical problems. Specifically, moisture plays an important role in the volumetric deformation of expansive subgrade soils. As a relationship between moisture variation and pavement performance exists, estimation of moisture variation in the subgrade soil could quantify pavement deformations. The objective of the current research is to investigate the moisture and suction variations of pavement sites due to real-time climatic loading, and to predict these results with numerical modeling. The selection of unsaturated parameters offers quite a challenge while modeling. The selection of unsaturated permeability and flow parameters is usually done in the laboratory by curve fitting because it is based on a specific condition of the soil which cannot be captured in a real-time field scenario. In this study, an attempt was undertaken to determine the variation of unsaturated hydraulic conductivity based on rainfall response data. Moisture sensors were installed at different

depths beneath the pavement and side slopes of a state highway and farm-to-market road in Dallas, Texas. During this study, a novel approach was taken to determine the flow parameters from field soil water characteristic curves. Field-based values were used in the PLAXIS 2D environment for transient analysis. The validity of the estimated parameters was confirmed, as FE results corresponded with direct field measurements. Analysis showed that change in suction at shallower depths recorded considerable variations. The study results indicated that FE modeling can provide effective information about subgrade matric suction variations.

INTRODUCTION

Expansive soils are usually clayey in nature and are susceptible to volumetric changes due to moisture variations. This volume-changing phenomenon induces larger stresses, which often cause cracking and settlement of pavement (Hossain et al. 2016; Djellali et al. 2011). Previous studies reported infrastructure damages associated with expansive clay ranging between 9 and 15 billion USD (Nelson and Miller 1992; Jones and Jefferson 2012). The Texas Department of Transportation (TxDOT) spends 25% of its annual maintenance and repair budget maintaining and repairing pavement distresses induced from expansive soil (Sebesta 2002).

The influence of moisture on changing the geotechnical properties of soil may lead to a shortened service life of pavement structures. Puppala et al., (2012) stated that severe pavement cracking can result in maintenance costs higher than the cost of construction. In particular, moisture redistribution under a pavement system has been identified as one of the major causes of pavement distress (Hedayati et al. 2015; Hossain et al. 2016). In-situ permeability can be an important indicator of moisture flow dynamics beneath pavement.

To consider the possible effects of moisture in the design procedures, many researchers have conducted field-based analyses to relate subgrade characteristics with environmental factors. Bayomy and Salem (2004) instrumented five different sites in Ohio. After monitoring them for a period of five years (1999-2003), the researchers reported the presence of seasonal moisture variations. Manosuthkij (2008) monitored four instrumented sites in Texas and found that when the mean moisture content, or the difference between the maximum and minimum moisture content of each month, was greater than 20%, edge cracking was likely to occur. In Ohio, Heydinger (2003) obtained data confirming both seasonal and temporary variations, due to precipitation, at two instrumented sites. Nguyen et al. (2010) instrumented two highway sites with 32 matric suction sensors and found an average matric suction of 40 kPa beneath the driving lane. The authors only mentioned the field data, however; no numerical modeling to simulate the field condition was reported.

One recent development in this area is the incorporation of numerical modeling to provide additional information on volumetric deformation. The finite element method (FEM) has been successfully utilized to account for the effects of many practical conditions more realistically than theoretical solutions based on infinite slab and other idealized assumptions (Kuo and Huang 2006). Previous researchers have used numerical modeling to predict the behavior of pavement built on expansive clay. Hedayati (2014) performed both unsaturated moisture diffusion and volume change in expansive subgrades. He preferred the Abaqus program for its ability to perform multiple nonlinear equations. Hashem et al. (2013) performed numerical modeling by Plaxis 2D software to simulate the behavior of flexible pavement built on expansive soil. Djellali et al. (2011) performed numerical modeling on expansive soil in Algeria. The authors concluded that the combined model, i.e., the Mohr-Columb model, shows that the majority of

displacements are in the shoulder side of the subgrade in pavement structures and soft soil in expansive subgrades, where the alligator cracking could be seen from field monitoring. Few researchers, however, have incorporated both field studies and the numerical environment. In addition, the use of realistic values of different soil parameters is always a challenge. Most of the researchers used laboratory-tested values in their numerical modeling. Laboratory testing captures a specific condition, whereas field conditions respond to climatic factors continuously. Therefore, incorporation of field values in numerical modeling is a necessity.

In the current study, attempts have been made to estimate the moisture and suction variations of expansive subgrades through both field instrumentation and numerical modeling. The study was conducted in North Texas, on two highways, designated as SH 342 and FM 2757. Moisture and suction sensors were installed in different depths to record the moisture variations with time. In order to do FEM, unsaturated soil permeability and flow parameters were obtained from field data rather than from laboratory testing. Suction and moisture variations were observed in the Plaxis 2D environment in flow mode. Eventually, FE results were compared with observed field measurements.

BACKGROUND OF THE STUDY

Developing a numerical model that captures the actual condition of the field requires exact soil parameters. Most of the previous studies used laboratory-based data for numerical modeling. Hedayati et al. (2014) performed numerical analysis on expansive subgrades and used a saturated permeability value of 3.54 x 10E-6 m/s for the modeling, even though the pavement subgrade is usually in an unsaturated state (Tom 2012). The authors also assumed the residual water content to be 0.11 m^3/m^3 based on Rawls & Brakensiek's 1989 study.

The twp most important design parameters for unsaturated conditions are hydraulic conductivity and flow properties. The following sections describe the background of unsaturated permeability and flow parameters, and determination of the two.

Unsaturated Hydraulic Conductivity

The most important factor affecting permeability is the interconnected void space (Ghorbanpourbabakandi, 2014). In expansive soil, permeability changes over time, especially after the formation of desiccation cracks. Vertical and horizontal permeability are not always the same. Bronswijk (1987) reported issues regarding flow mechanism changes in clay due to desiccation cracks. One of the major challenges while running the numerical modeling is the realistic value of hydraulic conductivity (Khan, Hossain and Ahmed 2017). Most of the researchers used the laboratory permeability value of saturated condition, which rarely exists in the field. Hossain (2012) used laboratory saturated hydraulic conductivity to simulate field behavior in the Plaxis environment. He used a value of 3.54E-9 m/s to account for both the horizontal and vertical permeability, and experienced discrepancies between the field and numerical results. Further, the author used reduced values of permeability at the crest of the slope, based on the rationale proposed by Zhan et al. (2007) that the increased infiltration rate in open cracks can be determined by performing the infiltrometer test. Subsequently, Hossain (2012) obtained improved results, but discrepancies remained. Based on test results in 1997 by Favre et al., saturation levels change after rainfall. Finally, Hossain (2012) ended up selecting three different permeability values, 3.54E-6 m/s; 3.54E-7; and 3.54E-8 m/s, in the top 3 m of soil to account for higher permeability. Khan et al. (2017) performed a flow analysis on a cracked highway slope and had the same issue of selecting correct permeability values for numerical modeling. Several permeability functions are used to

predict the unsaturated permeability after obtaining the Van Genuchten fitting parameters. The following equation, the Van Genuchten - Mualem function, is used to predict unsaturated conductivity if the saturated permeability is known (Ghorbanpourbabakandi, 2014).

$$k(\psi) = k_s S_e^{0.5} \left[1 - \left(1 - S_e^{\frac{1}{m}}\right)^m\right]^2$$

Where, S_e = effective degree of saturation

Khan et al. (2017) used Albrecht and Benson's 2001 laboratory experiment results on drying clay samples, which reported that hydraulic conductivity can increase up to 500 times after drying. Omidi et al. (1996) reported higher values of vertical permeability after desiccation cracks. The authors connected the wetting and drying cycles of expansive clay with the wetting-drying test of Albrecht and Benson (2001) and Omidi et al. (1996), and used a ratio of 22 for vertical-to-horizontal permeability. However, none of these researchers attempted to use the field value of hydraulic conductivity in numerical modeling. Hence, attempts were conducted during this study to determine the field hydraulic conductivity of soil samples in both horizontal and vertical directions. After determining the required parameters, values were inserted for numerical modeling. The subsequent section describes the methodology adopted for determination of field permeability for both horizontal and vertical directions.

Soil Water Characteristic Curve

The soil water characteristic curve is a unique property of each soil and is related to the soil particle size distribution and structure of the pore space. It describes the amount of water stored in a soil at a given suction (Tuller and Or, 2003) and requires knowledge of SWCC to model water flow in unsaturated soil. SWCC can be formed for a specific soil experimentally through drainage experiments; however, it is more convenient

to express the characteristic functions using proposed empirical models. Such three popular models are Brooks and Corey (1966), Van Genuchten (1980), and Clapp and Hornberger (1978). These are simple mathematical expressions that approximately fit the shape of SWCC for a specific soil.

SWCC Formulation

The suction-based method has been used to determine moisture variations in soils (Hedayati et al. 2014). Previous researchers have tried to incorporate suction-induced shrinkage to determine the volume change of soil (Puppala et al. 2014). Suction-related properties can be determined from laboratory testing. Currently, pressure plate, Tempe cell, and filter paper techniques are used for determining SWCC (Hedayati et al. 2014). However, these tests are time and labor intensive, and are highly dependent on the operator's skill. Moreover, according to Zapata (2000), a limited number of geotechnical laboratories perform suction-based tests; hence, determination of SWCC from physical properties of soil has been attempted. In addition, researchers have been using statistical analyses, physical tests, Artificial Neural Network (ANN), and genetic programming (GP) to determine SWCC (Hedayati et al. 2014).

In the current study, the WP4C Dewpoint Potentiameter was utilized to determine the SWCC of the soil. The equipment, manufactured by Decagon Devices Inc., uses the chilled mirror hygrometer technique to measure the matric suction and can determine the suction state of soil in a relatively small amount of time. In 'precious' mode, the device takes several subsequent readings, until the successive readings occur within a pre-determined tolerance. It usually takes 15-20 minutes to record a value; hence, a complete SWCC can be obtained in a timely manner. The WP4C can measure matric suction up to 450 MPa (Decagon Devices 2017). The specimens were prepared with de-aired/distilled water in order to minimize the effect of osmotic suction, as it measures total

suction, while the objective of the test was to obtain matric suction. A non-linear least-square technique was used to complete the SWCC curve, as per Fredlund and Xing's equation.

$$\theta_w = \left[1 - \frac{\ln\left(1 + \frac{\psi}{\psi_r}\right)}{\ln\left(1 + \frac{1{,}000{,}000}{\psi_r}\right)}\right] \frac{\theta_s}{\left(\ln\left(e + \left(\frac{\psi}{a}\right)^n\right)\right)^m}$$

where, θ_w is the volumetric water content; θ_s is the saturated water content; ψ is the matric suction; and ψ_r, a, n, and m are fitting parameters.

Based on the laboratory investigation, the saturated volumetric moisture content (Θ_s) was found to be 0.46. The values of the shape parameters, α (=0.06) and n (=1.8), were found after being fitted with the Van Genuchten equation.

SWCC Parameter Values

Hedayati et al. (2014) determined that saturated water content (Θ_s) was 0.56 m^3/m^3, but used the value for residual water content (Θ_r) proposed in literature. The authors determined the Van Genuchten flow parameters (α, n, m) from obtaining a SWCC curve from soil index properties.

Schaap et al. (2001) determined the unsaturated hydraulic properties of soil for 12 textural classes of USDA textural triangles. The authors reported the value of residual water content, saturated water content, α, and n for clay samples as 0.098, 0.459, 0.015 and 1.25, respectively.

Tuller et al. (2003) tabulated unsaturated flow parameters for various soil textural classes from the unsaturated soil hydraulic database (UNSODA). They reported values of residual water content, saturated water content, α, and n for clay samples as 0.102, 0.51, 0.021, and 1.20, respectively. None of the previous researchers attempted to record both laboratory and field-based SWCC. Alam (2017) reported both field and lab scale SWCC

parameters. The author conducted percolation analysis in vegetated lysimeters in the top cover soil of a landfill. Based on the laboratory testing conducted using a Tempe cell and dewpoint potentiometer, values of α, n, and m were reported as 0.0031, 1.6, and 0.375, respectively. The values obtained from field water characteristic curves were 0.02, 1.52, and 0.3421, respectively. As can be seen, the value of α changed from 0.0031 to 0.02 as the SWCC changed to FSWCC.

METHODOLOGY

Description of Site

The study area was selected, based on TxDOT maintenance records, over State Highway 342 (SH 342) in Lancaster, Texas, in Ellis County and FM 2757 in Kaufman County. The locations are always accessible and free from any utility lines, and both had experienced cracking due to expansive subgrades. The site location is presented in Figure 5:1(a), and photos of the sites are presented in Figure 5:1(b).

The SH 342 test site is located on a two-lane highway, with 11 ft. wide lanes. Each side of the road has an 11 ft. wide shoulder. The pavement is fairly level with the ground, and is flanked on both sides by grass and dense trees. Edge drops several inches in depth were observed in the pavement shoulder. No bodies of water were observed near the project site. The test site in Kaufman County was located on a farm-to-market road identified as FM 2757 in Forney, Texas. The low-volume road consisted of two lanes, each measuring 11 ft. wide, with no shoulder. The side slopes on both sides were covered with grass and dense trees. Based on the collected soil samples, it was found that more than 85% soil passed through the 200 No. sieve. The liquid Limit (LL) varied between 50 and 64, and the plasticity index (PI) ranged between 28 and 42. Per the sieve analysis and Atterberg limits, the soil was classified as high plastic (CH) clay.

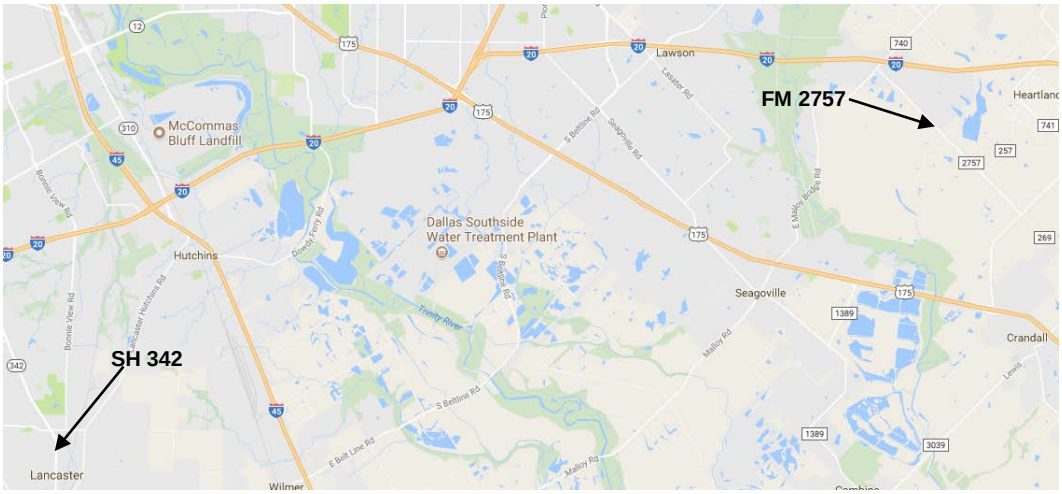

(a) (b)

Figure 5:1 (a) Location of SH 342 site, (b) SH 342 in Ellis County, Texas

Sensor Selection and Installation

A comprehensive field instrumentation layout was designed to monitor moisture variations in the subgrade soil. The installation for both of the sites was performed beneath the northbound lane, from the centerline towards the edge. Decagon 5TM moisture sensors were used to measure the volumetric moisture content, which was converted to gravimetric water content, using the soil's specific gravity and unit weight. An ECRN-100 high resolution rain gauge was installed on-site to record rainfall events, and an EM50 data logger was placed to collect the data from the moisture sensors and

the rain gauge. The data logger can measure the data continuously and can store up to 36800 scans (Decagon Devices 2017). Water potential probes were also installed in SH 342 to record the suction changes.

During installation, a 24 in. (0.6 m) wide and 18 in. (0.5 m) deep trench was excavated. Boreholes were drilled up to desired depths to collect soil samples. After installing moisture and suction sensors in the boreholes up to a depth of 4.5 m, the boreholes were backfilled. Finally, the trench was backfilled. Upon repaving the surface, sensors were connected to the data loggers, and a roadside rain gauge was installed. The instrumentation plan is shown in Figure 5:2, and some instrumentation photos are exhibited Figure 5:3.

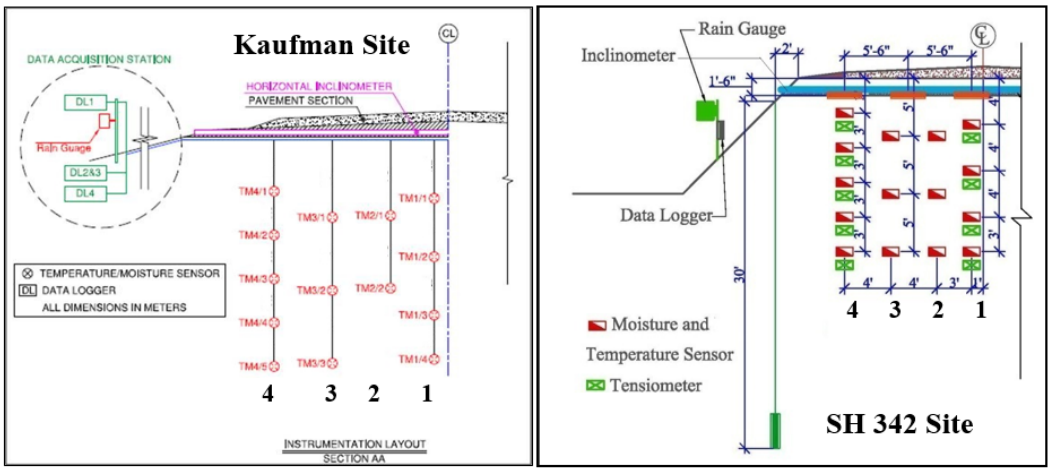

Figure 5:2 Instrumentation at two field sites

(a) (b)

Figure 5:3 (a) Instrumentation plan for pavement, (b) Field instrumentation on SH 342

Determination of Vertical Permeability

A roadside tipping bucket rain gauge was installed to obtain hourly rainfall data. Moisture variations, due to rainfall, in a borehole located in SH 342 are described below. Installed sensors were programmed to store data hourly, and the collected data was averaged into daily values. The moisture variation was monitored based on the daily averages. Sensors at 4 ft. (1.2 m), 8 ft. (2.4 m), 12 ft. (3.7 m), and 15 ft. (4.5 m) depth were installed in the center borehole of the pavement. The notation mentioned in the figure refers to the depth at which the sensor is installed, e.g., TM 8 stands for the temperature and moisture sensor at 8 ft. (2.4 m) depth. Moisture variation curves produced from the readings are shown in Figure 5:4. Most sensors registered instantaneous responses to rainfall. TM 15, located 15 ft. below the ground surface, recorded no appreciable changes in moisture content for any rainfall amounts. The average soil moisture at this depth was recorded as 19%, which was considered as the point of saturation at this depth. The values at which the moisture content readings stabilized were considered the equilibrium moisture contents for the remaining depths.

The equilibrium moisture content for TM 4 was 11%. Sensors TM 8 and TM 12 showed average moisture contents of 6% and 15%, respectively.

Seasonal variation is dependent on the initial moisture content, ground water table, soil type, and soil compaction level. Therefore, it is possible for moisture variations in some locations to exhibit a seasonal pattern, while others do not. The collected data showed that all sensors at SH 342 maintained an equilibrium moisture content that changed only as a response to rainfall.

Sensors at varying depths experienced individual peaks in response to each rainfall event. Moisture contents rose 1% to 15% in amplitude and were likely limited to the temporary saturation point at each respective depth. Since temporary variations occurring within a short time period can induce volumetric deformation in expansive clay, the temporary rises in moisture content are important to consider. The largest increases were seen during periods of extended rainfall events from February 2015 to May 2015. Continuous climatic loading prevented the dissipation of moisture, allowing for such high increases. TM 8 experienced greater rises in moisture content than TM 12, a result that can be attributed to the sensor's proximity to the ground surface. Excessive moisture dissipated after the continuous rainfall ceased, resulting in a decrease in moisture content.

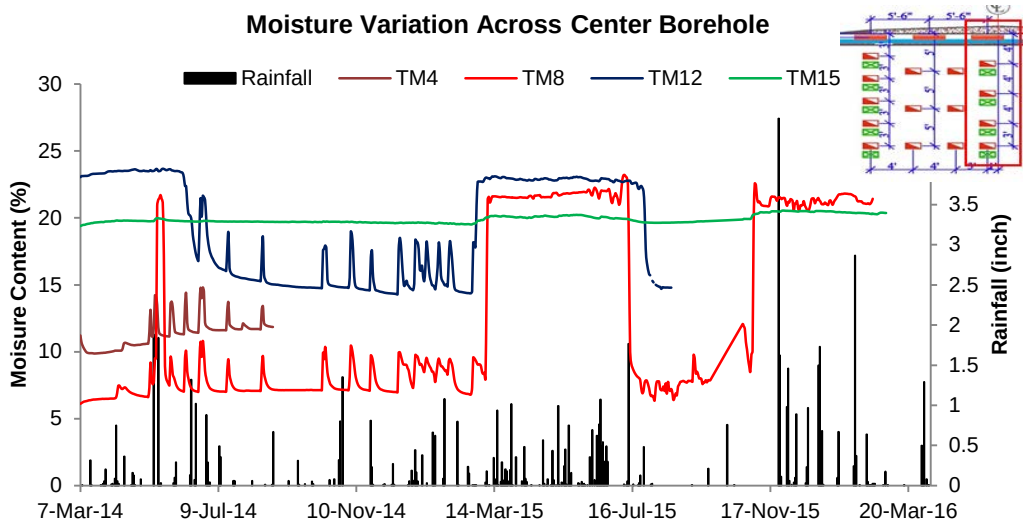

Figure 5:4 Moisture variation in center borehole

In order to determine the vertical permeability from real-time moisture data, two rainfall events were considered, as presented in Table 5:1. Based on the individual rainfall intensity amounts presented in Table 5:1, significant spikes in moisture content were observed to occur at different times at the different depths. The time-dependent moisture variations at the 1.2 m and 2.4 m locations are presented in Table 2. In the case of the rainfall event of July 17, 2014, sensors at 1.2 m experienced an increase of moisture content at 2:00 p.m., whereas sensors at 2.4 m experienced the increase at 4:00 p.m., a two-hour delay between the sensors' responses (Table 5:2). The vertical field permeability can be determined by finding the ratio between the vertical distance traveled by the water and the time required to travel that distance. Hence, the 2 hr. (7200 sec.) time difference can be equated to travelling a distance of 1.22 m between the two sensors located at the same borehole, leading to a permeability value of 1.69E-04 m/s.

Table 5:1 Duration and Intensity of Rainfall at SH 342

Time	Rainfall (mm)		Rainfall (mm)
7/17/2014 11:00 AM	1.4	11/22/2014 6:00 PM	1.4
7/17/2014 12:00 PM	1.8	11/22/2014 7:00 PM	1.0
7/17/2014 1:00 PM	0.5	11/22/2014 8:00 PM	1.4
7/17/2014 2:00 PM	1.2	11/22/2014 9:00 PM	1.4
7/17/2014 3:00 PM	2.0	11/22/2014 10:00 PM	1.0
7/17/2014 4:00 PM	0.2	11/22/2014 11:00 PM	0.6
		11/23/2014 12:00 AM	0.2
		11/23/2014 1:00 AM	0.2
		11/23/2014 2:00 AM	0.2
		11/23/2014 3:00 AM	0.2
		11/23/2014 4:00 AM	0.0
		11/23/2014 5:00 AM	0.2
		11/23/2014 6:00 AM	0.0
		11/23/2014 7:00 AM	0.2

A similar phenomenon was observed in the same pair of boreholes for another rainfall event on November 23, 2014. The sensor at 1.2 m experienced the increase of moisture at 2:00 a.m., and the sensor at 2.4 m experienced the increase at 8:00 a.m. (Table 5:2). Given a time lag of 6 hours (21600 sec), the permeability value was 5.65E-5 m/s. It is interesting to note that the vertical permeability value obtained from the first rainfall event was three (3) times greater than the value obtained from the second rainfall event.

Table 5:2 Variation of VMC in Response to Rainfall at Different Depths of SH 342

Time	1.2 m.	2.4 m	Time	1.2 m.	2.4 m
7/17/2014 12:00 PM	0.174	0.366	11/22/2014 11:00 PM	0.176	0.338
7/17/2014 1:00 PM	0.174	0.366	11/23/2014 12:00 AM	0.176	0.337
7/17/2014 2:00 PM	***0.217***	0.366	11/23/2014 1:00 AM	0.176	0.338
7/17/2014 3:00 PM	0.274	0.385	***11/23/2014 2:00 AM***	***0.210***	0.338
7/17/2014 4:00 PM	0.273	***0.461***	11/23/2014 3:00 AM	0.244	0.338
7/17/2014 5:00 PM	0.270	0.468	11/23/2014 4:00 AM	0.245	0.338
			11/23/2014 5:00 AM	0.248	0.338
			11/23/2014 6:00 AM	0.249	0.339
			11/23/2014 7:00 AM	0.249	0.343
			11/23/2014 8:00 AM	0.247	***0.392***
			11/23/2014 9:00 AM	0.245	0.415
			11/23/2014 10:00 AM	0.243	0.417

Effect of Rainfall Duration and Intensity on Permeability

The differences in values of vertical permeability can be attributed to rainfall duration intensity. The rainfall event in July 2014 was observed to have a higher intensity than the rainfall event in November 2014, resulting in the differences in permeability. The cumulative rainfall amount on July 14 was 7.1 mm in six (6) hours, whereas it was 8 mm over a period of thirteen (13) hours on November 23. Table 5:1 states the details of these two rainfall events. For example, on July 17, 2014 at a depth of 4 ft., an additional 1.2 mm of rainfall, following a previous cumulative rainfall of 3.7 mm, resulted in a change in moisture content. The volumetric moisture content rose from 17.4% to 21.7%. A similar increase in moisture content was not observed simultaneously at a depth of 8 ft. Rather,

after 2.2 mm of additional rainfall, the deeper sensors recorded an increase from 36.6% to 46.1%, which was two hours after the sensors at 4 ft. experienced an increase in moisture readings. A similar phenomenon was observed on November 23, 2014. A rainfall event from the previous day yielded a change in volumetric moisture content of 17.6% to 21.0% at a depth of 4 ft. Sensors at 8 ft., however, did not experience a change in moisture at the same time. After a period of six (6) hours and an additional 0.6 mm of rain, the moisture content increased from 34.3% to 39.2%. Based on the difference of the permeability values for two different rainfall events, it can be concluded that, given an equal amount of rainfall, a shorter period of rainfall correlates to a higher intensity and thus greater permeability through the soil. Conversely, lower intensity correlates to lower permeability. An average of these two values, 1.13E-04 m/s, was used for numerical modeling.

Determination of Horizontal Permeability

The same approach was taken to determine permeability in the horizontal direction. Horizontal permeability was studied by observing the time lag between moisture readings from the edge and center boreholes at the FM 2757 Kaufman County site. The moisture distribution, in response to rainfall, in the edge and center boreholes is presented (Figure 5:5).

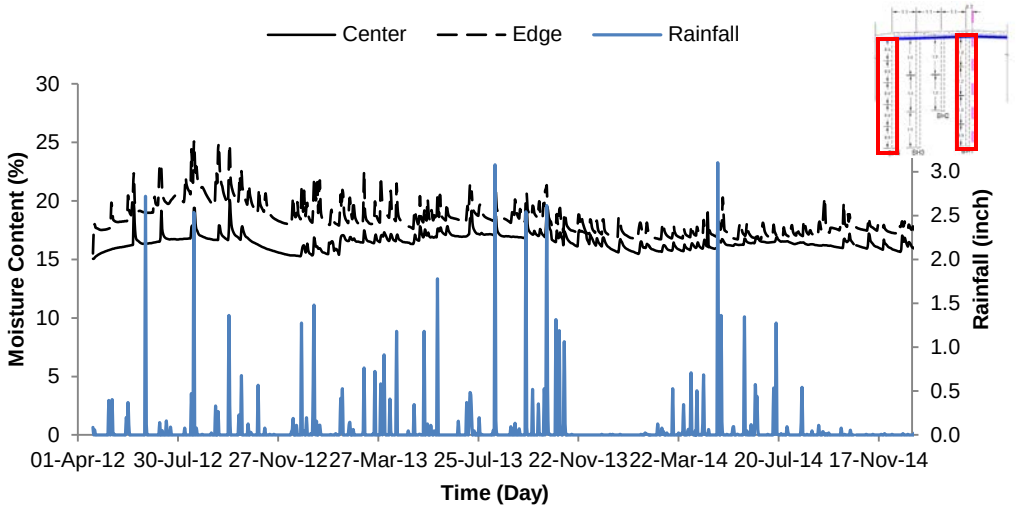

Figure 5:5 Edge and center moisture variations in FM 2757

The sensors installed at the edge and center exhibited similar responses after rainfall. Moisture content increased after precipitation and returned to its equilibrium value after the rain ceased. Sensors were programed to collect hourly data; however, data was averaged for each day while plotting against rainfall to simplify the computations. The average moisture content for the center borehole was recorded around 15-16% and experienced a 3-4% increase in amplitude after rainfall. Similarly, the edge borehole exhibited the same trend, while having an average moisture content somewhat higher than that of the center borehole. The increase can be attributed to edge moisture intrusion from the grassy side slope. Hourly data was used for determination of horizontal permeability, as presented in the next section.

Two rainfall events were considered for determination of horizontal permeability. On August 18, 2012, a time lag of five hours and an additional 26.8 mm of rainfall existed between moisture content increases at the edge and center boreholes for both sensors installed at 1.2 m (Table 5:3). The sensor at the edge had a peak in moisture content at 1:00 a.m., whereas the sensor at the center peaked at 6:00 a.m. Five hours were

required for the water to travel 3.29 m between the boreholes, resulting in a horizontal field permeability of 1.83E-04 m/s.

Table 5:3 Rainfall Event of August 18, 2012 at FM 2757

Time	Edge	Center	Rainfall (mm)
8/18/2012 12:00 AM	0.314	0.229	7.0
8/18/2012 1:00 AM	***0.373***	0.229	5.8
8/18/2012 2:00 AM	0.367	0.229	0.0
8/18/2012 3:00 AM	0.367	0.228	0.0
8/18/2012 4:00 AM	0.383	0.228	19.6
8/18/2012 5:00 AM	0.365	0.228	7.2
8/18/2012 6:00 AM	0.352	***0.262***	0.0
8/18/2012 7:00 AM	0.354	0.271	0.0
8/18/2012 8:00 AM	0.355	0.269	0.0
8/18/2012 9:00 AM	0.354	0.268	0.0

Similarly, a difference of nine hours and 13.5 mm of rainfall were observed between the edge and center boreholes on September 29, 2012 (Table 5:4). Given the time lag of nine hours (32400 sec.) and a distance of 3.29 m, horizontal permeability of 1.02E-04 m/s was obtained. Once again, rainfall events with higher intensity resulted in higher field permeability. The rainfall event of August 18, 2012, with 39.6 mm of rain in 9 hours, exhibited a higher permeability value than that of September 29, 2012 with 27.3 mm in 15 hours. As such, 1.8 times permeability value was recorded with increased rainfall intensity from 1.82 mm/hr. to 4.4 mm/hr. Average values of 1.02 and 1.83, 1.43E-04 m/s, were used for numerical modeling.

Table 5:4 Rainfall Event of September 29, 2012 at FM 2757

Time	Edge	Center	Rainfall (mm)
9/29/2012 6:00 AM	0.290	0.221	0.2
9/29/2012 7:00 AM	0.290	0.221	0.1
9/29/2012 8:00 AM	0.290	0.221	0.0
9/29/2012 9:00 AM	***0.387***	0.222	0.5
9/29/2012 10:00 AM	0.392	0.221	0.8
9/29/2012 11:00 AM	0.380	0.222	0.5
9/29/2012 12:00 PM	0.361	0.222	0.8
9/29/2012 1:00 PM	0.355	0.222	0.8
9/29/2012 2:00 PM	0.352	0.222	0.0
9/29/2012 3:00 PM	0.352	0.222	0.8
9/29/2012 4:00 PM	0.351	0.222	2.8
9/29/2012 5:00 PM	0.351	0.228	4.6
9/29/2012 6:00 PM	0.351	***0.273***	2.4
9/29/2012 7:00 PM	0.350	0.269	3.8
9/29/2012 8:00 PM	0.348	0.267	5.2
9/29/2012 9:00 PM	0.348	0.265	4.0

Field Soil Water Characteristic Curve (FSWCC)

The second challenging task, after obtaining the field permeability, was to determine the field-based unsaturated flow parameters. After generating the SWCC curve and determining the required parameters, attempts were made to determine the SWCC from field data. As many undetermined factors exist in the field, it was expected that parameters obtained from the field curve would be more realistic.

FSWCCs were developed, based on the field-instrumented moisture content sensors and tensiometers (Ahmed, Hossain, Alam and Khan 2017). Alam et al. (2017) determined field-based SWCC in vegetated lysimeters from similar instrumentation, and determined a total of three curves: upper bound, lower bound and the average, based on the scattered plot of the FSWCC. The FSWCC curve obtained from instrumented pavement is shown in Figure 5:6. Data from each FSWCC was fitted with the following Van Genuchten's equation (Van Genuchten 1980).

$$\theta = \theta_r + (\theta_S - \theta_r) \left\{\frac{1}{1 + (\alpha\psi)^n}\right\}^m$$

Where, ψ = soil suction (tensiometer data), Θ = volumetric moisture content (moisture sensor data). α and n are the shape parameters and $m = 1 - n^{-1}$. The saturated VMC (Θ_s) based on the field SWCC was 0.46 and residual VMC (Θ_r) for was found to be 0.11. The values of shape parameters, α (=0.089), n (=3.8) and m (=0.74) were found after being fitted with the Van Genuchten equation.

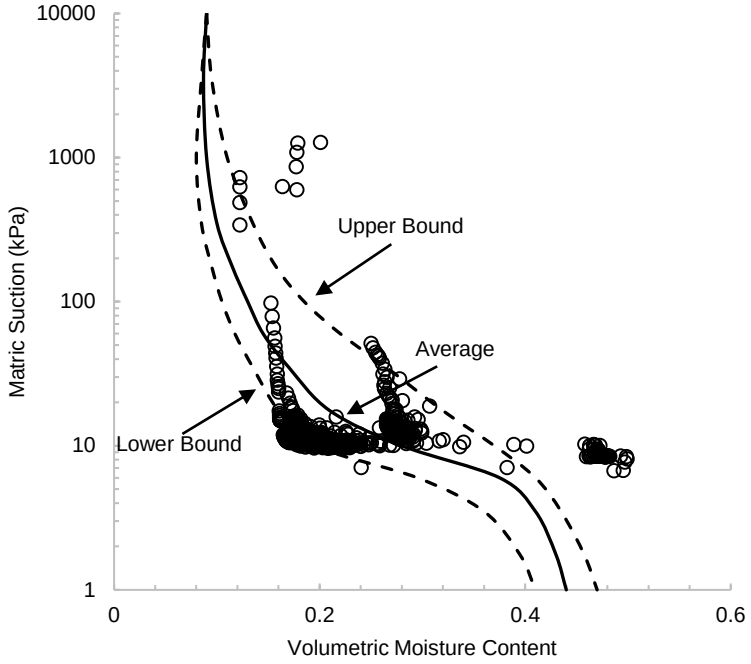

Figure 5:6 Field-based SWCC from SH 342 field data

It can be observed that the fitting parameters obtained from field and laboratory SWCC were not same. Field conditions present some undetermined factors and heterogeneity, and, most importantly, represent a continual portrayal of the actual condition. Hence, fitting parameters obtained from field SWCC were utilized in numerical modeling.

Table 5:5 Van Genuchten Fitting Parameters from FSWCC

	Fitting Parameters			Θ_s	Θ_r
Field	α	n	m		
SWCC	0.089	3.8	0.74	0.46	0.11

RESULTS AND DISCUSSION

The following sections contain the instrumented results, model calibration for the numerical analysis, and comparison of the FEM output with field measurements. The result section discusses both moisture and suction data; however, validation is only presented for suction results. In addition, although sensors measuring various parameters (e.g., moisture, and suction) were installed at different locations of subgrades, this paper focused on moisture and suction data from one borehole (center) to briefly present the behavior of expansive subgrades in response to climatic loading.

Instrumented Results

The recorded data indicates a significant change of moisture content (Figure 5:7a), hence corresponding variation of suction value (Figure 5:7b), at shallower depth (4 ft.). Stable moisture content and suction values were observed at a deeper depth (15 ft.). The moisture sensors recorded values at volumetric basis, which were converted to gravimetric values. Shallower sensors exhibited a constant moisture content of 6%, followed by a temporary increase up to 10% in response to precipitation. In contrast, sensors at 4.5 m depth recorded a constant value of 20%, with minimal response to environmental loading. A similar observation was made for suction sensors, where the deeper ones were almost constant, while fluctuation of suction values was observed for shallower sensor.

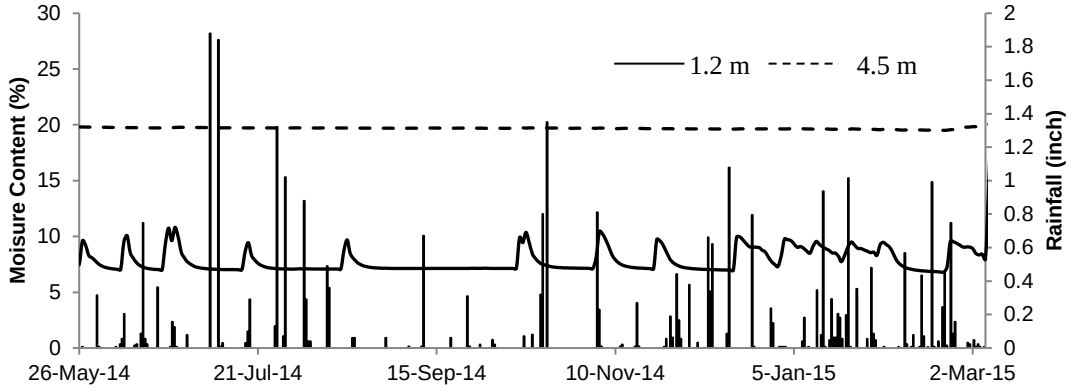

(a)

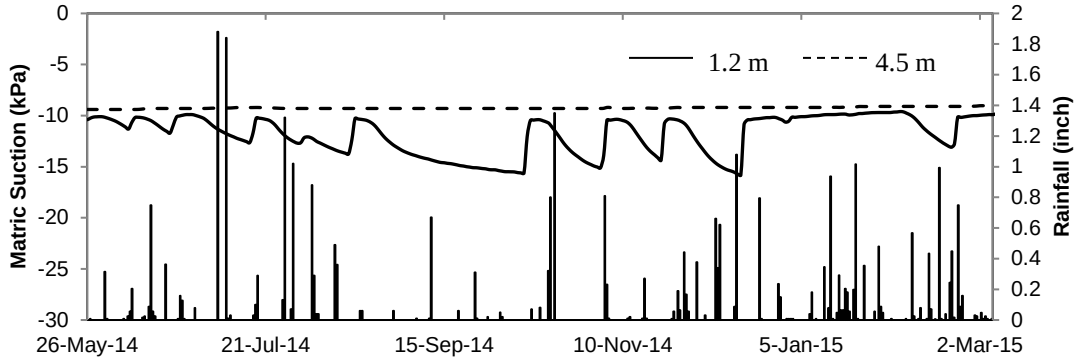

(b)

Figure 5:7 (a) Moisture variation and (b) Suction variation in center borehole of SH 342

Model Calibration

Rainfall and suction values from 8/12/2014 to 9/12/2014 were used for calibration of the model. Parameters obtained from field SWCC were utilized in a flow analyses in Plaxis to incorporate the unsaturated flow condition. Several trials were performed until the observed suction values were in good agreement with the sensor recordings. Typical model outputs exhibited the changes in saturation and suction values before and after

rainfall (Figure 5:8). As the pavement is symmetrical, only half of the geometry was used for modeling purposes.

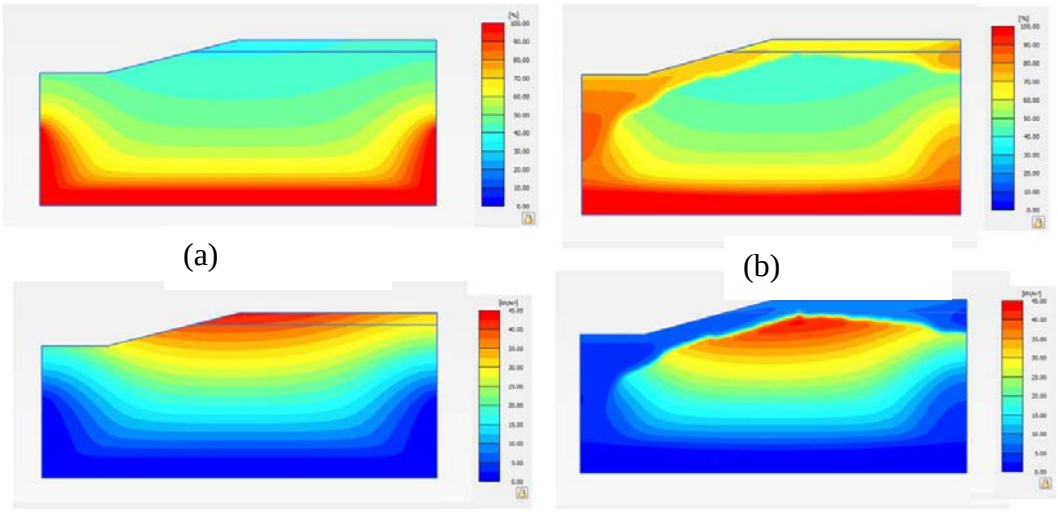

(a) (b)

(c) (d)

Figure 5:8 (a) Saturation level before rainfall (b) Saturation level after 4 days of rainfall (c) Suction level before rainfall (d) Suction level after 4 days of rainfall

Finite Element Results

Several rainfall events were recorded between 10/21/2014 and 12/17/2014; hence, corresponding moisture and suction changes were observed in the subgrade moisture sensors. FE results showed the smallest variations at deeper depths. The comparison of the model and field data is shown in Figure 5:9. The modeling behavior was similar to the observed values in the field. The suction change pattern was similar, and the values were close to those observed in the field. As the suction sensors located at 4.5 m recorded no variation of suction, values of 1.2 m were only compared with the field data. Rainfall events between October and November 2014 were used for the first case, while the following case represents the consecutive months. It can be observed that the suction values increased when there was no rainfall event, and dropped

immediately after the rainfall event, which was captured in the numerical environment also.

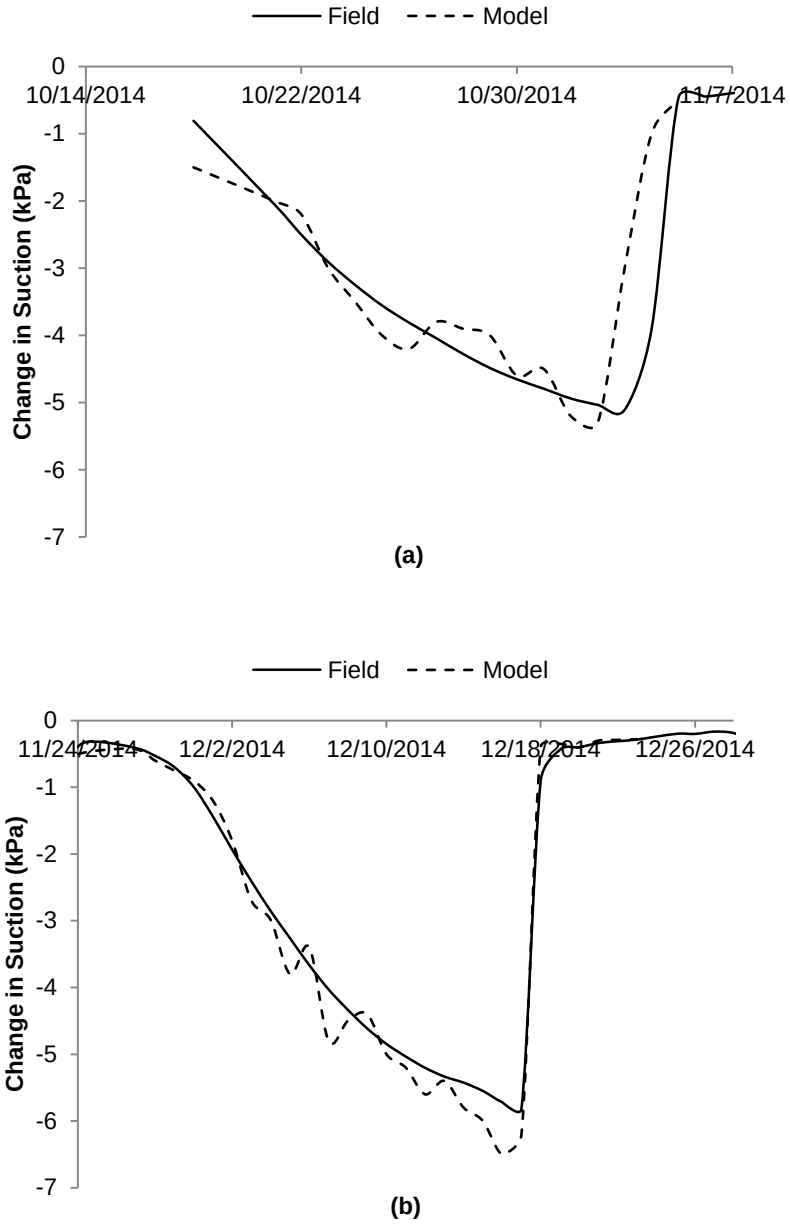

Figure 5:9 Field and numerical model comparison for rainfall event of (a) October 2014 and (b) November 2014

Minor differences in the change in suction values were observed for both cases. Without considering the effect of evaporation, the absence of heterogeneity of soil in the numerical environment might lead to the differences. However, the numerical model was successful in capturing the increase of suction during an absence of rainfall and subsequent drop after rainfall.

CONCLUSION

Moisture and suction changes in the subgrades of a 2-lane state highway and farm-to-market road were monitored through field instrumentation and modeled in a numerical environment. The sites were instrumented with moisture and suction sensors and rain gauges to record hourly rainfall. SWCC of the soils was determined, using both laboratory testing and field data. Field-based SWCC parameters were used for numerical modeling, as it represents the actual condition of the field. In addition, horizontal and vertical permeability were determined from response to rainfall of moisture sensors installed in the sites. The real-time data was used for climatic loading, and results were compared with the sensor results in the field. Moisture and suction sensors at deeper depths (4.5 m) recorded no variations, which was also captured in numerical modeling. Sensors at 1.2 m experienced temporary changes due to rainfall. FE results also captured the change in suction values during and after rainfall events. The study indicated that FE modeling, using SWCC and permeability from field data, can provide effective information regarding subgrade moisture and suction changes.

CHAPTER 6

USE OF MODIFIED MOISTURE BARRIER TO MITIGATE PAVEMENT EDGE CRACKING IN NORTH TEXAS

Ahmed, A.[1], Hossain, M.S.[2]

[1]Graduate Research Assistant, Department of Civil Engineering, The University of Texas at Arlington, 416 Yates Street, NH 119, TX 76019; Email: asif.ahmed0@mavs.uta.edu

[2]Professor, Department of Civil Engineering, The University of Texas at Arlington, 416 Yates Street, NH 404, TX 76019; Email: hossain@uta.edu

(Shortened version of this paper has been submitted to 97th Annual Meeting of Transportation Research Board, Submission ID: 18-05256)

ABSTRACT

Pavement serviceability can be reduced as the result of seasonal climatic variations in subgrade soil. Variations in moisture may alter material properties as well as cause shrinking and swelling in expansive subgrades. This study reflects two-fold objectives: (1) establish the rationale of selecting a modified moisture barrier to prevent moisture from entering the subgrade, and (2) observe the benefits of the selected barrier with respect to preventing moisture variations in subgrade. The modified moisture barrier that was used in this study was a combination of a 40 mil LLDPE geomembrane and an 8-oz. HDPE geocomposite. Based on the observation of edge moisture intrusion, the moisture barrier, consisting of a geomembrane and a geocomposite (geonet sandwiched between two nonwoven geotextiles) was placed in a 50 ft. section in FM 987 in Kaufman County, Texas. A control section along the same roadway was instrumented and monitored for comparison. Variations in subgrade moisture content were monitored using in-situ moisture sensors and geophysical testing in the form of electrical resistivity imaging (ERI). Deflections and moisture contents were continuously monitored in both

the barrier section and the control section. The field monitoring results clearly indicated that the moisture barrier significantly reduced the water infiltration near the edge of the pavement and reduced the movement of the pavement by 80%.

INTRODUCTION

Expansive soils can impact the structures that are built upon them. In fact, estimates show that damages to structures, resulting from expansive soils, range from 9 billion USD to 15 billion USD annually (Steinberg 1989; Nelson and Miller 1992; Jones and Jefferson 2012). More than half of these damages occur on highways and streets (Steinberg 1989). Expansive soil is found throughout the United States; in fact, only six of the contiguous United States do not identify as having expansive soils (Steinberg 1989). Expansive soils extend across Texas, in particular. Repair and maintenance account for 25% of the Texas Department of Transportation's annual expenditures (Sebesta 2002), and the maintenance costs associated with severely cracked pavement can exceed construction costs (Puppala et al. 2012). Therefore, it is important to address the expansive subgrade soil at the design stage if at all possible, or at the maintenance stage if the facility has already been constructed and is experiencing distresses associated with expansive soils.

The relationship between expansive soils, moisture content, and pavement are as follows. Expansive soils expand when they gain moisture and shrink when they lose moisture. As a result, soil layers above the expansive soils move upward when the expansive soils gain moisture and move downward when the expansive soils lose moisture. If the layers of expansive soil experience the same moisture changes, then the entire structure would just move up and down with changing moisture. However, the expansive soil layer may have areas with soils of different characteristics or different moisture contents, and, as a result, the soil layers above the expansive soils can exhibit

differential movement, causing damage to buildings, highway pavements, and airport pavements resting on shallow foundations.

Pavement distresses can appear as a result of the swelling and shrinking actions of expansive soils. Longitudinal cracks form on the surface of the pavement as a result of the expansion and contraction of subgrade soil, and moisture intrusion from the edge of pavement causes longitudinal cracks near the edge of the pavement. These longitudinal cracks near the edge of pavement are known as edge drops. In addition to the distresses caused by vertical movement, areas of expansive soil near areas of soil that are not expansive will cause differential movement, resulting in worse pavement distresses. Excessive moisture coupled with inadequate drainage has been reported as a major source of failure of flexible pavements (Elseifi et al., 2001). Excessive moisture weakens the subgrade soil and aggregate layers, leading to low shear strength and ultimately reducing the bearing capacity of the subgrade.

Moisture control is an overall indicator of the performance of pavement. Previous researchers (Eleseifi et al., 2001, Christopher et al. 2000, Henry and Banya 2002) discussed different approaches to mitigating moisture intrusion in pavements by increasing the drainage capability after precipitation. The objective of this paper is to discuss the efficiency of geosynthetics in preventing moisture from entering the subgrade. Based on the observations and limitations of the previous studies, this paper covers expansive soil treatment methods, evaluates the effectiveness of using geosynthetics as barriers compared to the conventional method, discusses the rationale of using a modified barrier in this study, provides data on the selection of geosynthetic layers, and presents preliminary results on the efficiency of a newly designed geocomposite membrane system.

The objective of this research was to assess the effectiveness of employing a modified (horizontal/sloped) moisture barrier to prevent the intrusion of moisture into the expansive subgrade soil and the pavement distresses resulting from this moisture variation. Moisture variations through moisture sensors and electrical resistivity, vertical deformation through inclinometers, and rainfall amounts through a rain gauge were monitored in a typical two-lane pavement. A monitored control section and a monitored experimental section contained the modified moisture barrier. Effectiveness of the modified moisture barrier was assessed through pavement performance. The geotechnical properties of the subgrade soil were determined through site investigation. A conclusion as to the effectiveness of the modified moisture barrier is presented.

EXPANSIVE SOIL TREATMENT METHODS

Transportation agencies have attempted numerous methods to control volume changes which can be categorized either as a method of (1) alteration of expansive soil by mechanical, chemical, or physical means or (2) control of subgrade moisture conditions (Snethen 1979; Hammitt and Ahlvin 1973, and FHWA 1980).

Mechanical means of altering expansive soil include ripping, scarifying, and then compacting the soil with moisture and/or density control; sub-excavation and replacement with granular, non-swelling or chemically-treated materials; and the use of fills over expansive soils to reduce heave as a result of the external load. Physical means of alteration involve the mixing of granular or non-swelling material into the expansive soil. Chemical alteration is where chemical additions to the expansive soil are used to alter the soil properties. The primary method for chemical alteration in expansive soils is lime stabilization.

Pre-wetting of the subgrade and isolation of the subgrade soil from moisture variations are two methods of controlling the subgrade moisture conditions. Pre-wetting

or ponding is based upon the idea that allowing pre-swelling to occur before construction will reduce the volume change that occurs after construction. Limitations include its application only before construction and the increased construction time.

Isolation of the subgrade soil from moisture variations will obviously prevent the subgrade soil from changing in volume, as the moisture variations would be minimal or nonexistent. Physical barriers with waterproofing membranes can be used for this purpose. Asphalt membranes sprayed over the subgrade, ditches, verge slopes, back slopes, full-depth asphalt pavement with a sprayed-on asphalt or synthetic fabric membrane beneath the ditch, full-depth asphalt pavement with paved ditches in cut sections, and vertical synthetic impermeable fabric membrane cutoffs have been used as physical moisture barriers.

BARRIER WITH GEOSYNTHETICS

Compared with physical alteration and removal of the native soil, controlling the moisture is more suitable in terms of construction difficulty, time, and cost, especially when the problem is extensive in amplitude. Elsefi et al. (2001) presented the difficulty of including moisture variations quantitatively in pavement design and rehabilitation; however, moisture drainage after precipitation events must be addressed during original design and construction practices. Therefore, a drainage system, like a permeable aggregate base, is a good solution and is reported as a popular trend by NCHRP Synthesis 239 (Christopher et al., 2000). Free-draining aggregates typically require treatment with asphalt or Portland cement, increasing the cost of the roadway significantly (Elseifi et al. 2001, Christopher et al. 2000). Therefore, the use of geosynthetics may be more beneficial than a drainage layer, as it serves several functions in addition to drainage. For example, geotextiles can serve the function of reinforcement of a particular layer; separation, drainage, or filtration; stress absorption;

and a moisture barrier (Koerner, 2005). Elseifi et al. (2001) reported three types of geosynthetics (i.e., geotextile, geonet, and geocomposite) which are designed to perform drainage functions, but at the same time act as multipurpose fabric. Henry and Barna (2002) listed the additional advantages of using geosynthetics over the drainage layer (with free draining material) as: (i) drainage is combined with separation and reinforcement, (ii) system is thinner than the free-drainage-base-aggregate layer, and (iii) geosynthetics are readily available and easy to place. Tensar Co. (2015) compared its commercial geocomposite (RoaDrain) with 4-inch open-graded base layer (OGBL) and reported the flow rate as 1.5 - 5 times higher than typical OGBL, while the permeability was stated as approximately 20 times higher.

BARRIER USED IN THIS STUDY

After the usage of geosynthetics in pavement moisture control was justified, designing the moisture barrier was the next step of the study. This section describes the modification of a geocomposite capillary barrier drain (GCBD) to the modified barrier used in this study.

Drainage of the water from its unsaturated state, before positive pore pressure develops, offers great serviceability to pavement structures. Henry and Stormont (2000) developed GCBD to drain water from soils at negative pore water pressure. After precipitation events, water infiltrates to fine soil and accumulates at the interface of a layer of larger pored soil (capillary barrier). Eventually, the water breaks into the lower layer (Figure 6:1a) when soil water suction reaches the entry suction of the underlying layer (Henry and Barna, 2002). Placing a transport layer, i.e. fine sand, between these two layers (Figure 6:1b) increases the amount and rate of drained water significantly. Based on experimental and numerical investigation, Stormont and Morris (1997) stated that using the sand layer as the transport layer, and gravel as the capillary barrier is

effective. A system of geosyntheics (Figure 6:1c) performs the same action of transport and capillary barrier based on the advantages described in the previous section. The upper geotextile acts as a transport layer, while the geonet acts as capillary barrier. A geonet is a geosynthetic with large, open pores that replaces the underlying coarse soil, as shown in Figure 6:1a.The third component is a separator geotextile. It prevents the underlying soil from intruding into the pore spaces of the geonet (capillary barrier).

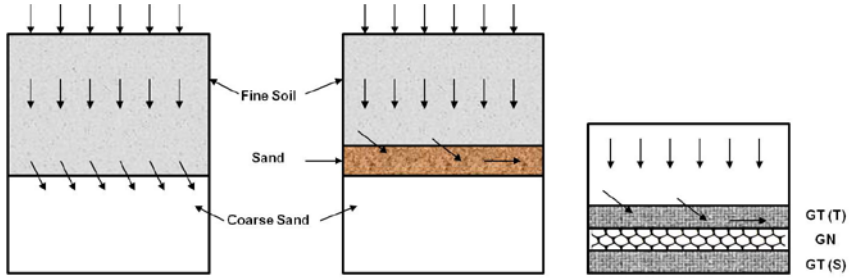

Figure 6:1 Lateral drainage in unsaturated soil with (a) capillary barrier, (b) transport layer above a capillary barrier, (c) GCBD with overlying soil (Redrawn from Henry et al. 2002)

The barrier used in this study is referred to as a modified moisture barrier. It uses the same concept of the GCBD, but has an additional component. An impermeable geomembrane is installed beneath the geocomposite system. As the separator geotextile remains in direct subgrade soil, there is a high possibility of soil intrusion into the geotextile, as it is not impermeable. Therefore, the whole system might not be effective in long-term field conditions if a clogging issue occurs. In order to combat this issue, a completely impermeable layer was added at the bottom. A complete section is presented in Figure 6:2.

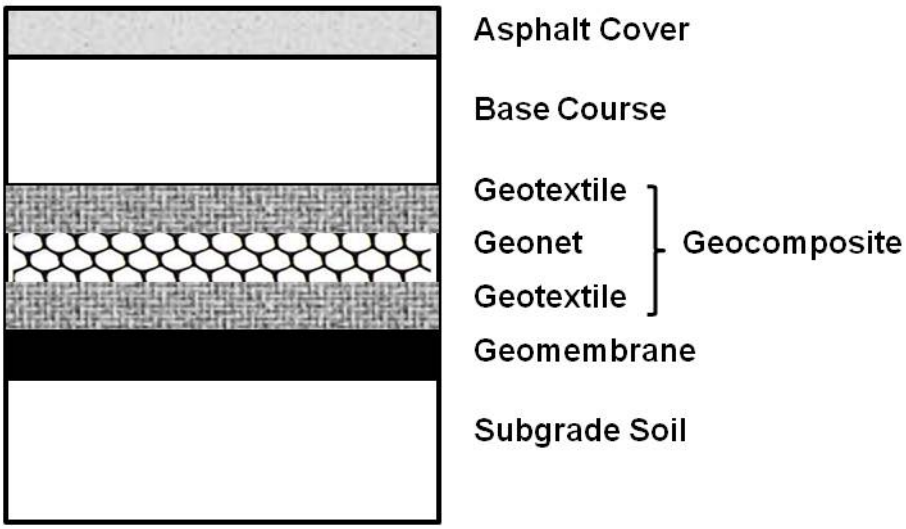

Figure 6:2 Geosynthetics barrier used during the study

MOISTURE BARRIER IN TXDOT

The Texas Department of Transportation seeks to improve the state of highways and streets constructed on top of expansive soils. Beginning in the mid-1990s, vertical moisture barriers were employed by them in areas where expansive clays had required repeated maintenance work (Jayatilaka and Lytton 1997). Vertical moisture barriers were able to reduce the development of pavement roughness, with deeper barriers being more effective, but the method proved to be more expensive, and construction difficulties were experienced. Additionally, this study establishes that maximum vertical movement due to expansive soils occurs at the edge of pavement.

Steinberg (1985) studied the effectiveness of vertical geomembranes in addressing pavement distresses associated with expansive soils in Texas. The author concluded that vertical geomembranes were feasible for construction and resulted in generally smoother pavement surfaces. He attributed this to reduced moisture variations in the expansive subgrade soil. It is recommended that the use of horizontal and/or vertical geosynthetics be studied further.

Al-Qadi and Elseifi (2002) studied the effectiveness of a geocomposite as a moisture barrier, installed as a separate layer underneath the Virginia Smart Road. To establish the effectiveness of the barrier, ground penetrating radar (GPR) and time-domain reflectometry were utilized. The authors concluded that the barrier, which can be categorized as a horizontal barrier, effectively reduced the amount of water that was able to reach the subgrade soil.

Based on the aforementioned case studies, it is evident that vertical moisture barriers incur construction difficulties. In most of the cases, the depth of the barrier was 2.44 m (8 ft.), based on the observation that the active zone was around this depth (Jayatilaka and Lytton, 1997). Digging up to 2.44 m and refilling back through several miles requires construction expertise to prevent moisture from penetrating through the altered pavement location. In addition, a horizontal moisture barrier can only be implemented during the construction phase (Elseifi et al., 2001). Therefore, a barrier scheme which can be performed both during and after construction of the roadway with minimal construction difficulties is needed. To this end, a modified barrier that combines both horizontal and semi-vertical barriers and can be deployed both during and after construction was used in this study. The depth of the barrier was 0.30 m (1 ft.), indicating less complexity during installation. Based on the studies of Hedayati (2014) and Ahmed et al. (2017), it is apparent that pavement is more vulnerable to longitudinal cracking at the edge. Therefore, it is more customary to control the moisture intrusion from the edge to ensure the longevity of the roadway. In order to do so, the current barrier scheme was adopted.

METHODOLOGY

Site Selection

This study focuses on the application of a modified moisture barrier to prevent longitudinal pavement cracking due to an expansive subgrade. Based on TxDOT maintenance records, a pavement site that showed distress, such as longitudinal pavement cracking assumed to be caused by an expansive subgrade, was selected. The site was selected away from flood zones, and utilities such as gas, electricity, water, etc. were determined to be located far enough away not to interfere with the study. It is a representative rural pavement site, and is accessible at all times for research purposes. The site is also located near a pavement where maintenance is being performed, which is conducive for instrumentation feasibility. Considering the aforementioned criteria, a section of farm-to-market road (FM) 987 was selected in Kaufman County, Texas, near Post Oak Bend, TX.

Site Description

The FM 987 site is located along FM 987, between Oak Bend Drive and Country Bend Drive, near Kaufman, TX. There are residential properties on both sides of the site. The road has two 12 ft. lanes with 1 ft. shoulders. On both sides of the road, there are drainage ditches with moderate slopes, where water was puddling. The road experienced longitudinal cracking near the edge of the lane and along the shoulder.

General Soil Description

From the United States Department of Agriculture (USDA)'s General Soil Map, it was determined that the FM 987 site contains general soil number 39, which is described as Houston Black-Heiden-Wilson soil in the Texas Blackland Prairie. Houston Black, Heiden, and Wilson soils are generally clayey and very slowly permeable. The Texas Blackland Prairie is associated with nearly-level or gently rolling plains and contains

flowing streams that generally flow southeastward. Soils common to the Texas Blackland Prairie are clayey soils with high shrink-swell properties, which are known as expansive clays. Houston Black and Heiden soils are both expansive clay soils. The location also contains loamy soils, such as Wilson soil, that are formed in interbedded sandstone and shale. The Texas Blackland Prairie is an ecological region of Texas that contains black, calcareous, alkaline, heavy clay soils.

Geocomposite Property Requirement

The geocomposite used should have the stiffness required to sustain traffic loading without considerable deformation, as well as adequate flow capacity to drain water (Christopher et al., 2000). The geosythetic used during the current study was checked against both flow and strength properties according to AASHTO Standard M 288. For example, in order to be compatible with the drainage requirement of geotextiles, the geosynthetic should have AOS less than 0.22 m, the permittivity value should be greater than 0.1 sec^{-1}, and the grab tensile strength should be greater than 700 N. Taking all of the standards into consideration, a HDPE resin with nonwoven polypropylene geotextile fabric was selected (Table 6:1). Again, to have the similar drainage capability of a 4 inch OGBL, the selected geocomposite should have a transmissivity of 0.00035 to 0.001m^2/sec (Christopher et al., 2000). The selected geocompostite had a transmissivity of 0.0007 m^2/sec, which was in the suggested range. Meeting all of the criteria, commercially-available SKAPS TRANSNET was used. It consists of SKAPS GeoNet made from HDPE resin, with nonwoven polypropylene geotextile fabric heat-bonded on both sides of geonet. Similar to a bottom liner used in landfills, a 40-mil impermeable, linear, low density, polyethylene geomembrane manufactured by Brawler Industries was used.

Table 6:1 Geosynthetic Properties Used in the Study

Property	Test Method	Unit	Value
Geotexile			
AOS	ASTM D4751	mm	0.18
Permittivity	ASTM D4491	sec^{-1}	1.26
Permeability	ASTM D4491	cm/sec	0.3
Grab Tensile Strength	ASTM D4632	N	1001
GeoComposite			
Ply Adhesion	ASTM D7005	g/cm	178
Transmissivity	ASTM D4716	m^2/sec	$7*10^{-4}$
Geonet			
Thickness	ASTM D5199	mm	6.98
Tensile Strength	ASTM 7179	kN/m	11.35
Transmissivity	ASTM D4716	m^2/sec	$6*10^{-3}$
Geomembrane			
Thickness		mil	40
Tensile Strength	ASTM D6693	N	270
Puncture Resistance	ASTM D4833	N	267

Northbound Lane Instrumentation

The first day of installation was January 30, 2017. The first step in installation was to excavate a trench in the northbound lane of the road (Figure 6:3). A sawcutting tool was used to cut through the roadway, and the material was removed using a backhoe. The excavated trench was 36” wide, 24” deep, and extended from the edge of the roadway to the centerline. The depth and length of the trench were verified before

continuing the construction sequence. The trench was then compacted with the rammer. Next, the sand bed was placed along the proposed location of the inclinometer casing. The inclinometer casing was then placed in the sand bed. After placing the inclinometer casing, sand was added on top of the inclinometer. The excavated materials were then used to refill the trench. Finally, the surface of the road was repaved.

Southbound Lane Instrumentation

On the second day of installation (January 31, 2017), the same size trench was excavated in the southbound lane of the road (Figure 6:3). Just as on the first day, a sawcutting tool was used to cut through the roadway, and the material was removed using a backhoe. The trench was the same dimensions as used for the northbound lane. Care had to be taken to ensure that the inclinometer placed underneath the northbound lane was not damaged during excavation of the southbound lane. Next, three 12 ft. boreholes were drilled in the trench. Disturbed soil samples were collected during drilling. Pipes were used to install sensors at depths of 3 ft., 6 ft., and 9 ft. After the boreholes were refilled with excavated materials and the trench was compacted, the sand bed was placed along the length of the trench. The inclinometer casing was placed along the sand bed and connected to the previously placed inclinometer casing for the northbound lane. Similar to installation in the northbound lane, the inclinometer casing was covered with sand, and the trench was filled with the excavated material. The surface of the road was repaved.

Geosynthetics Instrumentation

On the third and final day of installation (February 1, 2017), a trench was excavated in the southbound lane that was 50 ft. long, 8 ft. wide, and 1 ft. deep. A sawcutting tool was used to cut through the roadway, and the material was removed using a backhoe. The 8 ft. wide excavation included 5 ft. of pavement and 3 ft. of grassy

side slope. After the excavation, the excavated area was compacted. To assist with placement of the geomembrane, a thin sand bed was placed on top. The next step was to place the geomembrane on top of the thin sand bed. The top of the geomembrane was swept in preparation of the placement of the geocomposite. The geocomposite (geonet sandwiched between geotextiles) was placed on top of the geomembrane. The excavated portion was refilled with the excavated soil.

(a)

(b)

(c)

(d)

(e)

(f)

(g)

(h)

(i)

(j)

Figure 6:3 (a) Excavation of trench, (b) Compaction of the trench by rammer, (c) Placing inclinometer casing, (d) Borehole to install sensors, (e) Putting sensors into boreholes, (f) Saw cutting at edge of road, (g) Excavation for installing geosynthetics, (h) Putting geomembrane in position, (i) Geocomposite on top of geomembrane, and (j) Finished surface after installation.

Finally, a layer of limestone rock asphalt (LRA) aggregate was placed on top, and the surface was leveled with the roller compactor. The surface of the road was repaved. After completion of the roadwork, the sensors and rain gauges in both the control and experimental sections were connected to the data loggers for future data acquisition.

Collection of Soil Samples & Soil Test Results

Soil samples were collected from the site for soil classification. Relevant soil tests were performed according to ASTM standards. The particle-size distribution of the soil samples was determined by referring to ASTM D 422-63, Standard Test Method for Particle-Size Analysis of soils. All samples were composed of more than 50% clay, which indicated the presence of fine subgrade soil. The liquid limits were determined in accordance with ASTM D 4318 and varied between 32 and 89%. Plasticity ranged between 11 and 57%. The plasticity chart of the soil samples is presented in Figure 21. According to the Unified Soil Classification System (USCS), the sieve analysis, and the Atterberg limits, the soil was classified as high plastic clay (CH). The percentage passing the No. 200 sieve ranged between 51 and 87%, indicating the presence of fine subgrade soil.

Monitoring the Pavement Response

As discussed in the previous sections, the presence of moisture in the pavement is one of the most significant parameters for pavement performance, and measurement of moisture variations after construction is always a difficult task (Elseifi et al., 2001). With the advancement of electromagnetic techniques, indirect tests, such as the neutron probe, time or frequency domain reflectometry, and radiometry in remote sensing have become available for moisture measurement. Each method has its own advantages and disadvantages. For example, the neutron probe has a depth limitation of 1000 mm to 2000 mm, and remote sensing is effective in the top 100 to 150 mm of soil (Ahmed, 2017). Time domain reflectometry (TDR) measures the dielectric property of soil, which in turn provides the volumetric moisture content. The method is quick and automated, which has made it more acceptable. Consequently, 5TM moisture sensors, manufactured by Decagon Devices, were employed during this study for moisture measurement. The calibration of this type of moisture sensor is described elsewhere (Ahmed et al. 2017).

Three boreholes, each containing 12 sets of sensors, were installed in the two different sections of the selected roadway. As discussed earlier, a 50 ft. long pavement section was treated with geosynthetics, while another section of the pavement was untreated and is referred to as the control section. Each section had similar moisture sensors, as shown in Figure 6:4. As can be seen, the furthest sensor was installed at 12 ft. depth in both sections. Hossain et al. (2016) and Hedayati et al. (2015) installed moisture sensors up to 15 ft. of depth in similar expansive soil and recorded zero variations at this depth. Accordingly, the instrumentation depth was reduced to 12 ft. during this study.

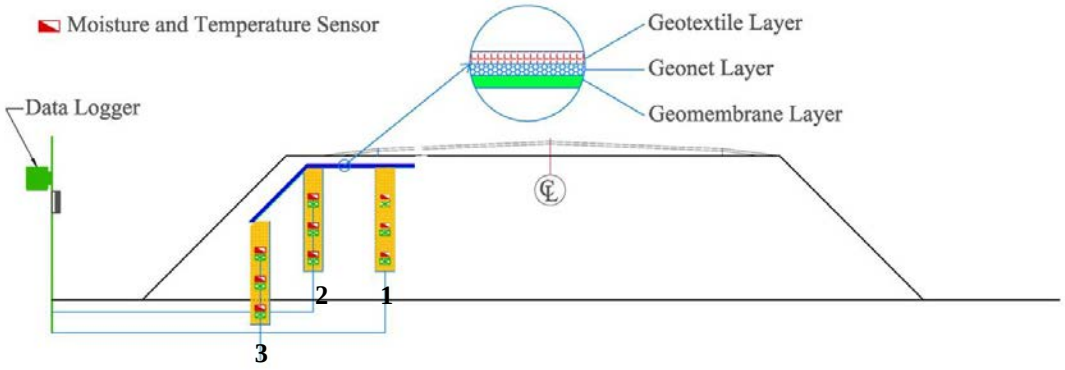

Figure 6:4 Instrumentation details at FM 987 for pavement monitoring

RESULTS AND INTERPRETATION

Field Instrumentation

The hourly sensor readings were averaged into daily readings. Only the results from borehole 1 from both sections are discussed here, as the data mirrors what was recorded by the remaining sensors. The barrier section moisture content remained near constant for all depths during the monitoring period, indicating its non-dependency on precipitation (Figure 6:5a). A gradual increase was noticed at the sensor installed at 6 ft., which can be attributed to capillary rise and groundwater movement. However, the control section moisture content responded to rainfall events at all depths (Figure 6:5b). For instance, the moisture content rose from 0.21 m^3/m^3 to 0.40 m^3/m^3 at 3 ft. depth in response to precipitation during the first week of March, 2017. Other sensors exhibited the same phenomenon. The increase in moisture content can severely affect the bearing capacity of the pavement subgrade and hence compromise the serviceability of the roadway.

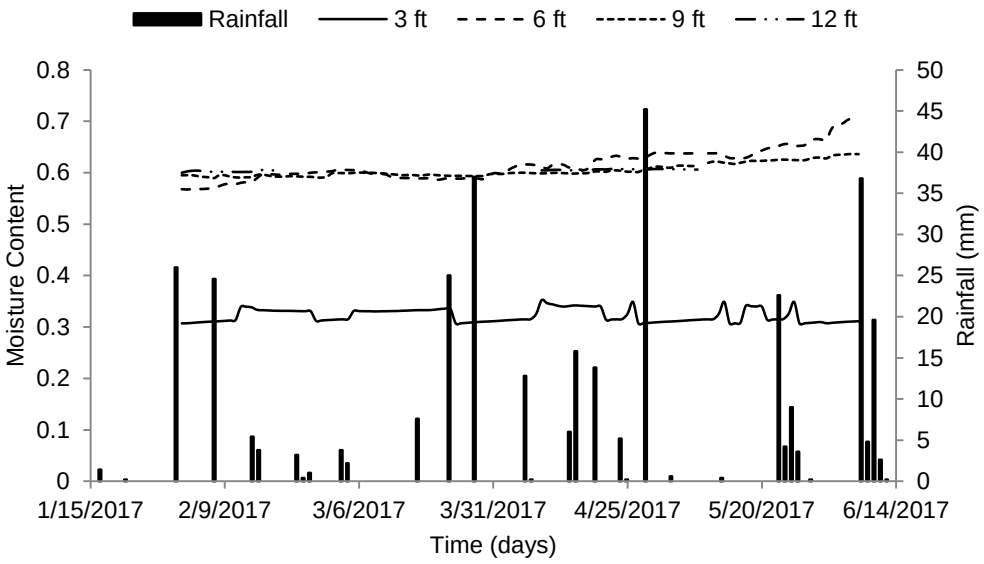

(a)

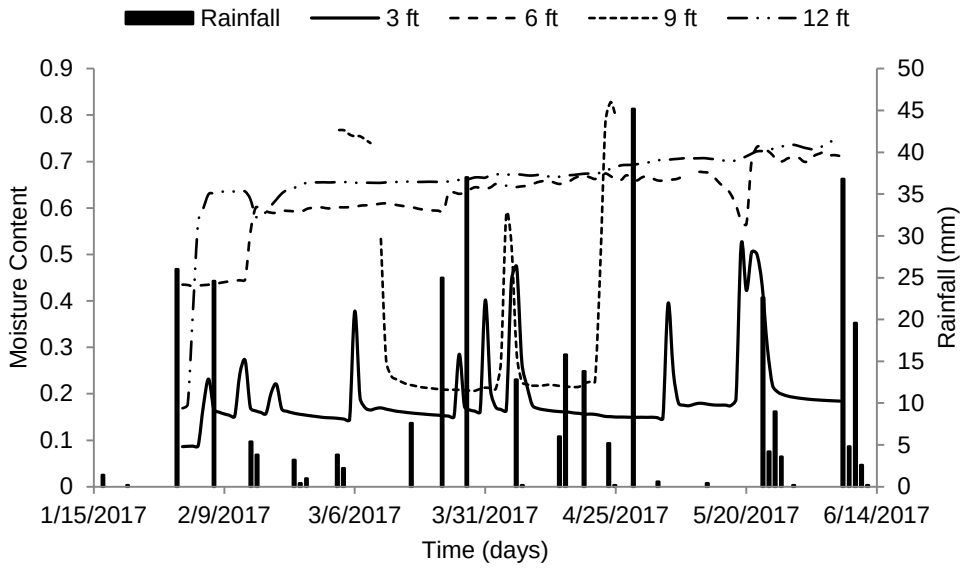

(b)

Figure 6:5 (a) Barrier section moisture content and (b) Control section moisture content

The moisture content measurements can be compared for each depth. Figure 6:6(a) exhibits a spike in the moisture content of the control section, resulting from 3 ft. of rainfall throughout the monitoring period. The barrier section displayed no spike in moisture content at the same depth; in fact, the barrier section exhibited a near-constant moisture content throughout the monitoring period. A similar phenomenon was observed for the depth of 6 feet, as shown in Figure 6:6(b). The moisture sensor at 6 ft. depth of the control section exhibited little spike, similar to what was exhibited at 3 ft., which can be attributed to the near-saturation state of the soil at the selected location. At this point, all of the medium's voids were almost filled with water. Cedergren (1974) reported a 50 percent reduction of pavement service life with as little as 10 percent of time with complete saturated state. On the whole, the constant moisture content, irrespective of rainfall events, indicates the effectiveness of the modified moisture barrier used in the study.

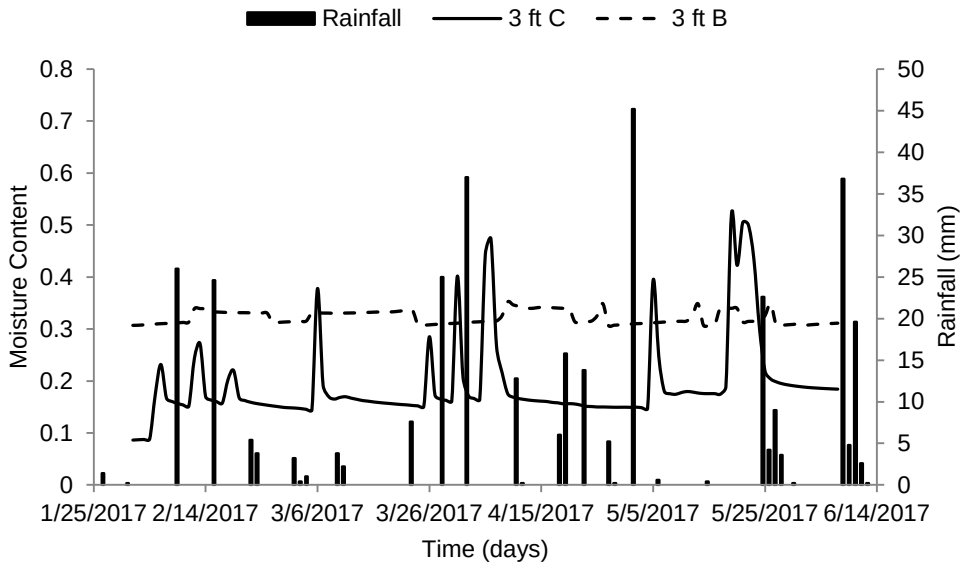

(a)

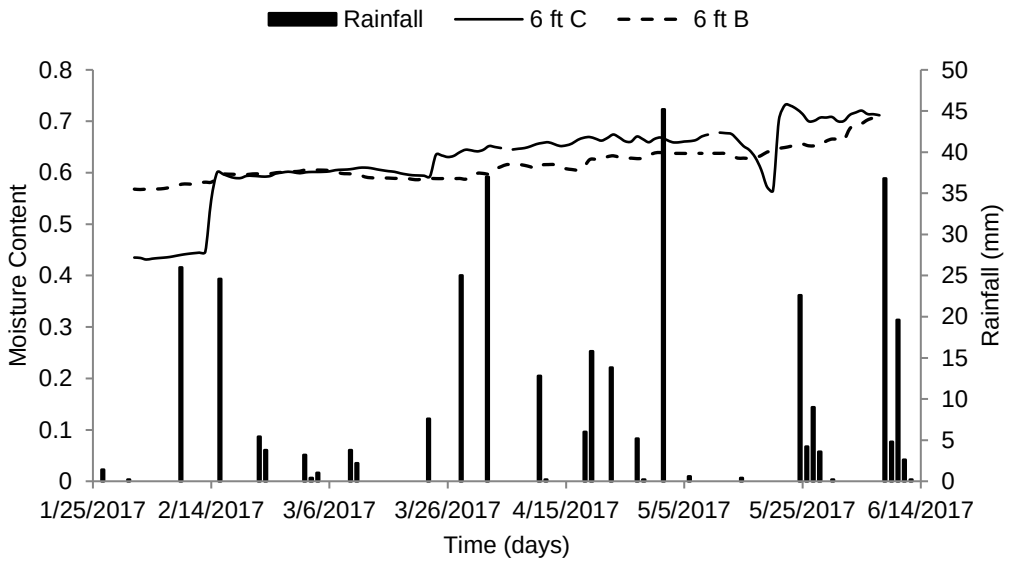

(b)

Figure 6:6 Moisture content comparison for borehole 1 at (a) 3 ft. depth and (b) 6 ft. depth

Monitoring Results from ERI

Excessive moisture, coupled with inadequate drainage, has been reported as a major source of flexible pavement failures. While moisture sensors provide point information, geophysical testing in the form of resistivity imaging was conducted in the grassy side slope of the pavement to get a continuous portrayal. The resistivity profile provides a comprehensive interpretation of the subsurface condition. The most interesting and important advantage of using ERI is that through its resistivity profile, it gives a clear idea of the moisture distribution within the test area.

The exact section of resistivity imaging can be seen in Figure 6:7 (a). An inverse relationship between resistivity and moisture was used to interpret the qualitative data presented in Figure 6:7. High readings of resistivity corresponded to lower moisture contents, while low readings of resistivity translated to higher moisture contents. The scale from red to blue in Figure 6:7 indicates levels of high and low resistivity values,

respectively. As can be noticed, the presence of moisture can be traced in the test section in May 2017 (Figure 6:7 b). Over the stated monitoring period in this paper, May experienced the highest rainfall (122 mm). As is customary and is reflected in the ERI test result, most of the precipitation acted as runoff (arrow sign in Figure 6:7 a) and accumulated in the slope. The control section without the barrier experienced comparatively more resistance (Figure 6:7c). Hedayati (2014) conducted resistivity imaging in a farm-to-market road in Kaufman, Texas and reported moisture intrusion from the grassy side edge. It appeared that the modified moisture barrier was directing the water to drain to the slope, as opposed to intruding inside the pavement. The results are in good agreement with the field instrumentation results depicted in Figure 6:5. Due to the water draining outside the pavement location, no immediate infiltration from the edge of the pavement was observed, which significantly reduced the moisture variation.

(a)

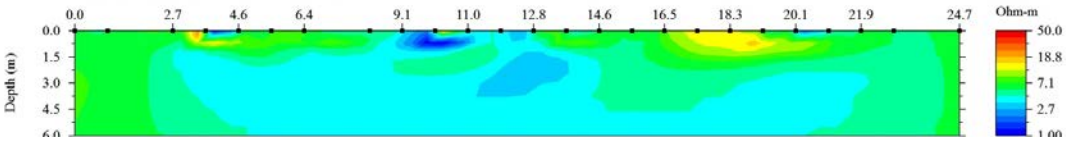

(b)

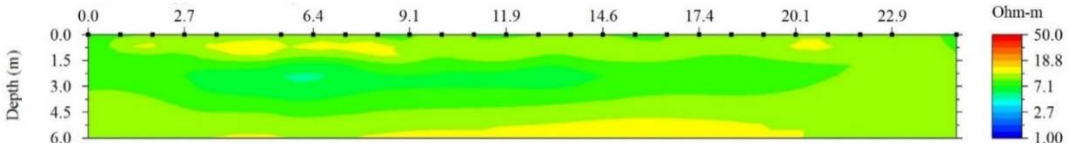

(c)

Figure 6:7 (a) ERI test section at FM 987; resistivity result beside (b) barrier section and (c) control section

Effect of Pavement Serviceability

High moisture content can reduce the bearing capacity of unbound bases and subgrades, leading to pavement distress. To evaluate the effect of using a moisture barrier on pavement serviceability, a horizontal inclinometer was used in both barrier and control sections. Topographic surveys and falling weight deflectometers (FWD) have been used by previous researchers to account for vertical movement (Hedayati 2014, Qadi et al. 2004). An inclinometer is also a useful tool for monitoring the vertical deformation underneath the whole pavement and locating local deformation (Machan and Bennett, 2008). While it provides the total portrayal of the pavement cross section, the major area of interest was the deformation at the edge of the roadway as it acts as the prime source of moisture intrusion. Figure 6:8 illustrates the comparison of edge deformation with and without the moisture barriers during the period between January 2017 and June 2017. As can be noticed, the section without the barrier exhibited the most movement. Given the uniformity of the pavement layers and subgrade, the control section recorded considerable swelling (25 mm) as a result of increased rainfall in May 2017. Accumulation of the moisture in an area without a geocomposite barrier might have led to the phenomenon. It may also be noticed that the area experienced shrinkage as a result of decreased precipitation in the following month. The opposite behavior was recorded in the barrier section with geocomposite, which did not exhibit precipitation-

dependent behavior. Thus, it appears that preventing water from entering subgrade might reduce the detrimental effect of cyclic swelling shrinkage of the expansive subgrade.

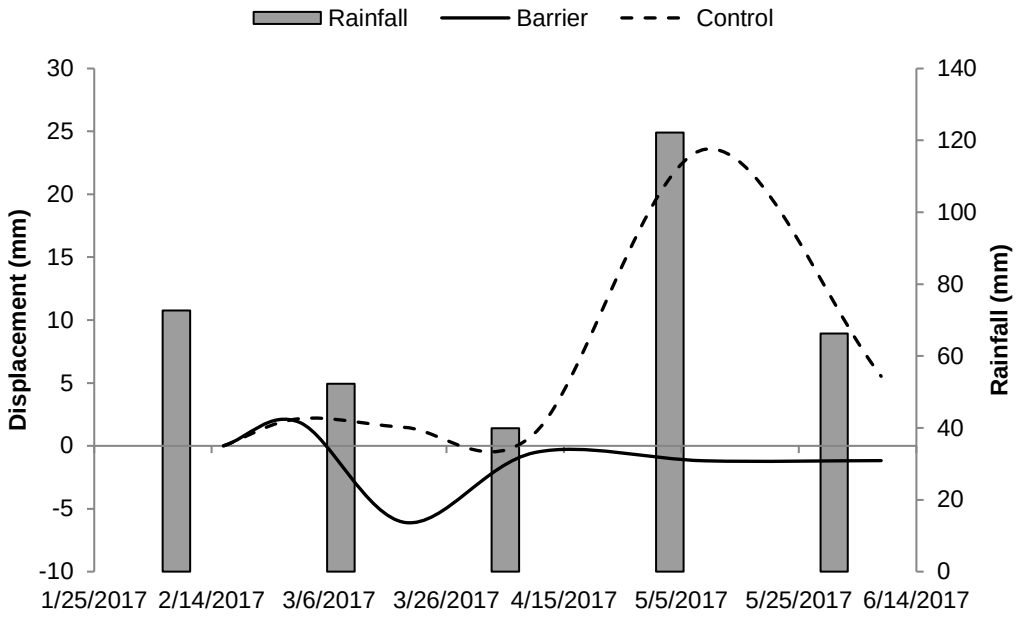

Figure 6:8 Measured deformation at edge of pavement with and without barrier

CONCLUSIONS

A 50 ft. long pavement section was modified with geomembranes and gecomposites at the edge to combat the moisture intrusion from that area. The modified barrier incorporated a three-layer system composed of geotextiles, geonets, and geomembranes to drain the precipitation to the roadside ditch. The monitoring plan included moisture sensor readings and resistivity imaging data, while pavement deformation was screened through an inclinometer. The field monitoring results exhibited that volumetric moisture content jumped from 0.20 m^3/m^3 to as high as 0.60 m^3/m^3 in the control section, whereas it maintained almost constant beneath the barrier, irrespective of rainfall events. Resistivity imaging also indicated an accumulation of moisture at the roadside ditch, indicating runoff of precipitation, while the control area remained drier.

Results from edge deformation monitoring indicated more movement in the control section after rainfall events, as the barrier section experienced 5 mm movement, in comparison with 25 mm in the control section. While the study is still ongoing, the preliminary results show the effectiveness of the modified moisture barrier.

CHAPTER 7

CONCLUSIONS AND RECOMMENDATIONS

Volumetric deformation due to cyclic swelling and shrinkage in expansive subgrades is a common phenomenon in Texas and leads to spending a significant portion of maintenance budgets on pavement repair. In order to improve the performance of the structure and reduce the frequency of maintenance, it is vital to have an accurate understanding of the relationship of subgrade moisture, pavement deformation and other parameters.

The main objective of this research was to study the real-time effects of environmental and climatic loading on pavement performance and to determine a viable solution. To this end, in-situ, real-time variations of moisture, temperature, and suction were monitored over several years, and a real-time moisture variation and deformation model was developed based on the collected data. To combat the moisture changes in subgrades, performance of a pavement section with a moisture barrier is also presented. In this chapter, findings are summarized and recommendations for future studies are presented.

MOISTURE VARIATION

- Results from field data indicated that moisture content variations change with depth. Moisture sensors nearer to the ground surface registered temporary increases as high as 15% in amplitude in response to rainfall events, while deeper sensors experienced less variation. Such increases in moisture content were likely limited to the temporary saturation point at each respective depth.
- Full saturation of the soil prevented appreciable changes in moisture content for sensors installed deepest in the subgrade at 15 ft. (4.5 m). The average value of

moisture content at this depth was approximately 20% for both the SH 342 and FM 2757 sites.

- Seasonal contributions to moisture variations were identified by observing the response of moisture content to wet and dry seasons. Periods of continuous high intensity rainfall prevented the dissipation of moisture, resulting in peaks in the seasonal trends. In contrast, moisture curves attained lower values during dry seasons.
- Instantaneous spikes in moisture content after individual rainfall events were indicative of temporary saturation induced by rainfall. As the free water moved downwards, moisture content readings returned to equilibrium.
- Comparison of moisture modeling with previous studies indicated that the model developed for this study can capture both seasonal and temporary variations. In addition, the developed model exhibited 90% similarity with the measured values in the site.

Moisture change was also traced by resistivity imaging, as listed below:

- Results from field monitoring from 2015-17 indicated repetitive behavior in consecutive seasons. The wet period was found to be from November to April, while the dry period was from May to October.
- Resistivity values at the top depth (approximately 3 ft.) recorded variations from 7 Ohm-m to 23 Ohm-m in response to seasonal variations.
- Below a depth of 3 m (10 ft.), resistivity values did not undergo significant fluctuations, which indicates the active zone in the study area.

TEMPERATURE VARIATION

- Sensor data from both the SH 342 and FM 2757 pavement sites found sinusoidal patterns in temperature variations that could be described with a first degree Fourier series. The cyclical trend was observed across all depths of subgrades.
- Subgrade temperatures closest to the ground surface generally exhibited daily variations. Signs of daily changes in temperature decreased with depth. Such temperature fluctuations likely grew smaller as a result of the high thermal inertia of soil.
- The lag time between sensors increased with depth. Sensors installed 15 ft. (4.5 m) in the subgrade attained their peaks as late as four months after sensors closest to the ground surface achieved their own maximum values.
- Warmer seasons registered a decrease in subgrade temperatures with increasing depth. The converse was observed for cooler seasons, when temperatures increased with depth. The existence of a reverse thermal gradient likely resulted in the observed temperature variations.
- A new ratio-based approach was adopted to develop a temperature model. In the current approach, temperature up to 12 ft. depth of subgrade can be determined from air temperature of the corresponding day.
- The developed model exhibited 90% similarity with the measured values at the site.

SUCTION VARIATION

- Tensiometers were installed in two boreholes in SH 342 to measure the in-situ suction variations. The sensors were installed at different depths, ranging from 3 ft. to 15 ft.

- Field monitoring of the suction sensors indicated that it is difficult to obtain an interpretable trend. Two sensors, located at 3 ft. and 4 ft., exhibited variations due to seasonal changes and rainfall, whereas other sensors maintained an almost-average value of -10 kPa.
- Previous studies indicated that it is difficult to obtain reliable suction data by field monitoring. One previous study indicated that most suction variations can be observed at shallower depths and in grassy side slopes, which may be the reason that the sensors installed beneath the driving lane in SH 342 were less sensitive.

DEFORMATION OF PAVEMENT

- In order to monitor the pavement performance, surveying and inclinometer activities were performed on a month-to-month basis.
- Seasonal deformation was observed in both sites, and both sites exhibited swelling and shrinkage behavior in each cycle.
- Edge crack and drop were observed in the sites after each summer. Such finding is also supported by previous studies. FM 2757 site exhibited longitudinal cracks in August/September of each year.

STATISTICAL MODELING

- Real-time moisture, temperature, and deformation modeling were carried out based on the collected data.
- The moisture model was able to capture both seasonal and temporary variations due to rainfall. However, the model is limited for expansive clay and homogenous layers of soil, excluding evaporation.

- While developing the temperature model, a ratio was developed between the air temperature and the temperature at a specific depth. Further, the ratio prediction equation was utilized to calculate the subgrade temperature at any depth. Soil heat parameters were not considered during the model development.
- In order to develop the deformation model, several parameters were considered, i.e., temperature, suction, rainfall, seasonal effect, etc. Eventually, the model captured both seasonal and temporary variations, incorporating time and rainfall amounts.

NUMERICAL MODELING

- This study focused on the challenging task of determining the critical flow parameters required for numerical modeling.
- Horizontal and vertical unsaturated hydraulic conductivity were determined, based on the field moisture flow data. The study found the permeability to be in a range of 10^{-4} to 10^{-5} m/s value.
- Van Genuchten flow parameters (a, n, and m), field soil water characteristic curve, were used, rather than the laboratory-based curve, to determine the flow.
- Numerical modeling in finite element software PLAXIS 2D, incorporating the field-based values, provided effective information regarding suction and moisture changes in subgrades.

PERFORMANCE OF MOISTURE BARRIER

- A modified moisture barrier, including a geocomposite and a gemembrane, was developed during the study to combat the moisture intrusion at the pavement subgrade.

- The modified moisture barrier, a combination of a 40-mil LLDPE geomembrane and an 8-oz. HDPE geocomposite (geonet sandwiched between two non-woven geotextiles) was placed in a 50 ft. section of a farm-to-market road.
- Volumetric moisture content jumped from 0.20 m^3/m^3 to as high as 0.60 m^3/m^3 in the control section without a barrier, whereas it was almost constant in the section with a barrier, irrespective of rainfall events.
- Deformation monitoring results indicated 5 mm of deformation in the barrier section compared to 25 mm in the control section, confirming the effectiveness of the barrier.

RECOMMENDATIONS FOR FUTURE WORK

- The study was conducted on two different sites of almost similar soil properties. Hence, the developed model and observations are valid for one specific type of soil. It is recommended that additional sites of different soil properties be studied also.
- While the sensors were programmed to provide readings at one-hour intervals, deformation readings were recorded monthly. It is recommended that elevation and deformation monitoring be carried out in more points and at smaller intervals.
- The test was carried out in flexible pavement only. A mix and match of flexible and rigid pavements would increase the usefulness of the study.
- Additional test sections should be considered, with different geometries (number and width of lanes), configuration (presence and width of shoulders), and types (i.e., interstate, state, farm-to-market).
- A high-accuracy suction sensor needs to be installed in order to capture the suction variations in the field.

- In this study, sensors were installed beneath pavement only. It is highly recommended that sensors be installed across the full width of the pavement and grassy side slopes, and at different depths in order to visualize the whole picture of moisture flow and other parameters.
- This study focused only on change of parameters (i.e., moisture, suction, temperature) with environmental loading. A focus on the decrease of soil strength (i.e., resilient modulus) with variations was completely absent. Incorporating the seasonal variations of resilient modulus is recommended.
- Different kinds of geomembranes and geocomposites should be tried in several pavement sections to check the effective properties of the barrier and ultimately result in developing a standard for selecting a moisture barrier.

REFERENCES

AASHTO (2006). Geotextile Specification for Highway Applications - M288-06, Standard Specifications for Transportation Materials and Methods of Sampling and Testing. American Association of State Transportation and Highway Officials, Washington, D.C., 20pp.

AASHTO (2004). Guide for Mechanistic Empirical Design of New and Rehabilitated Pavement Structures. Washington, D.C.: NCHRP Project 1-37A, Transportation Research Board of the National Academies.

Abd Rahim, and M.A. B., Picomell. M. (1989). "Moisture Movement under the Pavement Structure." Research Report 1165-1, Center for Geotechnical and Highway Research, University of Texas at El Paso, El Paso, Texas.

Abed, A. (2007) "Numerical simulation of a trial wall on expansive soil in Sudan." Plaxis Bulletin: 21, 14-18.

Adem, H. H., and S K Vanapalli. (2013) "Constitutive modeling approach for estimating 1-D heave with respect to time for expansive soils." International Journal of Geotechnical Engineering: 7(2), 199-204.

Advanced Geosciences, Inc. (2004). Instruction Manual for Earth Imager 2D Version 1.7.4. Resistivity and IP Inversion Software. Austin, TX, USA: Advanced Geosciences, Inc.

Ahlvin, R.G. (1962). “Flexible Pavement Design Criteria.” Journal of the Aero- Space Transport Division, Proceedings of the ASCE.

Ahmed, A., Hossain, M. S., Khan, M. S., Greenwood, K., & Shishani, A. (2017). Moisture Variation in Expansive Subgrade through Field Instrumentation and Geophysical Testing. In International Congress and Exhibition" Sustainable Civil Infrastructures: Innovative Infrastructure Geotechnology" (pp. 45-58). Springer, Cham.

Ahmed, A., Hossain, M.S., Khan, M.S. and Shishani A. (2017). Data Based Real Time Moisture Modeling in Unsaturated Expansive Subgrade. Second Pan-American Conference on Unsaturated Soils. November 12-15, Dallas, Texas.

Ahmed, A., Hossain, M.S., Alam M.J. and Khan M.S. (2017). “Moisture Distribution in unsaturated Subgrade through Field Instrumentation and Numerical Modeling”. Proc., Second Pan-American Conference on Unsaturated Soils, Geo-Institute of ASCE, Dallas, Texas.

Aizebeokhai, A. P. (2010). "2D and 3D geoelectrical resistivity imaging: Theory and field design." Scientific Research and Essays, 5(23), 3592-3605.

Alam, M.J., Hossain, M.S., Ahmed A. and Khan, M.S. (2017). “Comparison of deep percolation of flat and slope section vegetated lysimeters using field soil water characteristic curve.” Proc., Second Pan-American Conference on Unsaturated Soils, Geo-Institute of ASCE, Dallas, Texas.

Albrecht, B.A., Benson, C.H., (2001). Effect of desiccation on compacted natural clays. J. Geotech. Geoenviron. Eng. 127 (1), 67–75.

Al-Qadi, I. L., Lahouar, S., Loulizi, A., Elseifi, M. A., & Wilkes, J. A. (2004). Effective approach to improve pavement drainage layers. Journal of Transportation Engineering, 130(5), 658-664.

Al-Rawas, A.A., Hago, A.W. and Al-Sarmi, H. (2005). “Effect of lime, Cement and Sarooj (Artificial Pozzolan) on the Swelling Potential of an Expansive Soil from Oman.” Building and Environment 40, pp.681–687.

Amarasiri, A. L., Kodikara, J. K., & Costa, S. (2011). Numerical modelling of desiccation cracking. International Journal for Numerical and Analytical Methods in Geomechanics, 35(1), 82-96.

Angulo-Jaramillo, R., et al. (1997). "Seasonal variation of hydraulic properties of soils measured using a tension disk infiltrometer." Soil Sci. Soc. Am. J., 61(1), 27-32.

ASTM (2008). Standard test method for one-dimensional swell or collapse of cohesive soils (ASTM D4546). American Society of Testing and Materials.

Austin, R.A. and Gilchrist, A.J.T. (1996). “Enhanced Performance of Asphalt Pavements Using Geocomposites.” Geotextiles and Geomembranes 14. pp.175-186.

Bae, A., Stoffels, S. M., Antle, C. E., & Lee, S. W. (2008). Observed evidence of subgrade moisture influence on pavement longitudinal profile. Canadian Journal of Civil Engineering, 35(10), 1050-1063.

Baker, P. D. (1978). “Tree Root Intrusion into Sewers.” Progress Report No. 2: Analysis of Root Chokes by Species.” Engineering and Water Supply Department, Sewerage Branch, SA, Australia, August.

Barksdale, R. D., Brown, S. F., & Chan, F. (1989). Potential benefits of geosynthetics in flexible pavement systems (No. 315).

Basma, A.A., Tuncer, E.R. (1991). “Effect of Lime on Volume Change and compressibility of Expansive Soils. Transportation Research Record (1295).

Bayomy, F. and Salem, H. (2004). “Monitoring and modeling subgrade soil moisture for pavement design and rehabilitation in Idaho: Phase III: Data collection and analysis.” Final Report, National Institute for Advanced Transportation Technology, University of Idaho.

Bell, F.G. (1996) “Lime Stabilization of Clay Minerals and Soils”. Engineering Geology 42, pp.223-237.

Biddle, P. G. (1983). “Patterns of Soil Drying and Moisture Deficit in the Vicinity of Trees on Clay Soils.” Geotechnique, 33, 2, 107-126

Biddle, P. G. (2001). “Trees Root Damages to Buildings.” ASCE Geotechnical Special Publication, 115, 1-23.

Bozozuk, M. (1962). “Soil Shrinking Damages Shallow Foundations at Ottawa, Canada.” Research Paper 163, Division Building Research, NRCC, Canada

Brown, S.F. (1996). “Soil mechanics in pavement engineering.” Geotechnique, v 46, n 3, Sep, 1996, p 383-426.

Browning, G. (1999). “Evaluation of Soil Moisture Barrier.” FHWA/MS-DOT-RD- 99-21 & 23; Final Report.

Bryant, J. T., Morris, D. V., Sweeney, S. P., Gehrig, M. D., and Mathis, J. D. (2001) “Tree root influence on soil-structure interaction in expansive clay soils.” Expansive Clay Soils and Vegetative Influence on Shallow Foundations, 2001, p 110-131.

Buhler, R.L., and A.B. Cerato (2007). Stabilization of Oklahoma Expansive Soils Using Lime and Class C Fly Ash. Proc., Geotechnical Special Publication No. 162 – Problematic Soils and Rocks and In Situ Characterization, ASCE, Denver, CO, pp. 1-10.

Burmister, DM. (1943) "The theory of stresses and displacements in layered systems and applications to the design of airport runways." Highway research board annual meeting. Washington, DC. (23), 126–144.

Cameron, D. A. (2001). “The Extent of Soil Desiccation near Trees in a Semi-Arid Environment Footings Group.” IE Aust SA, 17.

Cedergren, H. R. (1974). Drainage of highway and airfield pavements, Wiley, New York.

Cedergren, H.R., K.H. O’Brien, and J.A. Arman, (1973). Guidelines for the Design of Subsurface Drainage Systems for Highway Structural Sections, Final Report Number FHWA-RD-73-14, Federal Highway Administration, Washington, D.C.

Chabrillat, S., Goetz, A.F., Krosley, L., Olsen, H.W. (2002). Use of hyperspectral images in the identification and mapping of expansive clay soils and the role of spatial resolution. Remote Sens. Environ. 82 (2), 431–445.

Chandra, D., R. L. Lytton, and W. Yang (1988). Effects of Temperature and Moisture on Low Volume Roads, Publication FHWA/TX-89/473-2. FHWA, Texas Department of Transportation.

Chen, F. H. (1988). Foundation on Expansive Soils, American Elsevier Science Publication, New York.

Chen, L., & Bulut, R. (2015). Numerical analysis of vertical moisture barriers in controlling expansive soils in presence of soil cracks. In IFCEE 2015 (pp. 2102-2111).

Chou, L. (1987) “Lime Stabilization: Reactions, Properties, Design and Construction.” TRB State of the Art Report 5, Transportation Research Board, National Research Council, Washington D.C.

Christopher, B. R., Hayden, S. A., & Zhao, A. (2000). Roadway base and subgrade geocomposite drainage layers. In Testing and performance of geosynthetics in subsurface drainage. ASTM International.

Clarke, C. R. (2006). "Monitoring Long-Term Subgrade Moisture Changes with Electrical Resistivity Tomography." Proc., Fourth International Conference on Unsaturated Soils, American Society of Civil Engineers, Carefree, Arizona, USA, 258-268.

Croft, J.B. (1967). “The Influence of Soil Mineralogical Composition on Cement Stabilization.” Geotechnique, vol. 17, London, England, pp.119–135.

Cutler, D. F. and Richardson, I. B. K. (1981). “Trees and buildings.” Construction Press: London.

Dafalla, M. A., Al-Shamrani, M. A., Puppala, A. J., & Ali, H. E. (2011). Design guide for rigid foundation systems on expansive soils. International Journal of Geomechanics, 12(5), 528-536.

Das, B. M. (2013). Advanced soil mechanics, 4th Ed., CRC Press, Boca Raton, FL.

Decagon Devices, Inc. (2017). “5TM Water Content and Temperature Sensors.” <http://manuals.decagon.com/Manuals/13441_5TM_Web.pdf> (March 28, 2017).

Decagon Devices, Inc. (2017). “WP4C Dew Point Potentimeter.” <http://manuals.decagon.com/Manuals/13588_WP4C_Web.pdf> (Apr. 5, 2017).

Department of the Army USA (1983) “Foundations in Expansive Soils, 1 September 1983.” Technical Manual TM, 5-818-7.

Dessouky, S. H., Oh, J., Ilias, M., Lee, S. I., & Park, D. (2014). Investigation of various pavement repairs in low-volume roads over expansive soil. Journal of Performance of Constructed Facilities, 29(6), 04014146.

Dhowian, AW (1990). "Field performance of expansive shale formation." Journal of King Abdulaziz University (Engineering Sciences): 2, 165–82.

Djellali, A., Abdelhafid O., and Behrooz S. (2012). "Behavior of flexible pavements on expansive soils." Int. J. of Transp. Eng., 1(1), 1-14.

Driscoll, R. (1983). “The Influence of Vegetation on the Swelling and Shrinkage of Clay in Britain.” Geotechnique, 33 (2), 93-105

Elseifi, M. A., Al-Qadi, I. L., Loulizi, A., and Wilkes, J. (2001). ‘‘Performance of a geocomposite membrane as a pavement moisture barrier.’’ Transportation Research Record 1772, Transportation Research Board, National Research Council, Washington, D.C., 168–173.

Evans, R. P.; McManus, K. J. (1999). “Construction of Vertical Moisture Barriers to Reduce Expansive Soil Subgrade Movement.” Transportation Research Record 1652, 7th International Conference on Low-Volume Roads, pp.108-112.

Favre, Fabienne, Pascal Boivin, and M. C. S. Wopereis (1997). "Water movement and soil swelling in a dry, cracked Vertisol." Geoderma 78(1): 113-123.

FHWA (1980). "Expansive Soils in Highway Subgrades: Summary." Report FHWA-TS-80- 236, U.S. Department of Transportation, Washington, D.C.

Fityus, S.G. (1999). A soil moisture based method of estimating ys. Australian Geomechanics, 34(3): 15–23.

Florides, G, and S Kalogirou (2004). "Measurements of ground temperature at various depths." 3rd International Conference on Sustainable Energy Technologies. Nottingham, UK.

Fredlund, D. G. (2006). Unsaturated soil mechanics in engineering practice. Journal of geotechnical and geoenvironmental engineering, 132(3), 286-321.

Fredlund, D. G., & Xing, A. (1994). Equations for the soil-water characteristic curve. Canadian geotechnical journal, 31(4), 521-532.

Fredlund, D. G., Xing, A., & Huang, S. (1994). Predicting the permeability function for unsaturated soils using the soil-water characteristic curve. Canadian Geotechnical Journal, 31(4), 533-546.

Fredlund, D.G. and Rahardjo (1993). Soil Mechanics for Unsaturated Soils, John Wiley & Sons, Inc., New York.

Fredlund, DG (1983). "Prediction of ground movements in swelling clays." 31st Annual Soil Mechanics and Found Engineering Conference. Minneapolis, MN: University of Minnesota.

Fredlund, M. D., Stianson, J. R., Fredlund, D. G., Vu, H., & Thode, R. C. (2006). Numerical modeling of slab-on-grade foundations. In Unsaturated Soils 2006 (pp. 2121-2132).

Gay, D. A. (1994). Development of a predictive model for pavement roughness on expansive soils (Doctoral dissertation, Doctoral Dissertation, Texas A&M University).

Gay, D. A., & Lytton, R. L. (1988). Moisture Barrier Effects on Pavement Roughness. Measured Performance of Shallow Foundations, Geotechnical Special Publication, (15).

Ghorbanpourbabakandi A. (2014). Leachate Recirculation Modeling Using Vertical Wells In Bioreactor Landfills. MS Thesis. The University of Texas at Arlington.

Giroud, J.P. and Han, J. (2004a). “Design Method for Geogrid-Reinforced Unpaved Roads. I. Development of Design Method.” Journal of Geotechnical and Geoenvironmental Engineering, pp.775-786.

Giroud, J.P. and Han, J. (2004b). “Design Method for Geogrid-Reinforced Unpaved Roads. II. Calibration and Applications.” Journal of Geotechnical and Geoenvironmental Engineering, pp.787-797.

Gould, S.J.F., Kodikara, J., Rajeev, P., Zhao, X.L., and Burn, S. (2011). A void ratio - water content - net stress model for environmentally stabilized expansive soils. Canadian Geotechnical Journal, 48(6): 867–877. doi:10.1139/t10-108.

Gupta, R., McCartney, J. S., Nogueira, C. D. L., & Zornberg, J. G. (2008). Moisture migration in geogrid reinforced expansive subgrades.

Hammitt, G. M., & Ahlvin, R. G. (1973). Membranes and Encapsulation of Soils for Control of Swelling. Publication of: Frost I Jord/Norway/, 2(Workshop Proceedings).

Hardcastle, J.H. (2000). “Engineering Properties of Soils- Some Suction Concepts”. University of Idaho, Department of Civil Engineering, CE 561 Class Handouts, fall semester, Lecture 22.

Hashem, M. D. and Abu-Baker, A. M. (2013). "Numerical modeling of flexible pavement constructed on expansive soils." Eur. Int. J. Sci. Tech., 2(10), 19-34.

Hearn, G J, T Hunt, J Aubert, and J Howell. (2008). "Landslide impacts on the road network of Lao PDR and the feasibility of implementing a slope management program." International conference on management of landslide hazard in the Asia.

Heath, W, B S Saros, and J W F Dowling. (1990). Highway Slope Problems in Indonesia. London, UK: Transport & Road Research Laboratory.

Hedayati, M. (2014). “Rainfall induced distress in low volume pavements.” PhD Dissertation, University of Texas at Arlington, Arlington, TX.

Hedayati, M. and Hossain, S. (2015). “Data based model to estimate subgrade moisture variation case study: Low volume pavement in North Texas.” Transp. Geotech., 3, 48-57.

Hedayati, M., Hossain, M. S., Mehdibeigi, A., and Thian, B. (2014). “Real-time modeling of moisture distribution in subgrade soils.” Proc., Geo-Congress 2014: Geo-characterization and Modeling for Sustainability, Geo-Institute of ASCE, Atlanta, GA, 3015-3024.

Henry, K. S., Stormont, J. C., Barna, L. A., & Ramos, R. D. (2002, September). Geocomposite capillary barrier drain for unsaturated drainage of pavements. In GEOSYNTHETICS: STATE OF THE ART-RECENT DEVELOPMENTS. PROCEEDINGS OF THE SEVENTH INTERNATIONAL CONFERENCE ON GEOSYNTHETICS, 7-ICG, HELD 22-27 SEPTEMBER 2002, NICE, FRANCE. (Vol. 3).

Henry, Karen S., and John C. Stormont. (2000) "Geocomposite capillary barrier drain." U.S. Patent No. 6,152,653. 28 Nov.

Heydinger, A. G. (2003). “Evaluation of seasonal effects on subgrade soils.” Transp. Res. Rec., 1821(1), 47-55.

Heydinger, A.G. (2003) Evaluation of Seasonal Effects on Subgrade Soils. Transportation Research Record: Journal of the Transportation Research Board, Vol. 1821, pp. 47-55.

Hicks, R.G. (2002). “Alaska Soil Stabilization Design Guide.” FHWA-AK-RD-01- 6B.

Hillel, D. (1982). Introduction to Soil Physics. Academic Press, New York.

Horak, E. (1983). “Waterbound Macadam Bases.” M.E. thesis, Department of Civil Engineering, Univ. of Pretoria, Republic of South Africa.

Horak, E. and Triebel, R.H.H. (1986). “Waterbound Macadam as a Base and a Drainage Layer.” Transportation Research Record 1055. pp. 48-51.

Hossain, Jubair. (2012). Geohazard Potential of Rainfall Induced Slope Failure on Expansive Clay. PhD Dissertation, the University of Texas at Arlington, Arlington, TX.

Hossain, S., Ahmed, A., Khan, M., Aramoon, A., and Thian, B. (2016). “Expansive subgrade behavior on a state highway in North Texas.” Proc., Geotech. and Struct. Eng. Congress 2016, American Society of Civil Engineers (ASCE), Phoenix, 1186-1197.

Houston, S. L., H. B. Dye, C. E. Zapata, K. D. Walsh, and W. N. Houston. (2011). "Study of expansive soils and residential foundations on expansive soils in Arizona." Journal of performance of constructed facilities. 25 (1), 31- 44.

Huang, S., Barbour, S. L., and Fredlund, D. G. (1998). "Development and verification of a coefficient of permeability function for a deformable unsaturated soil." Can. Geotech. J., 35(3), 411-425.

Huang, YH. (1993). Pavement Analysis and Design. New Jersey: Prentice-Hall.

Hufenus R., Rueegger, R., Banjac, R., Mayor, P., Springman, S.M. and Brönnimann, R. (2006). “Full-Scale Field Tests on Geosynthetic Reinforced Unpaved Roads on Soft Subgrade.” Geotextiles and Geomembranes 24, pp.21-37.

Jaksa, M. B., Kaggwa, W. S., Woodburn, J. A., and Sinclair, R. (2002). “Influence of Large Gums Trees on the Soil Suction Profile in Expansive Clays.” Australian Geomechanics, 71(1), 23-33.

Jayatilaka, R., & Lytton, R. L. (1997). Prediction of expansive clay roughness in pavements with vertical moisture barriers (No. FHWA/TX-98/187-28F,).

Jayatilaka, R., Gay, D. A., Lytton, R. L., and Wray, W. K. (1993). "Effectiveness of Controlling Pavement Roughness Due to Expansive Clays with Vertical Moisture Barriers." Research Report 1165-2F, Texas Transportation Institute, Texas A&M University, College Station, Texas.

Jones, L. D., and I. Jefferson (2012). Expansive Soils. In ICE Manual of Geotechnical Engineering, Volume 1: Geotechnical Engineering Principles, Problematic Soils and Site Investigation, ICE Publishing, London, UK, pp. 413-441.

Khan, M.S., Hossain M.S. and Ahmed A. (2017). “Determination of Spatial Variation of Unsaturated Vertical Permeability”. Proc., Second Pan-American Conference on Unsaturated Soils, Geo-Institute of ASCE, Dallas, Texas.

Khan, M. S., S. Hossain, A. Ahmed, and M. Faysal (2017). Investigation of a shallow slope failure on expansive clay in Texas. Engineering Geology, Vol. 219, pp. 118-129.

Kodikara, J., Rajeev, P., Chan, D. and Gallage, C. (2014). "Soil moisture monitoring at the field scale using neutron probe." Can. Geotech. J., 51(3), 332–345.

Koerner, R.M. (2005). Design with Geosynthetics 5th Ed. Pearson Prentice Hall, Upper Saddle River, NJ.

Kota, P.B.V.S., Hazlett, D., and Perrin, L. (1996). “Sulfate-bearing soils: Problems with calcium-based stabilizers.” Transportation Research Record 1546, pp.62-69.

Kuntiwattanakul, P., I. Towhata, K. Ohishi, and I. Seko (1995). Temperature Effects on Undrained Shear Characteristics of Clay. Soils and Foundations, Vol. 35, No. 1, pp. 147-162.

Kuo, C. and Huang, C. (2006). "Three-dimensional pavement analysis with nonlinear subgrade materials." J. Mater. Civil Eng., 18(4), 537-544.

Kutner, M. H., Nachtsheim, C., Neter, J., & Li, W. (2005). Applied linear statistical models. McGraw-Hill Irwin.

Lei, S., J. L. Daniels, Z. Bian, and N. Wainaina (2011). Improved Soil Temperature Modeling. Environmental Earth Sciences, Vol. 62, No. 6, pp. 1123-1130.

Lenz, R.W. (2011). Manual Notice: Pavement Design Guide.

Leong, E. C., and Rahardjo H. (1997). "Permeability functions for unsaturated soils." J. of Geotech. Geoenviron. Eng., 123(12), 1118-1126.

Little, D., Males, E. H., Prusinski, J.R. and Stewart, B. (2000). “Cementitious Stabilization.” 79th Millennium Rep. Series, Transportation Research Board.

Little, D.N. (1999). “Evaluation of Structural Properties of Lime Stabilized Soils and Aggregates, Vol. I. Summary of Findings.” National Lime Association Publication.

Lu, Y. (2015). Temperature Effect on Unsaturated Hydraulic Properties of Two Fine-Grained Soils and its Influence on Moisture Movement under an Airfield Test Facility. MS Thesis. Arizona State University.

Luo, R., & Prozzi, J. A. (2010). Development of longitudinal cracks on pavement over shrinking expansive subgrade. Road Materials and Pavement Design, 11(4), 807-832.

Lytton, R. L. (1977). "The Characterization of Expansive Soils in Engineering." Presentation at the Symposium on Water Movement and Equilibria in Swelling Soils, American Geophysical Union, San Francisco, California.

Lytton, R. L. (1994). "Prediction of Movement in Expansive Clay." Geotechnical Special Publication No. 40, American Society of Civil Engineers, New York, New York.

Lytton, R. L. (1995). "Foundations and Pavements on Unsaturated Soils." Proc., First International Conference on Unsaturated Soils, Paris, France, 3, 1201-1220.

Lytton, R., Aubeny, C., & Bulut, R. (2005). Design procedure for pavements on expansive soils. Texas Transportation Institute, Texas A & M University System.

Machan, G, and V G Bennett (2008). Use of inclinometers for geotechnical instrumentation on transportation projects: State of the practice. Washington, DC: Transportation Research E-Circular (E-C129).

Manosuthikij, T. (2008). “Studies on volume change movements in high PI clays for better design of low volume pavements.” PhD Dissertation, University of Texas at Arlington, Arlington, TX.

Mahedi, M., Cetin, B. and White, D. (2018). Performance Evaluation of Cement and Slag Stabilized Expansive Soils. In *Proceedings, 97th Annual Meeting, Transportation Research Board, Washington, DC*.

Mahedi, M., Hossain, M.S., Faysal, M. and Khan, M.S. (2017). Potential Applicability of Impact Echo Method on Pavement Base Materials as a Non-Destructive Testing Technique. In *Proceedings, 96th Annual Meeting, Transportation Research Board, Washington, DC.*

Mahedi, M., Hossain, S., Faysal, M., Khan, M. S., & Ahmed, A. (2017). Prediction of Strength and Stiffness Properties of Recycled Pavement Base Materials Using Non-Destructive Impact Echo Test. In *International Congress and Exhibition" Sustainable Civil Infrastructures: Innovative Infrastructure Geotechnology"* (pp. 121-136). Springer, Cham.

Manzur, S. R. (2013). Hydraulic performance evaluation of different recirculation systems for ELR/Bioreactor landfills, PhD Dissertation, University of Texas at Arlington

Manzur, S.R., Hossain, M.S., Kemler, V, and Khan, M.S. (2016). Monitoring extent of moisture variations due to leachate recirculation in an ELR/bioreactor landfill using resistivity imaging. Waste Management, 38-48.

Marks, BD, and TA Haliburton (1969). "Subgrade Moisture Variations Studied with Nuclear Depth Gages." Highway Research Record: 276, 14-24.

McDowell, C. (1956). "Interrelationship of load, volume change, and layer thickness of soils to the behavior of engineering structures." Highway Research Board. No. 35, 754-772.

Meerdink, J. S., Benson, C. H., and Khire, M. V. (1996). "Unsaturated hydraulic conductivity of two compacted barrier soils." J. of Geotech. Eng., 122(7), 565-576.

Mehrotra, Ayan, Murad Abu-Farsakh, and Kevin Gaspard (2016). "Development of subgrade Mr constitutive models based on physical soil properties." Road Materials and Pavement Design: 1-15.

Messing, I., and Jarvis, N. J. (1990). "Seasonal Variation in Feld Saturated Conductivity in Two Swelling Clay Soils in Sweden." Eur. J. Soil Sci., 41(2), 229-237.

Morris, C. E., & Stormont, J. C. (1997). Capillary barriers and subtitle D covers: estimating equivalency. Journal of Environmental Engineering, 123(1), 3-10.

Mowafy, Y.M., Bauer, G.E. and Sakeb, F.H. (1985). “Treatment of Expansive Soils: A Laboratory Study.” Transportation Research Record 1032, pp.34-39.

National Cooperative Highway Research Program (NCHRP). (2004). “Development of 499 the 2002 guide for the design of new and rehabilitated pavement structures.” Project 500 No. 1-37A, NCHRP Transportation Research Board, Washington, D.C. 501

Nelson, J D, D K Reichler, and J M Cumbers (2006). "Parameters for heave prediction by oedometer tests." 4th International Conference on Unsaturated Soils. Carefree, Arizona.

Nelson, J. D., Thompson, E. G., Schaut, R. W., Chao, K. C., Overton, D. D., & Dunham-Friel, J. S. (2011). Design procedure and considerations for piers in expansive soils. Journal of Geotechnical and Geoenvironmental Engineering, 138(8), 945-956.

Nelson, J., and J. D. Miller (1992). Expansive Soils: Problems and Practice in Foundation and Pavement Engineering. John Wiley & Sons, Inc., New York.

Nelson, John D., Overton, Daniel D., & Durkee, Dean B. (2001). Depth of wetting and the active zone. Paper presented at the Expansive Clay Soils and Vegetative Influence on Shallow Foundations, Houston, TX.

Nguyen, Q., Fredlund, D. G., Samarasekera, L., and Marjerison, B. L. (2010). “Seasonal pattern of matric suctions in highway subgrades.” Can. Geotech. J., 47(3), 267-280.

Dessouky, S., Oh, J. H., Yang, M., Ilias, M., Lee, S. I., Freeman, T., & Jao, M. (2012). *Pavement Repair Strategies for Selected Distresses in FM Roadways* (No. FHWA/TX-11/0-6589-1). Report FHWA/TX-11/0-6589-1. The University of Texas at San Antonio, San Antonio, TX.

Omidi, G.H., Thomas, J.C., Brown, K.W. (1996). Effect of desiccation cracking on the hydraulic conductivity of a compacted clay liner. Water Air Soil Pollut. 89 (1–2), 91–103.

Osman, M A, and A M.E Sharief (1987). "Field and laboratory observations of expansive soil heave." 6th International Conference of Expansive Soils. New Delhi, India.

Picomell, M. and Lytton, R. L. (1987). "Behavior and Design of Vertical Moisture Barriers." Transportation Research Record 1137, TRB, National Research Council, Washington, D.C., 71-81.

Picornell, M., Lytton, R. L., & Steinberg, M. L. (1984). Assessment of the effectiveness of a vertical moisture barrier. In Fifth International Conference on Expansive Soils 1984: Preprints of Papers (p. 354). Institution of Engineers, Australia.

Punthutaecha, K., Puppala, A.J., Vanapalli, S.K., Inyang, H. (2006). Volume change behaviors of expansive soils stabilized with recycled ashes and fibers. J. Mater. Civ. Eng. 18 (2), 295–306.

Puppala, A. J., M. Thammanoon, S. Nazarian, and L. R. Hoyos (2011). Threshold Moisture Content and Matric Suction Potentials in Expansive Clays Prior to Initiation of Cracking in Pavements. Canadian Geotechnical Journal, Vol. 48, No. 4, pp. 519-531.

Puppala, A. J., Manosuthikij, T., and Chittoori, B. C. (2014). “Swell and shrinkage strain prediction models for expansive clays.” Eng. Geol., 168(1), 1-8.

Puppala, A. J., T. Manosuthkij, S. Nazarian, L.R. Hoyos, and B. Chittoori (2012). In Situ Matric Suction and Moisture Content Measurements in Expansive Clay during Seasonal Fluctuations. In Geotechnical Testing Journal, 35(1), 1-9.

Puppala, A.J., Griffin, J.A., Hoyos, L.R. and Chomtid, S. (2004). “Studies on Sulfate-Resistant Cement Stabilization Methods to Address Sulfate-Induced Soil Heave.” Journal of Geotechnical and Geoenvironmental Engineering, 130, pp.391- 402.

Puppala, A.J., Manosuthikij, T., Chittoori, B.C. (2013). Swell and shrinkage characterizations of unsaturated expansive clays from Texas. Eng. Geol. 164, 187–194.

Puppala, A.J., Wattanasanticharoen, E. and Punthutaecha, K. (2003). “Experimental Evaluations of Stabilization Methods for Sulphate-rich Expansive Soils.” Ground Improvement Vol. 7, No. 1, 2003. pp. 25-35.

Qian, X., Koerner, R. M., & Gray, D. H. (2001). Geotechnical aspects of landfill construction and design. Prentice Hall.

Rao, R. R., H. Rahardjo, and D. G. Fredlund (1988). "Closed-form heave solutions for expansive soils." Journal of Geotechnical Engineering: 114 (5), 573- 588.

Raymond, G. and Ismail, I. (2003). “The Effect of Geogrid Reinforcement on Unbound Aggregates.” Geotextile and Geomembranes 21, pp.355-380

Ridgeway, H.H. (1982). Pavement Subsurface Drainage Systems, National Cooperative Highway Research Program Synthesis of Highway Practice Number 96, Transportation Research Board, National Research Council, Washington, D.C.

Rojas, E., Romo, M. O., Paul, G. and Refugio, C. (2006). “Analysis of deep moisture barriers in expansive soils. II: Water flow formulation and implementation.” International Journal of Geomechanics. Vol. 6 (5): 319-327.

Rollings Jr., R.S., Burkes, J.P., and Rollings, M.P. (1999). “Sulfate attack on cement-stabilized sand.” Journal of Geotechnical and Geoenvironmental Engineering, vol. 125 No.5, pp.364-372.

Rollins, K. M., & Christie, R. (2002). Pavement and Subgrade Distress-Remedial Strategies for Construction and Maintenance (I-15 Mileposts 200-217) (No. UT-02.17).

Romero, E., A. Gens, and A. Lloret (2001). Temperature Effects on the Hydraulic Behavior of an Unsaturated Clay. Geotechnical and Geological Engineering, Vol. 19, No. 3, pp. 331-332.

Russam, K. (1965). "The prediction of subgrade moisture conditions for design purposes." Moisture equilibria and moisture changes in soils beneath covered areas. Butterworth, Sydney, Australia: 233-236.

Ruttanaporamakul, P. (2012). “Resilient moduli properties of compacted unsaturated subgrade materials.” MS Thesis, University of Texas at Arlington, Arlington, TX.

Samouëlian, A., Cousin, I., Tabbagh, A., Bruand, A. and Richard, G. (2005). "Electrical resistivity survey in soil science: a review." Soil Tillage Research, 83(2), 173-193.

Sastry, S.S. (2012). Introductory Methods of Numerical Analysis. PHI Learning Private Limited, New Delhi, India.

Sebesta, S. (2002). “Investigation of maintenance base repairs over expansive soils: Year 1 report.” Report No. FHWA/TX-03/0-4395-1, Texas Transportation Institute, Texas A&M University, College Station, TX.

Sillers, W. S., and Fredlund, D. G. (2001). “Statistical assessment of soil-water characteristic curve models for geotechnical engineering.” Canadian Geotechnical Journal, v 38, n 6, December, 2001, p 1297-1313

Slope Indicator (2017). Accessed at http://www.slopeindicator.com/instruments/inclin-intro.php on August 29, 2017.

Snethen, D. R. (1979). “An Evaluation of methodology for prediction and minimization of volume change of expansive soils in highway subgrades. Research Report No. FHWA-RD-79-49., U. S. Army Eng. Waterway Exp. Sta. Vicksburg, MS.

Snethen, D.R. (2001). “Influence of Local Tree Species on Shrink/Swell Behavior of Permian Clays in Central Oklahoma.” Expansive Clay Soils and Vegetative Influence on Shallow Foundations, pp.158-171.

Stallings, S.L. (1999). “Roadside Ditch Design and Erosion Control on Virginia Highways.” MS Thesis, Virginia Polytechnic and State University, Blacksburg, Virginia, 170 pages.

Steinberg, M. L. (1977). "Ponding an Expansive Clay Cut: Evaluations and Zones of Activity." Transportation Research Record 641, TRB, National Research Council, Washington, D.C., 61-66.

Steinberg, M. L. (1980). "Deep Vertical Fabric Moisture Seals." Proc., Fourth International Conference on Expansive Soils, Denver, Colorado, 1, 383-400.

Steinberg, M. L. (1981). "Deep-Vertical-Fabric Moisture Barriers in Swelling Soils." Transportation Research Record 790, TRB, National Research Council, Washington, D.C., 87-94.

Steinberg, M. L. (1985). "Controlling Expansive Soil Destructiveness by Deep Vertical Geomembranes on Four Highways." Transportation Research Record 1032, TRB, National Research Council, Washington, D.C., 48-53.

Steinberg, M. L. (1989). "Further Monitoring of Twelve Geomembrane Sites in Texas." Report DHT-18, Departmental Information Exchange, State Department of Highways and Public Transportation, Austin, Texas.

Steinberg, M. L. (1992). "Controlling Expansive Soils: Twenty Texas Highway Projects." Proc., Seventh International Conference on Expansive Soils, Dallas, Texas, 1, 392-397.

Swanberg, J. H. (1946). "Temperature Variations in a Concrete Pavement and the underlying Subgrade." Highway Research Board Proceedings. Vol. 25.

Tabbagh, A., Dabas, M., Hesse, A., & Panissod, C. (2000). Soil resistivity: a non-invasive tool to map soil structure horizonation. Geoderma, 97(3), 393-404.

Talluri, N., Puljan, V., Manosuthikij, T., Puppala, A. J., & Saride, S. (2011). Prediction of Swell-Shrink Movements of Pavement Infrastructure. In Geo-Frontiers 2011: Advances in Geotechnical Engineering (pp. 2740-2749).

Tensar Co. (2017). Accessed in http://www.tensarcorp.com/Applications/pavement-rehabilitation on July 13, 2017.

Thompson, M.R. (1982). “Highway Subgrade Stability Manual.” Illinois Department of Transportation, Departmental Policies, MAT-10.

Thompson, M.R., (1966). “Lime Reactivity of Illinois Soils.” Journal of the Soil Mechanics and Foundations Division, ASCE, Vol. 92, No. SMS.

Thornthwaite, Charles Warren (1948). "An approach toward a rational classification of climate." Geographical review 38(1): 55-94.

Tripathy, S. and Rao, K. S. S. (2009). "Cyclic swell–shrink behaviour of a compacted expansive soil." Geotech. Geol. Eng., 27(1), 89-103.

Tucker, R.L. and Poor, A.R. (1978). “Field Study of Moisture Effects on Slab Movements.” Journal of Geotechnical Engineer, ASCE, 104(4), 403-415.

Tutumluer, E. and Kwon, J. (2005). “Evaluation of Geosynthetics use for Pavement Subgrade Restraint and Working Platform Construction.” Proc. of 13th Annual Great Lakes Geotechnical/Geoenvironmental Conference on Geotechnical Applications for Transportation Infrastructure, May 13, 2005.

Tuller, M., and Or, D. (2004). Retention of water in soil and the soil water characteristic curve. *Encyclopedia of Soils in the Environment*, *4*, 278-289.

TxDOT (1999). Test Procedure for determination of potential vertical rise. Austin: TxDOT.

Van Genuchten, M. T. (1980). “A closed-form equation for predicting the hydraulic conductivity of unsaturated soils.” J. Soil Sci., 44(5), 892-898.

Van Wijk, W.R. and D. A. De Vries (1963). Periodic Temperature Variations in a Homogeneous Soil. In Physics of Plant Environment, W. R. Van Wijk, ed. North-Holland Publ. Co., Amsterdam, pp. 102-143.

Vaswani, N.K. (1975). Case Studies of Variations in Subgrade Moisture and Temperature under Road Pavements in Virginia. Transportation Research Record 532, Transportation Research Board, National Research Council, Washington, D.C., pp. 30-42.

Wagner, J. F. (2013). “Chapter 9 – Mechanical properties of clays and clay minerals.” Handbook of Clay Science, Volume 5 (edited by F. Bergaya and G. Lagaly). Elsevier, Oxford, England, 347-381.

Wang, M W, J Li, S Ge, and S T Li (2013). "Moisture migration tests on unsaturated expansive clays in Hefei, China." Applied Clay Science: 79, 30-35.

Wanyan, Y., Abdallah, I., Nazarian, S., and Puppala, A.J. (2010). Expert system for design of low-volume roads over expansive soils. Transportation Research Record: Journal of the Transportation Research Board, 2154(1), 81-90.

Ward, W. H. (1953). “Soil Movements and Weather.” Proceeding of 3rd International Conference Soil Mechanics, Zurich, 2, 477-481.

Wesseldine, M.A. (1982). “House Foundation Failures Due To Clay Shrinkage Caused by Gum Trees” Transactions, Institution of Professional Engineers, NZ, March, CE9 (1).

Winterkorn, H.F. and H.Y. Fang (1972). Effect of Temperature and Moisture on the Strength of Soil-Pavement Systems, Report No. 350.4. Fritz Laboratory Reports, Bethlehem, PA.

Xu, Q, S. Liu, X. Wan, C. Jiang, X. Song, and K. Wang (2012). Effects of Rainfall on Soil Moisture and Water Movement in a Subalpine Dark Coniferous Forest in Southwestern China. Hydrological Processes, Vol. 26, No. 25, pp. 3800-3809.

Zapata, C. E., Houston, W. N., Houston, S. L., and Walsh, K. D. (2000). “Soil-water characteristic curve variability.” Geotech. SP, 99(1), 84-124.

Zapata, C.E., and W.N. Houston (2008). Calibration and validation of enhanced integration climatic model for pavement design. In Transportation Research Board.

Zhan, T. L. T., Ng. C. W. W., and Fredlund, D. G. (2007). “Field study of rainfall infiltration into a grassed unsaturated expansive soil slope.” Can. Geotech. J., 44, 392-408.

Zheng, J., and R. Zhang (2013). Prediction and Application of Equilibrium Water Content of Expansive Soil Subgrade. In Second International Conference on Geotechnical and Earthquake Engineering. Chengdu, China: ASCE, pp.754-761.

Zhou, Q. Y., Shimada, J., & Sato, A. (2001). Three dimensional spatial and temporal monitoring of soil water content using electrical resistivity tomography. Water Resources Research, 37(2), 273-285.

BIOGRAPHY

Asif Ahmed was born in Dhaka, Bangladesh. He earned his bachelor's degree in civil engineering from Bangladesh University of Engineering and Technology (BUET) in February, 2013. Considering the existing geotechnical issues like landslides, slope stability, and problematic soils in his native country, he decided to pursue higher education in geotechnical engineering. He began his graduate study in geotechnical engineering under the supervision of Dr. Sahadat Hossain at the University of Texas at Arlington from spring 2014. As a research assistant funded by the Texas Department of Transportation (TxDOT), his research works include but are not limited to unsaturated soil mechanics, expansive soil behavior, slope stability, pavement distress development, real-time data analysis, and finite element numerical modeling. He has also worked on different research projects, investigating failed highway slopes and geophysically evaluating existing highway sub-structures in North Texas. Mr. Ahmed has experience in the instrumentation of highway slopes and pavement sites. He has several publications in prestigious civil engineering journals and has presented at local, national and international conferences, such as the Transportation Research Board Meeting, Geo-Congress, etc. He was awarded 2nd prize in ASCE's annual national competition in the geo-poster category for presenting part of his doctoral work. He received an Outstanding Graduate Student Award in the Civil Engineering Department at UTA in 2015-16 and 2016-17. He is a student member of American Society of Civil Engineers (ASCE) and Deep Foundation Institute (DFI), and is an engineer-in-training (E.I.T.) in the State of Texas. He aims to be a part of the research and development area in the geotechnical engineering sector.